Effects of hyperglycemic and inflammatory conditions on proteoglycan synthesis in cultured human endothelial cells

Master Thesis in Clinical Nutrition

Trine Marita Reine

Faculty of medicine, Departement of Nutrition

UNIVERSITETET I OSLO

01 september 2008

Acknowledgements

This thesis describes work undertaken between august 2007 and august 2008 at the Department of Nutrition, University of Oslo, under the supervision of Professor Svein Olav Kolset.

First and foremost I would like to thank my supervisor, Svein Olav Kolset, for including me in his research group, for introducing me to the intriguing field of glycobiology, for always having time to spare in a seemingly overbooked schedule and for his invaluable guidance during this work.

I am also indebted to my co-supervisor Katja Svennevig for her guidance throughout the work of this thesis, both in the lab and during the process of writing. Her patience, encouragement and support have been invaluable to me.

I would also like to thank Parvin Mahzonni for technical assistance in the lab.

A special thanks to my husband Simen for always standing by my side – and to my daughter Marita, for making me see things in perspective. Also; thanks to my family and friends for putting up with me and supporting me throughout this process.

Finally, I would like to express my gratitude to fondsfinans for valuable financial support.

Oslo, 01 september 2008

Trine Marita Reine

Abstract

Background: Diabetes Mellitus (DM) is associated with both micro- and macro-vascular complications, linked to hyperglycemia and atherosclerotic chronic inflammation of the vessels. The endothelium is the prime organ to be exposed to hyperglycemia and is one of the main targets of diabetic complications. Proteoglycans (PGs) are important components of the healthy endothelium, and are also involved in a number of processes important to the development of DM and atherosclerosis. Thus, changes in PG expression might be linked to the development of diabetic complications.

Methods: Primary human umbilical vein endothelial cells (HUVEC) were established and cultured *in vitro*. In order to study the changes in PGs during DM, we mimicked the diabetic conditions by exposing endothelial cells to a hyperglycaemic or inflammatory environment. Hyperglycemic exposure was either high glucose (25.0 mM) or glucosamine (GlcN; 0, 0.1, 1.0, 2.0, 5.0 or 10.0 mM), and inflammatory conditions were created by adding pro-inflammatory cytokines interleukine-1α (IL-1α, 2 ng / ml) or tissue necrosis factor-α (TNF-α, 7 ng / ml). Low glucose (5.0 mM) was used as the control in all experiments. ^{35}S-sulfate labelling was performed 24 hours prior to harvesting. Radiolabelled macromolecules were obtained by gelfiltration chromatography; in some cases PGs were further isolated by ion-exchange chromatography, before separation on SDS-PAGE and visualization by film exposure. Cells cultured for Western blotting analyses were stimulated for 24 hours before harvesting, isolation of PGs by ion-exchange chromatography, SDS-PAGE separation, electroblotting and immunostaining against PGs perlecan and decorin.

Results: GlcN dose-response and time-response experiments indicated a suitable exposure of 1.0 mM GlcN for 24 hours in HUVEC. The major findings revealed a decreased biosynthesis and secretion of ^{35}S-PGs and of the individual PGs perlecan and decorin upon GlcN exposure. The effects of high levels of glucose were

inconclusive. Exposure of HUVEC to the pro-inflammatory cytokine IL-1α increased the total *de novo* synthesis of PGs, while the effects of TNF-α were inconclusive. Only decorin was increased by the cytokines, not perlecan. Both during hyperglycaemic and inflammatory conditions however, no effects on the heparan sulfate (HS) / choindroitin sulfate (CS) ratio of the total PG pool were observed, nor on the HS/CS composition of the individual PGs perlecan and decorin. Perlecan was demonstrated to be a HSPG in HUVEC.

Conclusions: The experiments indicated a suitable exposure of 1.0 mM GlcN for 24 hours in HUVEC, affecting PG expression without affecting cell viability. The decrease in PGs after GlcN exposure suggests an effect of hyperglycemia on PG expression trough the hexosamine pathway. GlcN is most likely to influence on the total expression of PGs. These effects were, however, not observed in cells exposed to high glucose. IL-1α, but not TNF-α, was indicated to increase PG expression. The HS/CS composition was not observed to be altered with high glucose or GlcN treatment. Decorin expression was altered upon cytokine exposure, but not perlecan. This might suggest a different effect on various PGs by inflammatory mediators. Additional analyses are clearly demanded to clarify the causes of the observed changes in PG expression; it must be elucidated whether these changes reflects changes in PG synthesis, degradation, or rather in glycosaminoglycan composition, length and sulfation.

Table of contents

1. Abbrevations

AGE	Advanced Glycation End products
BM	Basement Membrane
cABC	chondroitinase ABC
Cpm	Counts per minute
CS	Choindroitin sulfate
DAG	Diacylglycerol
DEAE	Diethylaminoethyl
DHAP	Dihydroxyacetone phosphate
DM	Diabetes Mellitus
DMSO	Dimethyl sulfoxide
DS	Dermatan sulfate
EC	Endothelial cell
ECM	Extracellular matrix
EDTA	Ethylenediaminetetraacetic acid
EGF	Epidermal growth factor
EGFR	Epidermal growth factor receptor
eNOS	endothelial nitric oxide synthase
FCS	Foetal Calf Serum
FGF	Fibroblast Growth Factor
GAG	Glycosaminoglycan
Gal	Galactose
GalN	Galactosamine
GalNAc	N-Acetyl Galactosamine
GAPDH	Glyceraldehyde-3 phosphate dehydrogenase

GFAT	Glutamine:fructose-6 phosphate amidotransferase
GlcA	Glucuronic acid
GlcN	Glucosamine
GlcNAc	N-Acetyl Glucosamine
Gln	Glutamine
Glu	Glutamic Acid
GLUT	Glucose transporter
HA	Hyaluronic acid / hyaluronan
HbA_{1c}	Glycated Haemoglobin A_{1c}
HG	High glucose
HS	Heparan sulfate
HUVEC	Human Umbilical Vein Endothelial Cell
IdoA	Iduronic acid
KS	Keratan sulfate
LG	Low glucose
$NADH/NAD^+$	Nicotinamide adenine dinucleotide
$NADPH/NADP^+$	Nicotinamide adenine dinucleotide phosphate
PAI-1	Plasminogen Activator Inhibitor - 1
PARP	Poly ADP-ribose polymerase
PBS	Phosphate Buffered Saline
PDGF	Platelet Derived Growth Factor
PG	Proteoglycan
PKC	Protein Kinase C
RAGE	Receptor for AGE
ROS	Reactive Oxygen Species
SLRP	Small Leucine Rich PGs

SMC	Smooth Muscle Cells
TGF-β	Transforming Growth Factor -β
UDP	Uridine diphosphate
VEGF	Vascular Endothelial Growth Factor

2. Introduction

The altered way of living of humans towards a more sedentary lifestyle with a higher consumption of sugar and fat, has lead to an increase in life-style related diseases such as metabolic syndrome and type II diabetes (1). Diabetes Mellitus (DM) reduce the life quality and life-expectancy of the patient, as well as being costly for the society. DM is associated both with hyperglycemia and atherosclerotic chronic inflammation of the vessels. The endothelium lining the vessels is the prime organ to be exposed to hyperglycemia and is one of the main targets of diabetic complications. The structurally diverse and widespread proteoglycans (PGs) are involved in a number of different processes important in the development of DM and atherosclerosis. Changes in PG expression could thus be involved in the development of diabetic complications. In order to study changes in endothelial PG expression during diabetic conditions, we mimic these conditions by exposing cultured human endothelial cells to hyperglycaemic conditions or inflammatory cytokines, and study the effects on proliferation, total PG production and changes in the expression of individual PGs.

2.1 Diabetes Mellitus

DM is responsible for 5 % of all deaths globally each year, and this number is likely to increase by more than 50 % over the next 10 years. In Norway there are probably between 90 000 and 120 000 people with diagnosed DM, and nearly as many may with undiagnosed DM (2). An estimated number of 171 million people are diagnosed with DM worldwide. The total number of diabetics will be more than doubled over the next 25 years, reaching a total of 366 million globally by 2030 (3). This increase is mostly due to an addition in the prevalence of type II DM, and occurs because of the growing trend towards obesity, unhealthy diets with a higher consumption of sugar and fat and more sedentary lifestyles (1).

DM is a group of metabolic diseases steadily increasing in prevalence all over the world. DM is characterized by chronic hyperglycemia caused by lacking production of – or response to –insulin. The anabolic hormone insulin decreases the amount of glucose in the blood by promoting glucose uptake by cells and increasing the capacity of the liver to synthesize glycogen. There are three main forms of DM: type I, type II and gestational DM, which have similar signs, symptoms and consequences, but different causes and population distribution. Type I DM is characterized by the autoimmune destruction of the insulin-producing β-cells of the pancreas, leading to failure to produce insulin and hence impaired uptake of glucose. In type II DM the hyperglycemia is caused by insulin-resistance or reduced insulin sensitivity in combination with reduced insulin secretion. The pancreas increases the production of insulin in response to lowered sensitivity in liver, muscle and fat. This extra workload exhausts the β-cells and the insulin production declines over time, resulting in a relative insulin-deficiency (4). Finally, gestational DM is defined as "any degree of glucose intolerance with onset or first recognition during pregnancy" (5). The hormones of pregnancy can cause insulin resistance in predisposed women. This condition typically resolves after delivery, but can have severe consequences for the foetus. The causes of type I DM is not clear, but it could possibly be triggered by for example viral infections in genetic susceptible individuals, and it often attacks young people. The much more common type II DM is on the other hand provoked by lifestyle factors and its prevalence increases with increasing age, although this age is now declining.

2.2 The endothelium

The endothelium is the thin layer of cells that line the interior surface of blood vessels, forming an interface between circulating blood in the lumen and the rest of the vessel wall. Endothelial cells (ECs) are specialized epithelium cells which line the entire circulatory system, from the heart to the smallest capillary. They synthesize

molecules released to the blood and to the extracellular matrix (ECM), and control the passage of materials into and out of the bloodstream. The endothelium senses mechanical and hormonal stimuli, and responds to this by releasing agents that regulate vasomotor function (NO, endothelin-1, angiotensin II), trigger inflammatory processes (NO, adhesion molecules) and affect homeostasis (6). Dynamic interactions between ECs and components of their surrounding ECM are necessary for the invasion, migration and survival of EC during angiogenesis. These interactions are mediated by EC receptors recognizing ECM components; integrins and cell surface PGs, and are also modulated by matrix proteinases that proteolytically degrade matrix components (7). Thus, the endothelium is either directly or indirectly involved in many human diseases such as atherosclerosis, coagulation disorders, malignant growth, and chronic diseases including DM and arthritis.

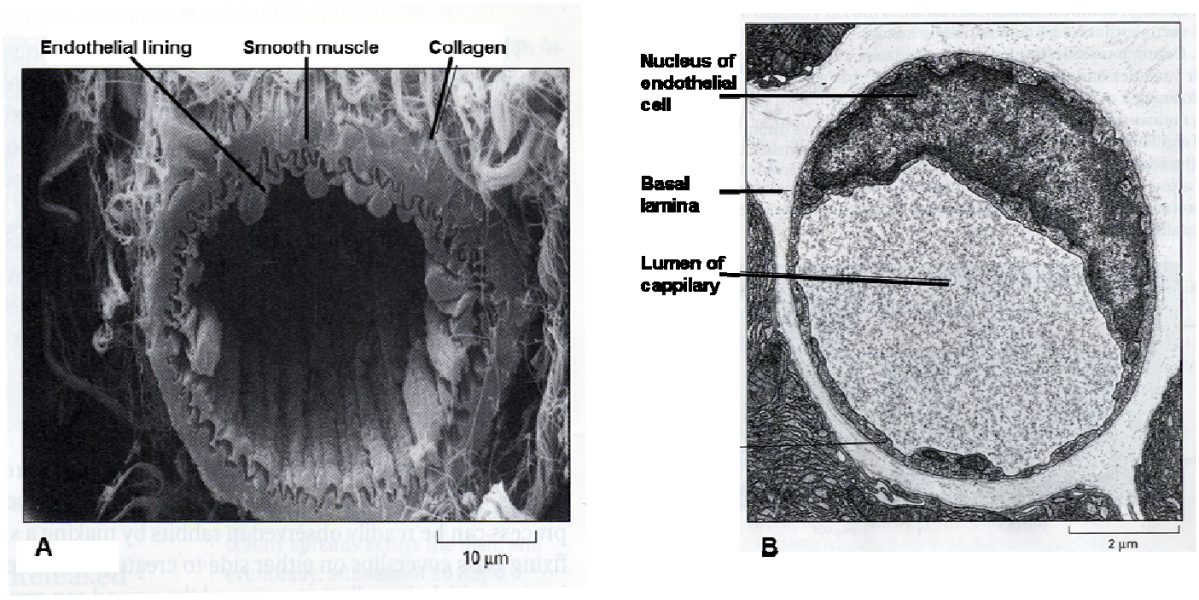

Figure 2.1. Illustration of different vessels and the endothelium. *A. A small artery in cross section showing the inner lining of endothelial cells and the surrounding layer of smooth muscle cells and connective tissue. B. Electron micrograph of a small capillary cross-section. The wall is formed by a single endothelial cell surrounded by basement membrane. From Alberts, B. et al, Molecular biology of the Cell, 3ed (8).*

The largest blood vessels (arteries and veins) have a thick tough wall of connective tissue and smooth muscle cells (SMC), and this wall is lined by a thin single layer of ECs, separated from the surrounding outer layers by a basement membrane (BM) (figure 2.1A). The amount of connective tissue and SMC in the vessel wall varies

according to the vessel's diameter and function, but the endothelial lining is always present. In the capillaries the walls consists of nothing but ECs and basal lamina as shown in figure 2.1B (8). Covering the endothelium luminally is the endothelial glycocalyx; a network of membrane-bound PGs and glycoproteins (9). Both plasma and endothelial derived soluble molecules are incorporated into this network, and a dynamic equilibrium exists between this layer of soluble components and the flowing blood. Figure 2.2 provide a schematic illustration of the construction of the endothelium.

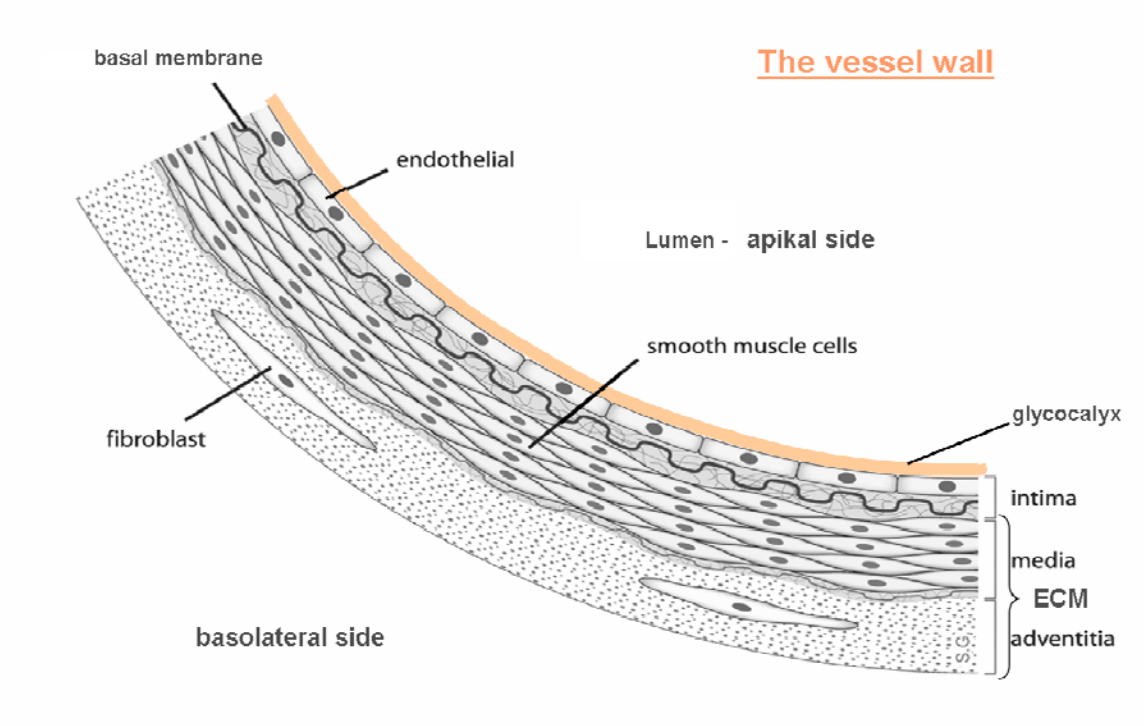

Figure 2.2. Structure of the vessel wall. *The blood vessels have a wall of connective tissue and smooth muscle cells (tunica media and adventitia), and this wall is lined by a thin single layer of ECs, separated from the surrounding outer layers by a basal membrane (tunica intima). PGs are important constituents of both the ECM and the basement membrane. Covering the endothelium luminal is the endothelial glycocalyx; a network of membrane-bound PGs and glycoproteins. Modified from: http://en.wikipedia.org/wiki/Image:Anatomy_artery.png*

2.3 DM complications

The chronic hyperglycemia of DM is important in the pathogenesis of specific DM-related micro- and macro- vascular complications (10). Diabetic microangiopathy can cause retinopathy, neuropathy and nephropathy (11). Macroangiopathy – mainly atherosclerosis of the coronary, carotid and peripheral arteries - increase the risk of myocardial infarction, stroke and diabetic foot disease. DM is thus an important cause of blindness, limb amputation and kidney failure, and 50% of diabetic die of cardiovascular disease. Hyperglycemia plays an important role in the development of microvascular complications, along with hypertension, smoking, hypercholesterolemia, dyslipidemia, obesity and hyperhomocysteinaemia (6). The risk of macroangiopathy is not so strongly related to hyperglycemia, but more so to the general risk factors of atherothrombosis, all of which create a constant damage to the vascular wall manifested by a low-grade inflammatory process and endothelial dysfunction.

The treatment of DM was very limited until insulin became medically available in 1921. Today the disease is usually managed with a combination of insulin supplementation, tablets (type II), dietary treatment, exercise, and weight loss. Two landmark studies, the DCCT (The Diabetes Control and Complications Trial) (12) and UKPDS (United Kingdom Prospective Diabetes Study) (13), showed that intensive control of hyperglycemia can reduce the occurrence of progressive retino- neuro- and nephropathy in diabetic patients. Important goals in preventing long-term diabetic complications are keeping fasting blood glucose concentration between 4 and 7 mM, and avoiding a postprandial concentration above 10 mM. The level of HbA_{1c} (glycated hemoglobin A_{1c}) reflects the average plasma glucose concentration over longer periods of time, and should be held below 7.5 % in diabetics (14).

2.3.1 Endothelial dysfunction

The endothelium is the prime organ to be exposed to the hyperglycemia of DM, and hyperglycemia is identified as a primary causal factor in the development of DM

complications, and might be responsible for impairment of significant functions of the endothelium (12;13). The endothelium is especially vulnerable to hyperglycemia because of the inability to regulate the glucose uptake, resulting in high intracellular levels during hyperglycemic conditions. ECs and SMCs express GLUT 1 (Glucose transporter 1) which is not responsive to insulin, but they do not express GLUT 2-5, and thus cannot regulate glucose uptake trough insulin action (15;16). Also, SMCs are able to downregulate GLUT 1, while ECs are not (16). This is reflected in the fact that diabetic complications appear to affect organs where cells do not require insulin for uptake, such as EC, mesangial cells in the renal glomerulus and neurons and Schwann cells in peripheral nerves.

Endothelial dysfunction is a key component in the pathogenesis of atherosclerosis. It is a broad term that implies an impairment of the normal functions of the endothelium. This is characterized by a shift toward reduced vasodilation caused by impaired NO generation, a proinflammatory state and increase in prothrombotic properties (17). Besides the vasodilatory effects, NO inhibits leukocyte adhesion to the endothelial cells, and reduce platelet aggregability and SMC proliferation, and thus protects against inflammation (18). Up-regulation of adhesion molecules, generation of chemokines and production of PAI-1 (plasminogen activator inhibitor-1) participate in the inflammatory response and contribute to the prothrombotic state.

Important changes associated with microvascular complications are the thickening of the basement membrane, reduction of glycocalyx dimensions (19;20), increased organ blood flow and vascular permeability, and abnormal blood viscosity, platelet function – all of which originates, at least in part, in the endothelial dysfunction. Macrocvascular complications include disease of the larger vessels, or essentially, atherosclerosis.

The thickening of the capillary BM observed in DM (21) is to a large part due to an increase in type IV collagen secretion by the capillary cells, reduced PG expression and alterations in ECM network formation. BM thickening could cause vascular dysfunction by several different mechanisms: Alterations in BM compounds could

affect vascular cell metabolism and impair functions such as migration, cell adhesion and growth. A decrease in negative charges due to altered PG composition could change the filtration properties of renal glomerular capillaries, and glycated extracellular proteins can bind to specific receptors and affect vascular cell metabolism and function directly. Degraded products of BM can alter vascular cell growth indirectly by initially activating macrophages, which then release vasoactive cytokines (21). Acute and long standing hyperglycemia is also associated with profound reduction of glycocalyx dimensions, and it is speculated that this damage to the glycocalyx contribute to the endothelial dysfunction in hyperglycemic conditions. The role of endothelial glycocalyx in atherogenesis is not well-established but data suggests that it is involved in the initiation and progress of the atherosclerotic process (19).

2.3.2 Mechanisms underlying endothelial dysfunction in DM

DM is associated with micro- and macro vascular complications; affecting the small vessels such as those supplying the retina, nerves and kidneys, and the large arteries of the limbs and coronary arteries, respectively. Hyperglycemia is established as a major risk factor contributing to the underlying endothelial dysfunction and low grade inflammation of this angiopathy (12;13). This relationship is illustrated in figure 2.4. There are four main hypotheses linking hyperglycemia to diabetic complications: increased hexosamine pathway flux, increased AGE (Advanced Glycation End products) formation, activation of PKC (protein kinase C) and increased polyol pathway flux (11;22), see figure 2.3 (22).

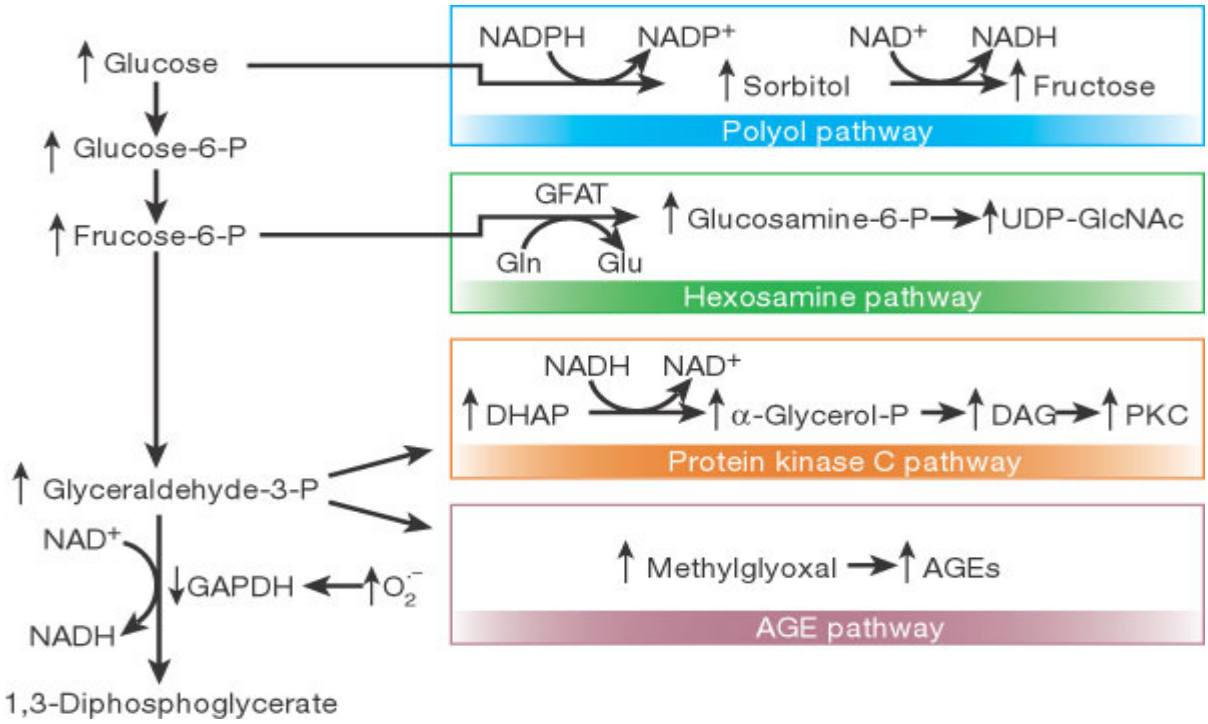

Figure 2.3. Overview of the metabolic pathways of glucose, linking hyperglycemia to diabetic complications. *Excess superoxide partially inhibits the glycolytic enzyme GAPDH (glyceraldehyde-3 phosphate dehydrogenase), thereby diverting upstream metabolites from glycolysis into pathways of glucose overutilization. This results in increased flux of DHAP (dihydroxyacetone phosphate) to DAG (Diacylglycerol), an activator of PKC, and of triose phosphates to methylglyoxal, the main intracellular AGE precursor. Increased flux of fructose-6-phosphate to UDP-N-acetylglucosamine increases modification of proteins by O-linked N-acetylglucosamine (GlcNAc) and increased glucose flux through the polyol pathway consumes NADPH and depletes glutathione. From Brownlee, M. Nature, 2001(22).*

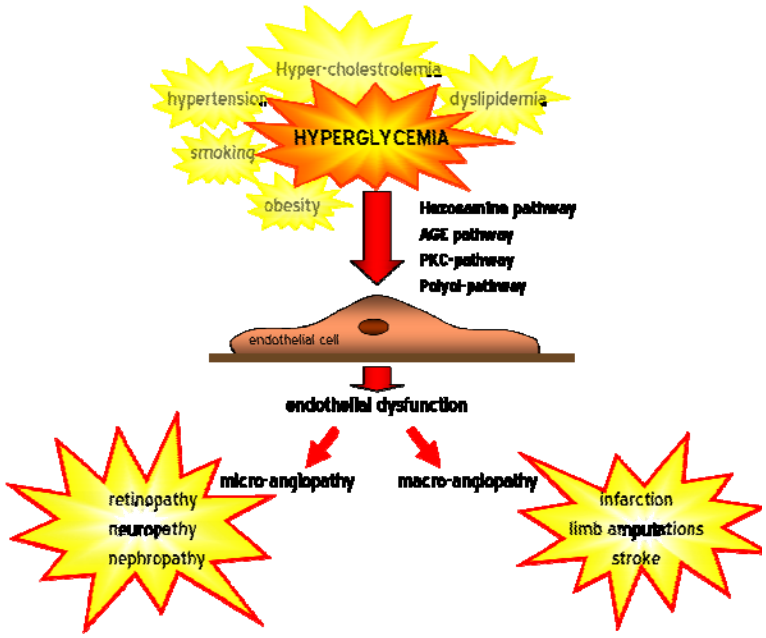

Figure 2.4. Illustration of the relationship between hyper - glycemia, endothelial dys- function and diabetic complications. *Diabetes is associated with micro- and macro vascular complications; affecting the small vessels such as those supplying the retina, nerves and kidneys, and the large arteries of the limbs and coronary arteries, respectively. Hyperglycemia is established as a major risk factor contributing to the underlying endothelial dysfunction and low grade inflammation of this angiopathy.*

The Hexosamine pathway

The increase of intracellular glucose and glucose metabolites will increase the flux trough several metabolic pathways. Shunting of excess intracellular glucose into the hexosamine pathway is one of the ways in which hyperglycemia might contribute to the diabetic complications. Exposure to excess glucosamine (GlcN) is thought to exert the same effects trough entering this pathway as indicated in figure 2.5. GlcN taken up by cells is phosphorylated into GlcN 6-phosphate by hexokinase, which then bypasses GFAT (glutamine:fructose-6 phosphate amidotransferase) to enter the hexosamine pathway.

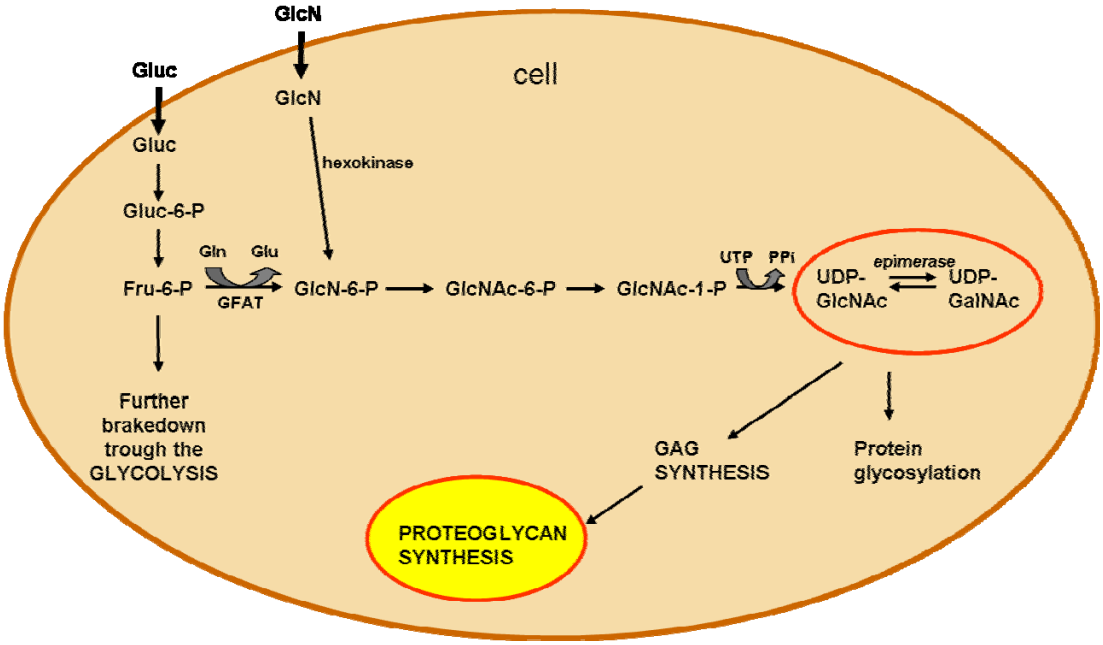

Figure 2.5. The hexosamine pathway. *Glucose (Gluc) is taken up by cells and metabolized trough the glycolysis or other metabolic pathways such as the hexosamine pathway. In the latter, glucose is converted to GlcN-6-phosfate (GlcN-6-P) by the enzyme GFAT (glutamine:fructose-6 phosphate amidotransferase). GlcN-6-P is further converted to N-Acetyl-Glucosamine-6-fosfate (GlcNAc-6-P) andGlcNAC-1-P, and then to the Uridine diphosphate-sugars UDP-GlcNAc and UDP GalNAc (N-Acetyl-galactosamine). The rate-limiting step of GFAT can be avoided by direct administration of GlcN, which is converted to GlcN-6-P by a hexokinase. UDP-GlcNAC and UDP-GalNAc are utilized for GAG (glucosaminoglycan) -synthesis and protein glycosylation. An increase in UDP-sugars is believed to increase the GAG-synthesis, and thus alter the PG expression. An increase in glucose availability will create excess superoxide, partially inhibiting the glycolytic enzyme GAPDH, and thereby diverting upstream metabolites from glycolysis into pathways of glucose overutilization. This results in increased flux of the hexosamine pathway, and possibly a change in PG expression.*

Some of the fructose-6-phospate from the glycolysis is converted by the enzyme GFAT into glucosamine-6-phosphate (GlcN-6P) and finally to UDP-GlcNAc, which is required for N-linked and O-linked glycosylation and the GAG (glucosaminoglycan) synthesis of PGs (23). The substrate affinity of GFAT is relatively low, and during normoglycemic conditions, the flux trough this pathway is scarce; about 1-2% of the incoming glucose enters this pathway (24). During hyperglycemia however, the flux is markedly increased (25). This increased production of GlcNAc could lead to altered modification of transcription factors, often resulting in pathological changes in gene expression. As an example, increased modification (O-GlcNAcylation) of the transcription factor Sp1 will result in increased expression of TGF-β (Transforming growth factor-β) and PAI-1, both of which have negative effects for diabetic blood vessels (26). Activation of the hexosamine pathway may result in many changes both in gene expression and protein function, which together could contribute to the pathogenesis of diabetic complications. It could also affect the synthesis of PGs directly by increasing the availability of UDP sugars, substrates of GAG synthesis.

AGE formation

Advanced Glycation End products (AGEs) are the results of a chain of chemical reactions after an initial glycation reaction, and the formation and accumulation of AGEs will increase in hyperglycaemic conditions. The formation of AGEs damage vascular cells in several ways; by modification of intracellular proteins, including proteins involved in the regulation of gene transcription, by modification of ECM components, interfering with matrix-matrix, matrix-cell and cell-cell interactions, and finally by modification of plasma proteins able to bind and activate RAGE (Receptors for AGE), inducing receptor mediated ROS (reactive oxygen species) production and activation of transcription factor NFκB. This will increase proinflammatory gene expression, including expression of cytokines and growth factors (TNF, IL, TGFβ) (11;18;27) as well as interleukins and adhesion molecules (28). The levels of AGE are increased in blood in persons suffering from DM (27).

The polyol pathway

The first enzyme of the polyol pathway, aldose reductase, normally has the function of reducing toxic aldehydes in the cell to inactive alcohols. When glucose concentration becomes too high aldose reductase will also catalyze the NADPH dependent reduction of glucose into sorbitol, which is further reduced to fructose by sorbitol dehydrogenase. Hyperglycaemic conditions increase the flux through this pathway, consuming NADPH and at the same time decreasing the regeneration of the critical intracellular antioxidant glutathione from glutathione disulfide by NADPH. By reducing the amount of glutathione, the polyol pathway increases susceptibility to intracellular oxidative stress (11;22).

The PKC pathway

DAG and PKC are critical intracellular signalling molecules that can regulate many vascular functions, including permeability, vasodilator release, endothelial activation and growth factor signalling. Hyperglycemia increases DAG (diacylglycerol) content, which activates PKC. This has a number of pathogenic consequences by affecting the expression of eNOS (endothelial nitric oxide synthetase), endothelin-1, VEGF (vascular endothelial growth factor), TGF-β and PAI-1, and by activating NF-κB and NAD(P)H oxidases. Activation of PKC can thus produce vascular damage including increased permeability, NO dysregulation, increased leukocyte adhesion and alterations in blood flow (11;22).

Each of these four pathogenic mechanisms reflects a single unifying process - the overproduction of superoxide by the mitochondrial electron transport chain generated during hyperglycemia. The glycolytic enzyme GAPDH (glyceraldehyde-3 phosphate dehydrogenase) catalyses the reduction of glyceraldehyde-3-phospate into 1,3-diphosphoglycerate. Superoxide overproduction will inhibit GAPDH by activating PARP (poly ADP-ribose polymerase), accumulating upstream glucose-metabolites, increasing the flux trough the mentioned pathways (10;22).

Hyperglycemia is the major determinant of microvascular disease, however, not of *macro*vascular disease. In macrovascular endothelium however, insulin resistance increase free fatty acid flux into the cells, increasing free fatty acid oxidation by the mitochondria. This cause mitochondrial overproduction of ROS just like hyperglycemia does in microvasculature, activating the same damaging pathways. (11;27) Also, sustained high blood sugar will increase the production of AGE causing dysfunctional changes in the endothelium making it less elastic and more permeable. Additionally, increased AGE formation is linked to the oxidation of LDL-particles, making them more atherogenic. Together this will increase the risk of atherosclerosis, thrombosis and heart infarction, making the formation of AGE a contributor to the development of cardiovascular disease in diabetics.

Inflammation

Hyperglycemia contributes to the chronic inflammation seen in endothelial dysfunction. Although inflammation is a protective response, this response is also the basis of chronic diseases such as atherosclerosis (18). The inflammatory response is initiated by the adhesion of circulating monocytes to selectins and integrins on the endothelium (This relationship is also illustrated in figure 2.15, section 2.5). The expression of these adhesion molecules are upregulated during hyperglycemia and inflammation. Monocytes extravase into the target tissue, where they differentiate into macrophages. In the ateroma, macrophages express scavenger receptors to bind modified LDL, and these receptors are also increased in hyperglycemia. Activated macrophages secrete a variety of biologically active products amplifying the inflammatory response, including the cytokines and growth factors, continuing the vicious cycle. Thus, hyperglycemia is associated with increased production of pro-inflammatory cytokines such as TNF-α, IL-1α and growth factors such as TGF-β (18). TNFα has been shown to be an independent risk marker both for cardiovascular disease and DM (29).

Cytokines are soluble mediators of the immune system. The major inflammatory endocrine cytokines TNF and IL-1 are increased by a variety of inflammatory

mediators, including hyperglycemia. Both induce endothelial activation with increased expression of adhesion molecules, secretion of additional cytokines and growth factors, and NO production. Activation of the transcription factor NFκB is crucial in cytokine regulation of gene expression in ECs. NFκB is also activated by TNF-α, IL-1, hyperglycemia, AGEs, Angiotensin II, oxidized lipids and insulin, and regulate the inflammatory response and vascular cell function by regulating genes like cell-adhesion molecules, ILs, PAI-1 and NOS (6), and are thus important in the pathogenesis of vascular disease in DM. TGF-β is an anti-inflammatory and pro-fibrotic growth factor, regulating cellular functions such as cell growth, death / apoptosis and differentiation. It is a potent inducer of ECM protein synthesis, also affecting PG synthesis. There is evidence that TGF-β play a major role in the development of diabetic nephropathy, in part by inducing the thickening of the BM. In contrast, TGF-β has potent anti-inflammatory effects on vascular cells, down-regulating cytokine-induced expression of adhesion-molecules (6).

2.4 Proteoglycans

PGs are diverse and widespread molecules, also found in the endothelium, and are important both in endothelial function and dysfunction. The production and structure of PGs change during hyperglycemia and inflammation, and are thought to influence the progression of diabetic complications (30-33). In order to understand this relationship, it is necessary to study changes in PG expression and structure in relation to hyperglycemia and inflammation.

2.4.1 Structure & Function

PGs are glycoproteins covalently attached to one or more GAG chains. GAGs are long, linear polymers of a repeating disaccharide, of variable length and variable degree of modifications by sulfation, acetylation and epimerization. The disaccharides are composed of an uronic acid and a hexosamine (The uronic acids are either glucuronic acid, GlcA or iduronic acid, IdoA and the hexosamines are

glucosamine, GlcN or galactosamine, GalN). These give rise to the different GAGs heparan sulfate HS/heparin (GlcA/IdoA + GlcNAc), choindroitin sulfate CS (GlcA + GalNAc), dermatan sulfate DS (IdoA+GalNAc), keratin sulfate KS (Gal + GlcNAc) and hyaluronic acid (hyaluronan) (GlcA + GlcNAc), see figure 2.6. Hyaluronic acid is an unsulfated GAG which does not occur as a PG bound to a protein, but rather in free form or in complexes with other ECM components. Heparin is distinguished from HS by a higher degree of sulfation and higher proportion of IdoA. DS is in fact a CS 4 –sulfate GAG where a large percentage of GlcA is epimerized to IdoA. One unique feature of most GAGs is sulfation at different positions, increasing the negative charge and the ability to interact with partner molecules.

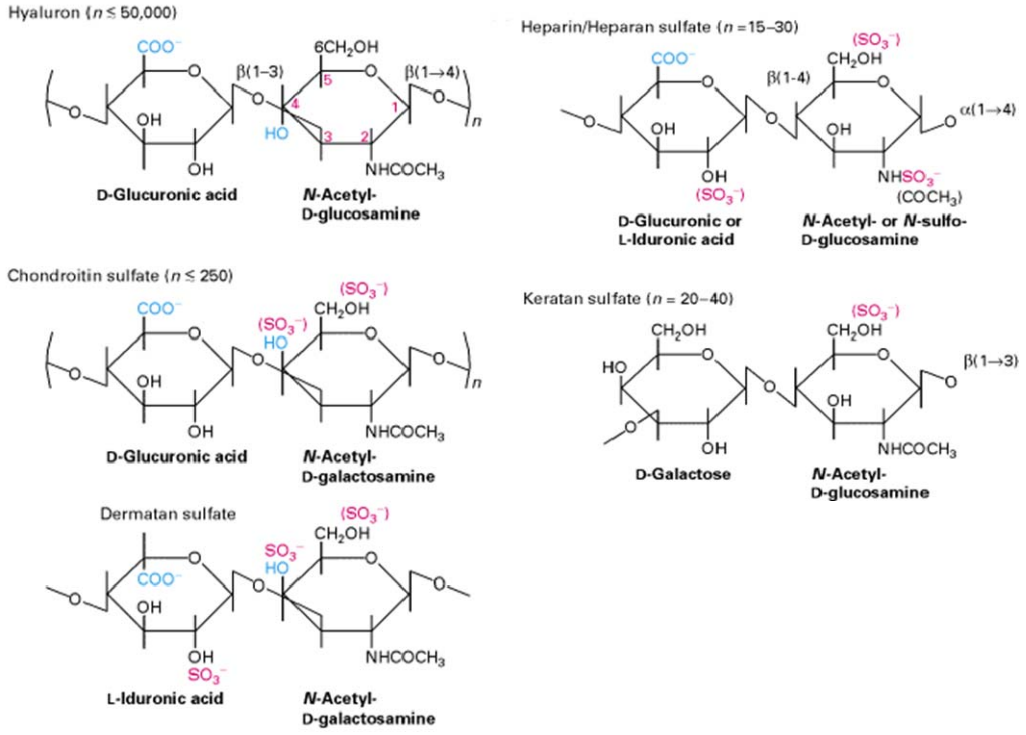

Figure 2.6. Structure of the different GAGs and their hexosamine and uronic acid building blocks*. The different GAGs are composed of repetitions of one of the above disaccharides. Each disaccharide is composed of a hexosamine (glucosamine GlcN or galactosamine GalN) and an uronic acid (glucuronic acid GlcA or Iduronic acid IdoA). These combinations give rise to the different GAGs heparan sulfate / heparin, Choindroitin sulfate), dermatan sulfate, keratin sulfate and hyaluronic acid (hyaluronan) which structures are indicated in this figure. The GAGs can be sulfated in the indicated positions. Taken from: http://courses.cm.utexas.edu*

The different PGs can be classified according to their GAGs, their topographical distribution, their functions or ultimately according to their core protein. They are referred to by trivial names that relate to structural or functional features of the respective macromolecules. The most common PGs are listed in table 2.1 along with some important features.

Table 2.1. Overview of the most common PGs *based on their localization (intracellular, cell surface and matrix) and some of their most common features (type and number of GAGs, size of core protein).*

PGs			PG	GAG sort / no	Protein core kDa
Intracellular			serglycin	HS/CS 8	17
Cell surface	**GPI-coupled**		glypican 1-5	HS/CS 3	57-69
	Integral		syndecan-1	3HS+2CS	30,6
			syndecan-2	2 HS	20,4
			syndecan-3	3HS+ 2CS	44,6
			syndecan-4	2 HS	19,5
			D-syndecan	2 HS	39
			β-glycan	CS/DS 1	36
Matrix	**Aggrecans (hyalectans - PGs interacting with Hyaluronan & lectins)**		versican	CS/DS 10-30	265-370
			aggrecan	KS/CS >100	220
			brevican	CS 1-3	100
			neurocan	CS 3-7	136
	SLRP's (small leucine rich)	**class I**	decorin	CS/DS 1	40
			biglycan	CS/DS? 2	35
		class II	fibromodulin	KS 2-3	41
			lumican	KS 3-4	38
			keratocan	KS 3-5	38
			PRELP	KS 2-3	44
			osteodherin	KS 2-3	42
		classIII	epiphycan	DS/CS 2-3	35
			osteoglycin	KS 2-3	35
	Basement - membrane		perlecan	HS/CS 3	400-467
			agrin	HS 3	250
			bamacan	CS 3	138

As table 2.1 illustrate, the PGs are very diverse. The size of the core protein ranges from 10 to > 500 kDa, and the number of GAG chains attached varies from 1 to >100 (23). Figure 2.7 illustrate the difference in size and structure in different PGs. The GAG chains vary in type and length, are modified in different ways, and in addition, several PGs carry GAGs of more than one type or have additional N-linked or O-linked sugar modifications. Also, ‘part-time’ PGs exists, proteins in which only a

portion has GAG chains attached. PGs are found intracellular (usually in secretory granules), at the cell surface, and as part of the ECM, including the BM and the glycocalyx. Their biological roles are as diverse as their structures, ranging from simple mechanical support in the ECM, to more intricate effects on processes such as cell adhesion, motility and proliferation. Most of the effects depend upon binding of proteins to the GAG chains, and certain functions are expressed by the free GAG chain, but some biological activities also depend upon the presence of the protein core in various ways.

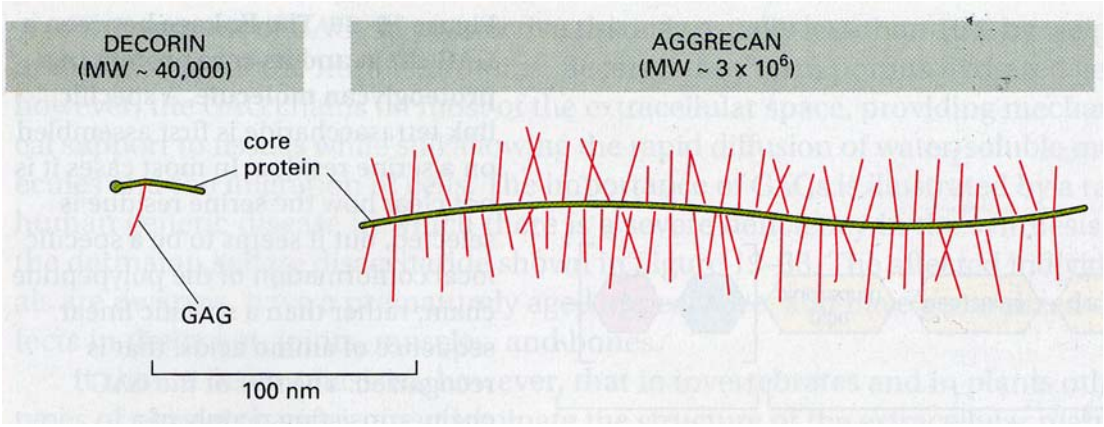

Figure 2.7. Illustration of the difference in size and structure of the different PGs. *Example of a large PG – aggrecan - and a small PG – decorin - found in the ECM. Both the size of the core proteins, and the number and kind of GAGs attached, vary amongst the different PGs, providing them with them distinct functions. Taken from Alberts, B. et al, Molecular biology of the Cell, 3ed (8).*

In the endothelium, PGs are found on the cell surface, in the underlying BMs and in the ECM in association with other matrix proteins such as collagen type IV, laminin, and fibronectin, as well as in the luminal glycocalyx of the vessels.

Matrix PGs

Secreted PGs constitute a major component of the ECM. The ECM is the extracellular macromolecular ground substance of connective tissue, and is generally composed of proteins like collagens, glycoproteins such as fibronectin, and PGs. It has a mechanical role in supporting and maintaining tissue architecture, but can also be described as a dynamic meshwork actively regulating critical cellular functions such as migration, survival, proliferation and differentiation (34). PGs have been

particularly well studied in cartilage in which they constitute over 90 % of the dry weight of the tissue (35). The GAGs tend to adopt highly extended conformations that occupy a huge volume relative to their mass, and they form gels even at very low concentrations. Their high density of negative charges attracts a cloud of cations, such as Na^+, that are osmotically active, causing large amounts of water to be associated with the matrix. This creates a swelling pressure that enables the matrix to withstand compressive forces and enable joints and tissue to absorb large pressure changes (8). The most common cartilage PG is aggrecan, which binds to HA (hyaluronic acid) and a link protein. Although aggrecan is "the cartilage PG", it is also found in other tissues. In the same way other PGs such as decorin, biglycan and perlecan are also found in cartilage (36). This illustrates the fact that the intrinsic properties of a tissue is not provided by a unique PG, but rather by the unique blend of several PGs and their organization in the ECM with other components.

Given the structural diversity of PG molecules, it would be surprising if their function in the ECM were limited to acting as a scaffold and a shock absorber in matrix. The GAGs can form gels of varying pore size and charge, and thus serve as selective sieves to regulate the traffic of molecules and cells according to size or charge. There is evidence that HSPGs such as perlecan has this role in the BM of the kidney glomerulus, which filters molecules passing into the urine from the bloodstream (37). PGs are thought to play a major part in intracellular signalling and the control of growth and differentiation. Matrix PGs can bind and regulate various secreted molecules, such as growth factors, cytokines, proteases and protease inhibitors. Subendothelial matrix-PGs can bind the LDL constituent apoB and thus be involved in the lesion initiation of atherosclerosis (38). Binding to growth factors indicate a role in regulating growth and differentiation. Binding of FGF (fibroblast growth factor) to HSPGs is required for its activation (39), whereas binding of TGF-β to the core protein of several matrix proteins such as decorin inhibits the activity of this growth factor (40). PGs also bind to and regulate many inflammatory mediators *in vitro*, suggesting that they serve an important role in modulating inflammatory responses *in vivo* (41). The ability of matrix PGs to bind and then activate or restrain

different signalling molecules under different conditions, can affect tissue maturation, angiogenesis, invasion and metastasis.

The matrix PGs comprises the largest class of PGs, and is usually divided in three subgroups according to structure and function; the aggrecans/hyalectans, the basement membrane PGs and the small leucine rich PGs (SLRP's) (42).

Aggrecan is one of the **hyalectans**; the matrix PGs interacting with hyaluronan and lectins. Many aggrecans thus binds to the same hyaluronan chain in matrix, forming enormous aggregates, as illustrated in figure 2.8. This PG has a relatively large core protein, and over 100 CS or KS GAG-chains. Other hyalectans are versican, brevican and neurocan.

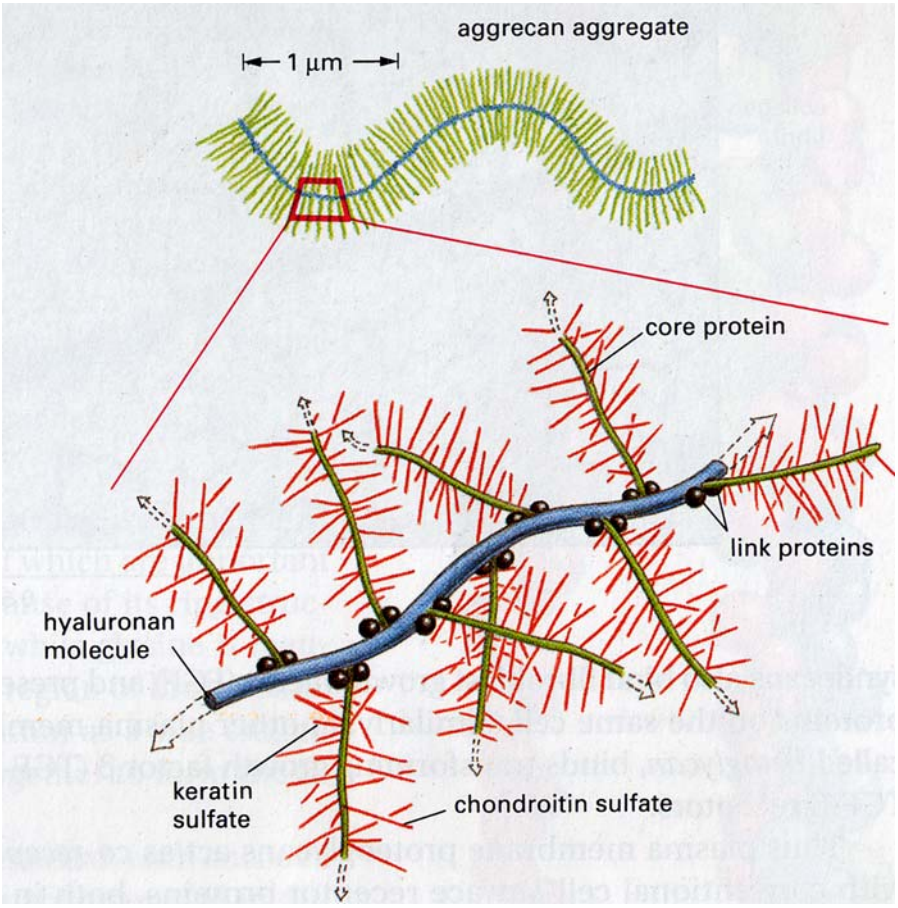

Figure 2.8. Schematic drawing of PG aggregate*. The giant aggrecan aggregate, consisting of about 100 aggrecan monomers noncovalently bound to a single hyaluronic acid chain trough two link proteins that binds both the core protein of the PG and the hyaluronan chain. Taken from Alberts, B. et al, Molecular biology of the Cell, 3ed (8).*

Basement membranes are flexible thin mats of specialized ECM that underlie the endothelium, separating it from the underlying connective tissue (figure 2.2). It serves structural and filtering roles as well as determining cell polarity, and consists of a network of molecules composed primarily of type IV collagen, laminins and HSPG. Three PGs are characteristically present in vascular and epithelial basement membranes: perlecan, agrin and bamacan (42). The first two primarily carries HS side chains, whereas the latter carries primarily CS, and the chimeric structural design of these PGs suggests that they may be involved in numerous biological processes (42). Perlecan is embedded in the BM of most endothelial cells, and derives its name from its appearance as a string of pearls. The molecular structure is illustrated in figure 2.9. The protein core of perlecan is ~ 470 kDa, together with numerous N-linked and O-linked oligosaccharides and 3 HS chains it can reach a molecular weight over 800 kDa (43). The various modules of perlecan and its HS chains can participate in a large number of molecular interactions, binding to growth factors such as FGF2, VEGF and PDGF (platelet-derived growth factor), and other protein constituents of the BM or cell surfaces (43). Perlecan is also found to carry CS chains.

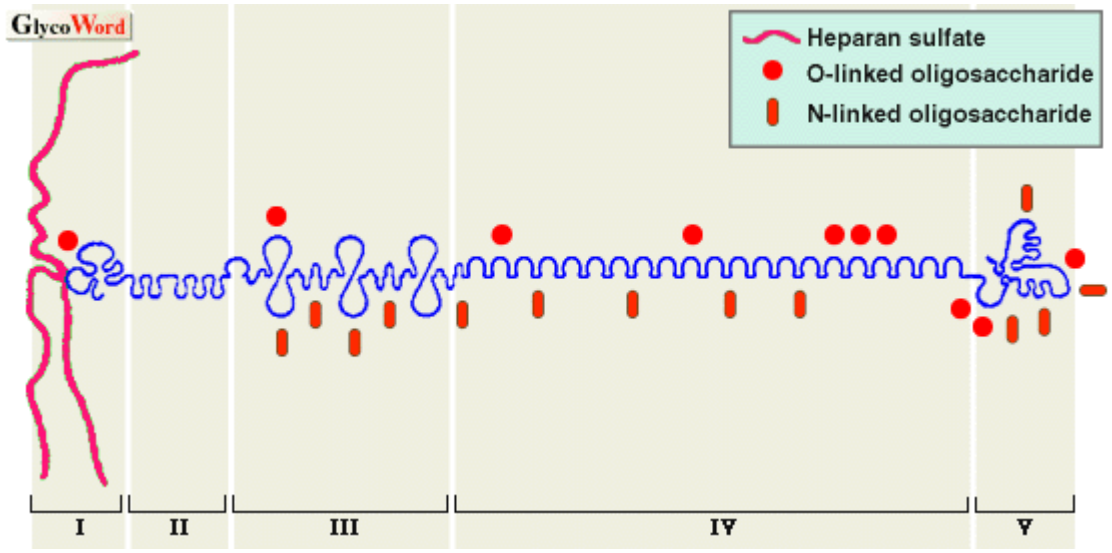

Figure 2.9. Schematic molecular structure of perlecan. *The large matrix- PG perlecan 450 kDa core protein is composed of five domains with distinct properties for interactions with other molecules. Three HS, or possibly CS GAG-chains can be attached to the amino-terminal end. Taken from Segev, A et al. (44).*

The family of **SLRP's** are all characterized by a central domain of leucine-rich repeats flanked by small cystein clusters, and further divided into three classes based on their protein and genomic organization (see table 1). These are non-aggregating and small KS/DS containing PGs. Decorin is a member of this group, with a protein core of ~ 40 kDa and a single CS/DS chains attached. Decorin contribute to the proper assembly of connective tissue by interacting with other matrix proteins. Decorin interacts with fibrillar collagens, inhibiting fibril formation, as well as fibronectin, thrombospondin, the complement component C1q, EGFR (epidermal growth factor receptor) and TGF-β. Through the latter interaction decorin is believed to function in the control of cell cycle (43;45)(http://www.cmb.lu.se/ctb/).

Figure 2.10. Schematic drawing of the molecular organization of small leucine-rich PG decorin. *This illustration does not represent the actual sizes of the core proteins or actual location of glycosylation sites. Decorin contains one CS or DS chain on the ~ 40 kDa core protein. Taken from http://www.glycoforum.gr.jp/science/word/proteoglycan/PGA04E.html*

Cell surface PGs

All cellular processes that involve molecular interactions at the cell-surface, such as cell-matrix, cell-cell and ligand-receptor interactions, are likely to involve PGs. Two major families of cell surface PGs have been identified; the syndecans and the glypicans. These bind a multitude of growth factors and ECM molecules, and have been implicated in several signal transduction pathways that regulate cell proliferation and cell shape. They are found on the surface of many cells serving as receptors for collagen, fibronectin and other matrix components. Syndecan also acts as a co-receptor by binding FGF and presenting it to the FGF receptor proteins on the same cell (46). Similarly, β-glycan binds TGF-β and presents it to TGF-β receptors.

HSPG binds the pro-inflammatory cytokines TNFα, IL-2, IL-6 and IFNγ and syndecan-1 is shown to be able to reduce inflammatory response in toxic shock (41).

The syndecans are a family of type I transmembrane proteins with an intracellular cytoplasmatic domain, while glypicans are attached to discrete cell membrane regions by a GPI lipid anchor. Syndecans carry HS chains near the tips of their extracellular domains and sometimes also have CS chains attached to the extracellular domains near the cell surface. The ectodomain region contains conserved sites for GAG attachment, cell interaction, and oligomerization. Numerous ligands are bound via their HS chains, and the response to this binding is flavoured by the identity of the core protein that bears the HS chains. Each of the syndecan core proteins has a short cytoplasmic domain that binds cytosolic regulatory factors. Additionally, all syndecans can be shed from the cell surface by proteolytic cleavage at a conserved site in the ectodomain near the cell membrane. This shedding is highly regulated and can be accelerated by various biological effectors, thereby making it an extremely important process in the regulation of syndecan function. The process of ectodomain shedding reduces the syndecan at the cell surface, a rapid mechanism to inactivate receptor-ligand interaction and signalling. Shedding also converts the cell surface HSPG into soluble effectors that may compete for the same ligand or may function in a remote location (47).

PGs are generally considered the most important backbone molecules of the glycocalyx, which has been shown to have vasculoprotective effects (19). The glycocalyx is situated at the luminal side of all blood vessels and is a negatively charged mesh of PGs, membranous glycoproteins, GAGs and associated plasma proteins. The volume of this dynamic layer depends on the balance between biosynthesis and the enzymatic or shear-dependent shedding of its components (figure 2.11). The endothelial glycocalyx is an important determinant of vascular permeability, both by size/steric and electrostatic hindrance. It can function as a mechanotransducer detecting and amplifying flow-induced shear-forces. The PGs in the glycocalyx contribute greatly to its functional importance by the GAG chain

variety arising from epimerization, elongation, and sulfation, able to bind a variety of plasma derived proteins. This could be receptors and their ligands, enzymes, growth factors, cytokines etc. In DM hyperglycemia is associated with reduction of glycocalyx dimensions, which is suspected to contribute to endothelial dysfunction, and the endothelial glycocalyx is also suggested to be involved in the initiation and progression of atherosclerosis (19).

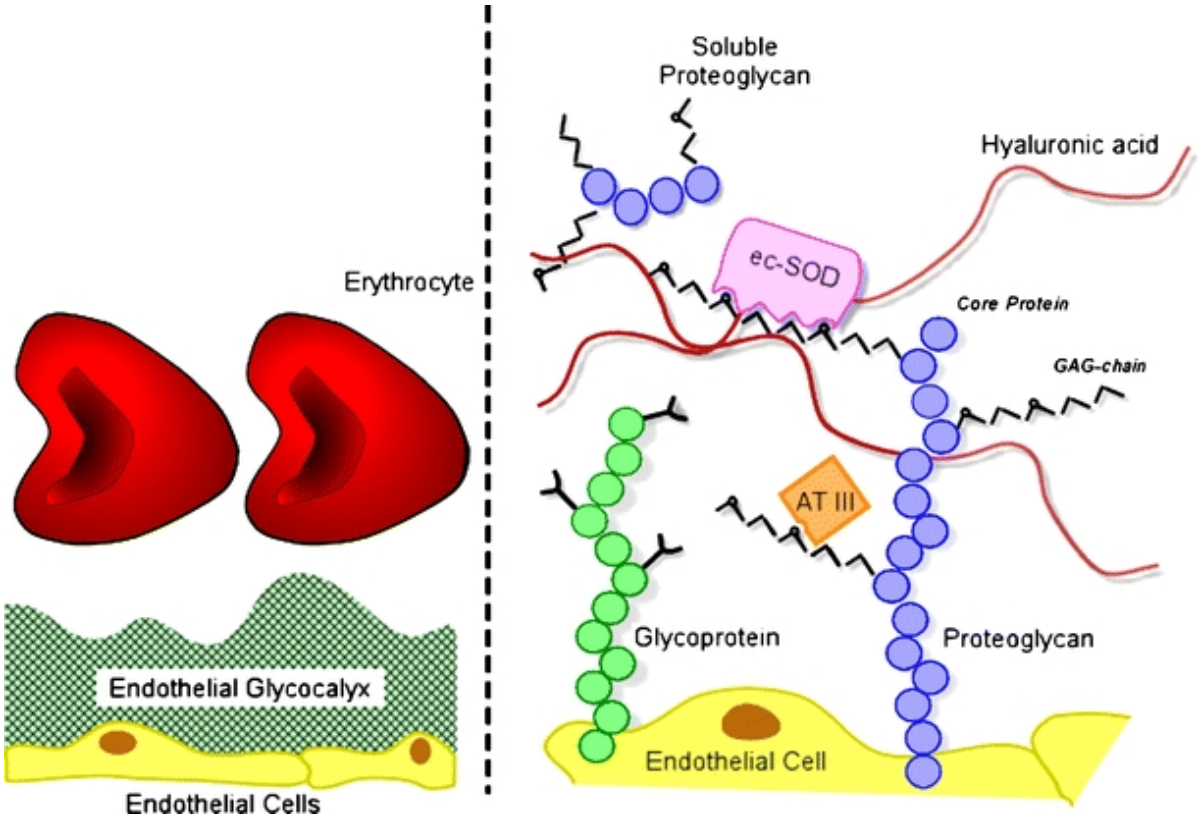

Figure 2.11. Schematic representation of the endothelial glycocalyx, showing its main components. Left*: The endothelial glycocalyx can be observed in vivo as a red blood cell exclusion zone, located on the luminal side of the vascular endothelium. It consists of membrane-bound and soluble molecules.* Right*: Components of the endothelial glycocalyx. Bound to the endothelial membrane are PGs, with long unbranched GAG-chains and glycoproteins, with short branched carbohydrate side-chains. Incorporated in and on top of this grid are plasma and endothelium-derived soluble components, including hyaluronic acid and other soluble PGs and various proteins, such as extracellular superoxide dismutase (*ec-SOD*) and antithrombin III (*AT III*). Together, these components form the endothelial glycocalyx that functions as a barrier between blood plasma and the endothelium and exerts various roles in plasma and vessel wall homeostasis. Note that this figure is not drawn to scale; its purpose is to illustrate glycocalyx composition. Figure and legend taken from Reitsma, S. et al, Pflugers Arch 2007(48).*

Intracellular PGs

Matrix and cell surface PGs are produced by cells that are engaged in ECM or tissue construction. However, several other cells do produce PGs, and particularly cells of the immune system and metastasing tumour cells will produce intracellular PGs. Intracellular PGs can include endocytosed PGs like glypican-1, nuclear PGs/GAGs and PGs in secretory and storage granules (49). Intracellular PGs interact with proteins in different ways; some of which are concentrating and protecting proteins organized into granules, assisting transportation of granule-contents to their destination, and presenting or releasing proteins (49;50). Serglycin is probably the dominating intracellular PG, found in granules of haematopoietic cells, ECs and SMCs. Human serglycin is a 17-30 kDa core protein which can potentially carry 8 HS/CS GAG chains. While the serglycin core protein is conserved, the identity, number and sulfation pattern of GAGs may differ between cell types, providing a range of different functions (32). Serglycin is stored in granules in mast cells, but is a secretory product of macrophages and endothelial cells, which increase during inflammation. It execute important functions related to the formation of storage granules and the retention of inflammatory mediators inside granules and vesicles (32;51), besides being important in the secretory processes of human monocytes (52). Secreted serglycin can regulate the activity or transport of partner molecules. Taken together, this implies a role for serglycin in the inflammatory process and in relation to DM.

Figure 2.12 illustrates the diverse functions of HSPG, both as intracellular, cell-surface and extracellular PGs.

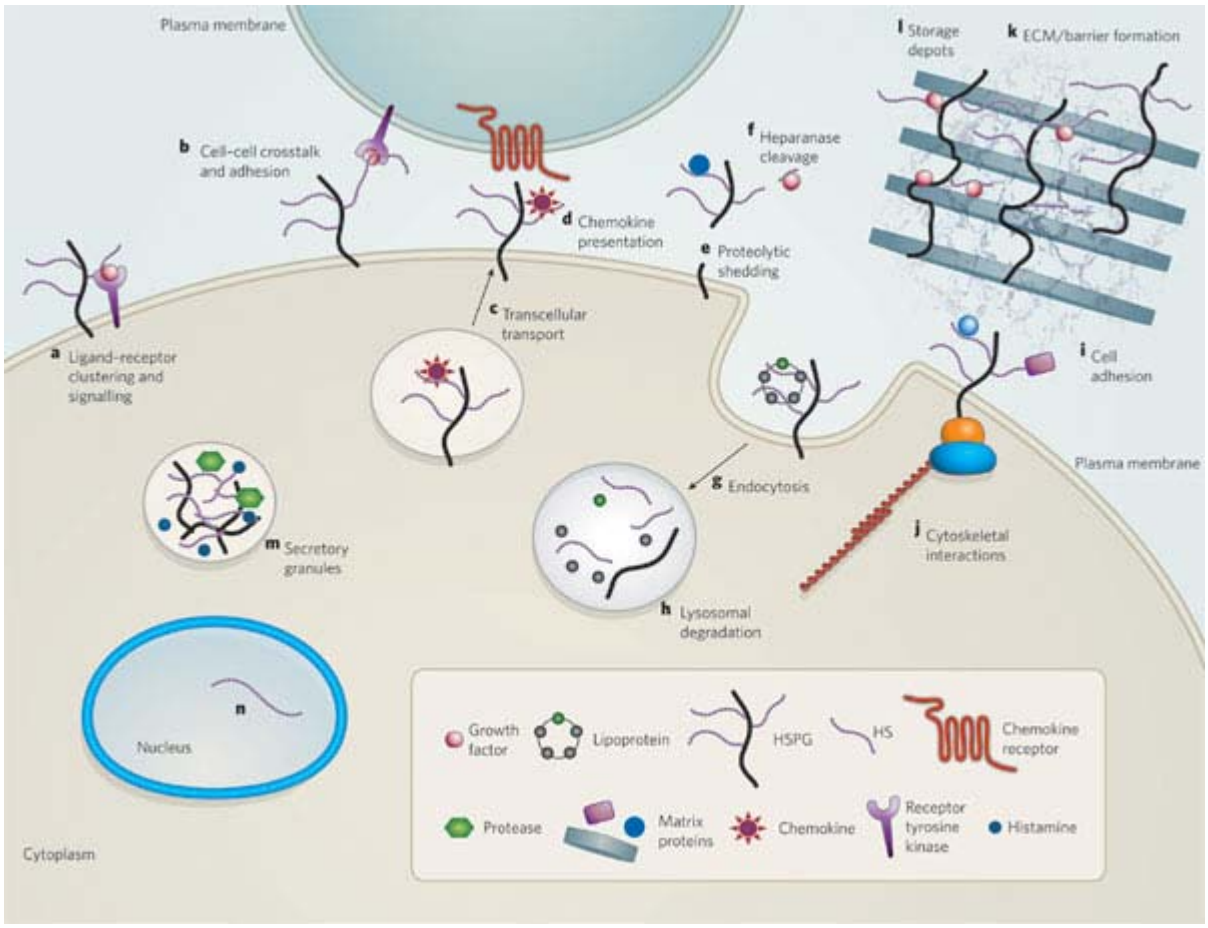

Figure 2.12. Overview of the functions of HSPGs*. HSPGs function as co-receptors for growth factors and their receptor tyrosine kinases, which are present either on the same cell (**a**) or on adjacent cells (**b**). They transport chemokines across cells (**c**) and present them at the cell surface (**d**). Proteolytic processing leads to the shedding of syndecans and glypicans from the cell surface (**e**), and heparanase cleaves the HS chains (**f**), liberating bound ligands (such as growth factors). Cell-surface HSPGs are actively taken up by endocytosis (**g**) and can recycle back to the surface or be degraded in lysosomes (**h**). HSPGs also facilitate cell adhesion to the extracellular matrix (**i**) and form bridges to the cytoskeleton (**j**). Secreted HSPGs are involved in the formation of organized extracellular matrices that form physiological barriers (**k**) and sequester growth factors and morphogens for later release (**l**). Serglycin carrying highly sulfated heparin chains is packaged into secretory granules of haematopoetic cells (**m**). Finally, some experiments suggest that HS chains exist in the nucleus (**n**), although their function in this location is unknown. Text and figure taken from Bishop, J.R., Nature 2007(50).*

2.4.2 Synthesis

PGs are produced in the ER and Golgi apparatus. After the ribosomal translation of the core protein, except for in KS, GAG synthesis is initiated by sequential addition of four monosaccharides donated by UDP-sugars; Xyl, Gal and GlcA into a

tetrasaccharide linker, as illustrated in figure 2.13. A xylotransferase will transfer xylose (xyl) from UDP-xyl to specific serine residues in the core protein. The xyl-enriched core protein is transported to the *cis*-Golgi where galactocyltransferases types I and II will add two galactoses (Gal) to the xyl, after which glucuronosyltransferase type I adds glucuronic acid (GlcA) completing the GAG-chain primary linker (8;53).

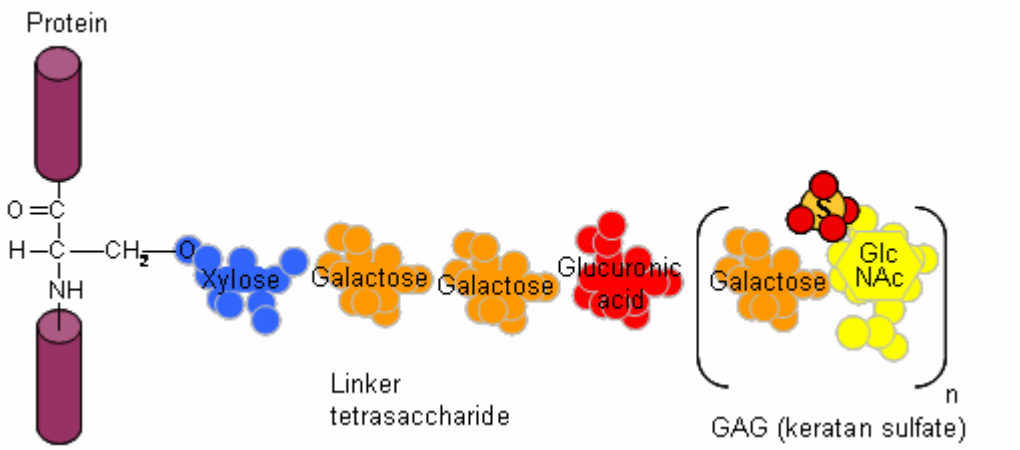

Figure 2.13.The tetrasaccharide primary linker of GAG-chains. *PG synthesis is initiated in Golgi by the transfer of a xylose from UDP-xyl to the serine residue in the core protein. Addition of two galactose molecules and a molecule of glucuronic acid completes the primary linker. The addition of the next saccharide determines whether the GAG chain will be CS/DS (addition of GalNAc) or HS/heparin (addition of GlcNAc). From this point onward the sugar chain is extended by addition of two alternating monosaccharides; GlcA and GlcNAc in HS/heparin, or GlcA and GalNAc in CS/DS. Shown here is KS. Taken from http://www.steve.gb.com/science/extracellular_matrix.html*

After completion of the linker saccharide, the addition of the fifth saccharide determines whether the GAG chain becomes CS/DS or HS/heparin. In the case of HS/heparin GlcNAc is added, in the case of CS/DS GalNAc is added (49;53). Figure 2.12 illustrate the different steps in the synthesis of these PGs. In KS on the other hand, the GAGs are initiated as N-or O-linked oligosaccharides and extended by alternating addition of GlcNAc and Gal. Whether GalNAc or GlcNAc is added to the primary linker could be determined by several factors; such as the amino acid sequence flanking the serine residue on the core protein, and the access of UDP-sugars and presence of GAG-synthesizing enzymes in the Golgi. Modifications of the linker region including phosphorylation, sulfation and epimerisation, has been

demonstrated and could be of importance; sulfation of the linker region has been observed only in DS/CS, not in heparin/HS (53).

Following chain polymerization the growing GAG-chain will undergo modifications including *N*-sulfation, epimerization and *O*-sulfation (31;49;53). These chain modifications take place in both the *cis*- and *trans*- Golgi, determining the final type and functionality of the PG. Epimerization of GlcA into IdoA change CS into DS, and the sulfation pattern distinguish HS from the more heavily sulfated heparin. Elongation and modification of GAG chains is catalyzed by different sets of enzymes in different sub domains of the Golgi apparatus. The chain elongation is probably dependent on these modifications; in particular will sulfation determine when chain elongation is terminated (53). There is also regional variability to the epimerization and sulfation within each GAG chain, giving rise to motifs required for specific interaction with growth factors, cytokines, matrix components, enzymes and other proteins. In contrast to HS/heparin and CS/DS, hyaluronan is assembled at the cell membrane, and is not modified afterwards. As a consequence it has no sulfate groups or modifications.

After synthesis and modifications PGs are transported from the Golgi to their destinations: the ECM, the cell surface or intracellular organelles. In endothelial and other polarized cells there is also an apical / basolateral sorting of the PGs.

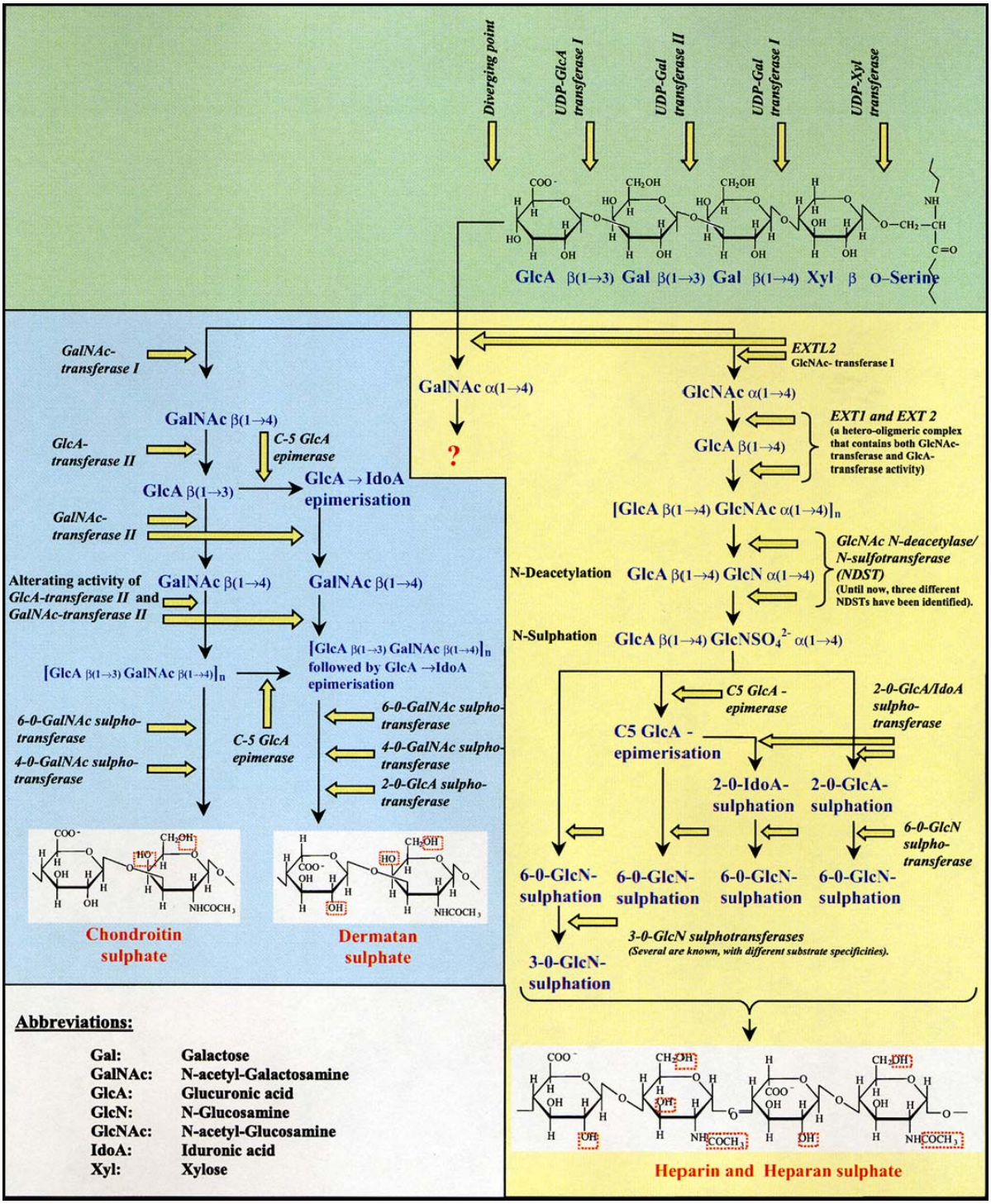

Figure 2.14.The different steps in the synthesis of CS, DS, HS and heparin glycosaminoglycan chains. *Taken from Prydz, K. et.al, J.Cell Sci. 2000 (53).*

2.5 PGs in hyperglycemia and inflammation

The synthesis and structure of PGs are shown to change during hyperglycemia, and are thought to influence the progression of diabetic complications. In order to understand this relationship, it is necessary to study changes in PG expression and structure in relation to diabetic conditions such as hyperglycemia and inflammation. Changes in PG expression in EC may affect important functions such as cytokine signalling, lipoprotein turnover and chemokine regulation, which are all relevant in DM. Hyperglycemia has been shown to decrease PG expression in cultured human endothelial cells (54).

DM is regarded as an inflammatory disease, and the endothelium is able to respond to inflammatory cytokines trough the binding with matrix and cell-surface PGs. Each cytokine bind to a specific cell-surface receptor, and subsequent cascades of intracellular signalling then alter cell functions. HSPG are known to bind several proinflammatory cytokines, amongst them TNF-α (41). The release of TNF-α and IL-1 is believed to increase vascular permeability and contribute to the atherosclerotic process. Elevated levels of IL-1α and TNF-α has been measured in persons with DM (18;29) Inflammatory cytokines (TNF-α) are increased in hyperglycemia in humans (55).

The uptake of lipoproteins is also an important feature of inflammation and the development of atherosclerosis. HSPG is important for uptake of lipoproteins, both in normal and in pathological lipoprotein metabolism. HS will bind LPL and lipoproteins in a complex on the cell surface, making HS important in the development of atherosclerosis (31;56).

Entry of leukocytes into tissues is a key feature of inflammation, and EC HSPG expression is required for several stages of this entry process. Endothelial HSPG is important in L-selectin binding to neutrophils, in chemokine presentation and in chemokine transportation across the endothelium. These roles of HSPG in leukocyte entry are illustrated in figure 2.15. Thus, HSPG is important in the inflammatory

process of DM (57). Different PGs are, however, observed to have contradictory effects, both anti – and pro- atherogenic. Although facilitating lipoprotein uptake and monocyte adhesion to the endothelium, increased HSPG in EC have also been associated with decreased monocyte binding to subendothelial matrix (24).

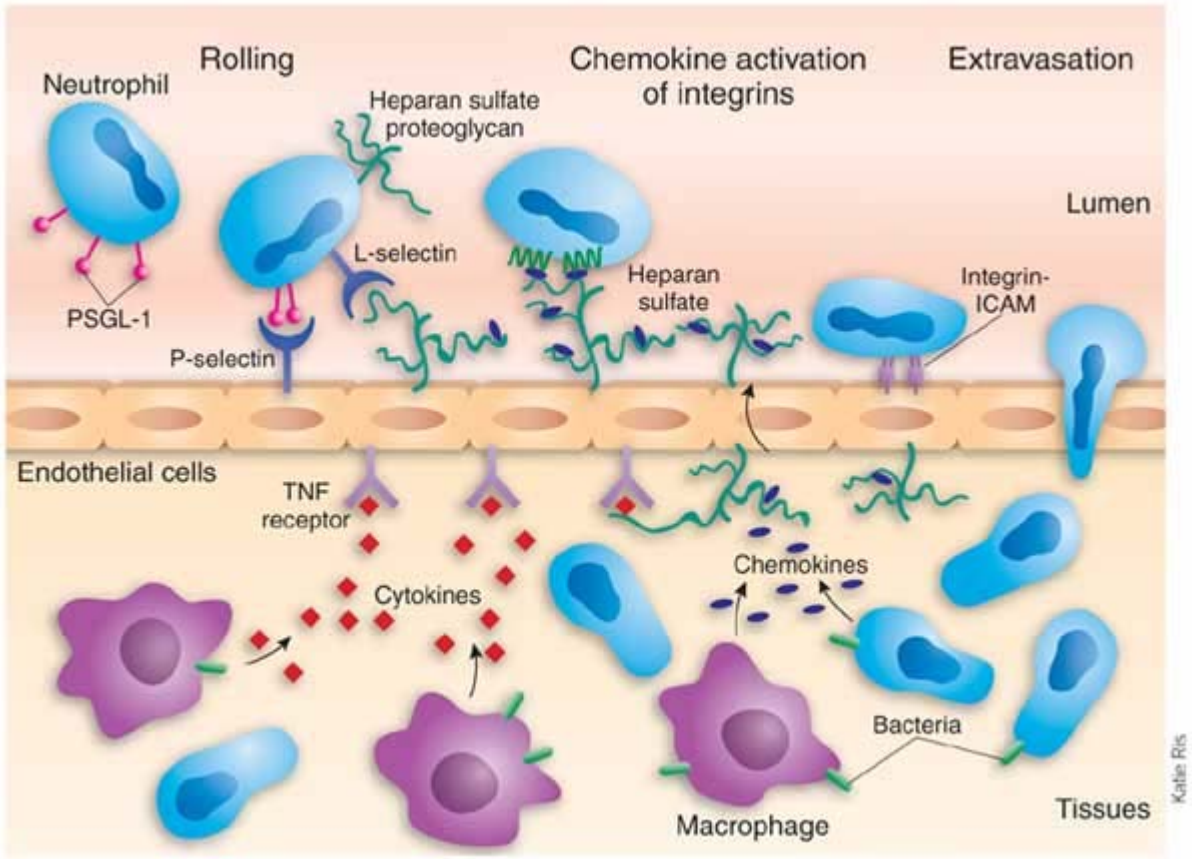

Figure 2.15*. *Role of HS in leukocyte entry into sites of inflammation. *In response to inflammatory stimuli from cytokines, ECs and resident macrophages in the vascular wall will produce both chemokines that attracts leukocytes into tissue, and cytokines that trigger the display of selectin luminally on ECs. Endothelial HSPGs act as coreseptors for chemokines. PSGL, P-selectin glycoprotein ligand-1; ICAM, intracellular adhesion molecule. Taken from Parish,C.R., Nat Immunol 2005 (57).*

3. Aims

DM is associated with several micro- and macrovascular complications, and in the course of prevention, it is important to obtain a better understanding of the underlying mechanisms.

The endothelium is the prime organ to be exposed to the hyperglycemia of DM, and hyperglycemia is identified as a primary causal factor in the development of DM complications, and might be responsible for impairment of significant functions of the endothelium (12;13). PGs are important components of the vascular tissue, influencing arterial properties such as viscoelasticity, permeability, lipid metabolism, cell adhesion, proliferation, hemostasis and thrombosis (23;31;35;42;43).

Endothelial dysfunction is a key component in the pathogenesis of atherosclerosis, and hyperglycemia contributes to the chronic inflammation seen in endothelial dysfunction. PG structure and composition are altered in atherosclerotic lesions, most evident in DM. Increased levels of IL-1α and TNF-α is observed in DM. DM associated quantitative and qualitative alterations of PGs are being increasingly reported, and are proposed to play an important role in the pathogenesis of diabetic complications (54;58;59). Studies have shown that exposing HUVEC (Human umbilical cord vein endothelial cells) to IL-1α and TNF-α increase PG synthesis (60) and hyperglycemia is also shown to alter the endothelial PG expression (54).

These studies were initiated to investigate the changes in endothelial PG expression during diabetic conditions. ECs were obtained from umbilical cords and cultured in vitro to study the response to hyperglycemia and inflammatory conditions. A hyperglycemic environment was mimicked both by exposing the cells to high glucose or to the glucose metabolite GlcN. Inflammatory conditions were created by exposure to each of the pro-inflammatory cytokines IL-1α and TNF-α.

Quantitative and qualitative effects on cell proliferation, total *de novo* PG synthesis and the individual PGs perlecan and decorin were investigated.

Specific aims

- To study the biological effects of GlcN on primary human endothelial cells
  - Effect on proliferation
  - Effect on total *de novo* PG biosynthesis and secretion
- To study the biological effects of hyperglycemia, using high glucose or GlcN on primary human endothelial cells
  - Effects on proliferation
  - Effects on total *de novo* biosynthesis and secretion
  - Effects on PG composition
- To study the biological effects of inflammation, using IL-1α and TNF-α on primary human endothelial cells
  - Effects on proliferation
  - Effects on total *de novo* biosynthesis and secretion
  - Effect on PG composition

4. Methods

4.1 Human Umbilical Vein Endothelial Cells (HUVEC)

HUVEC are primary ECs isolated from the vein of human umbilical cord.

Ethical approval for the use of human ECs from the Human Research Ethical Committee was obtained by our collaborators at Rikshospitalet. The use of umbilical cords was approved in advance by the mothers (61).

4.1.1 Isolation of HUVEC from umbilical cord

HUVEC were enzymatically isolated from infant umbilical cords of normal pregnancies using collagenase. This was done under sterile conditions and the cells were established as primary cell cultures. This was first done by E. A. Jaffe et al (62). The location of the vein of the umbilical cord is illustrated by figure 4.1.

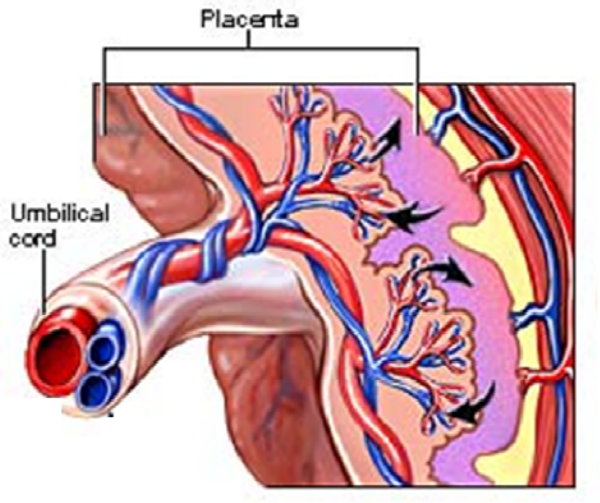

Figure 4.1. Illustration of the placenta and the umbilical cord. *HUVEC were obtained from the vein of the umbilical cord. The umbilical cord vein is shown in red in this figure, transporting oxygen rich blood from the mother to the foetus. Modified from http://dralaamosbah.blogspot.com/*

Procedure:

1. Umbilical cords were obtained from the local Obstetric and Gynaecology division at Rikshospitalet, Oslo, placed in a sterile container filled with cord

buffer and kept at 4°C. The cord was stored for a maximum of 3 days before processed

2. Injured parts were removed. Metal cannulas were placed in each end of the vein and the vein was then rinsed in PBS (phosphate buffered saline)

3. 10 ml 0.2 % collagenase was infused into the umbilical vein and incubated in 37°C for 10 min.

4. The collagenase solution containing the ECs was flushed from the cord by perfusion PBS.

5. The cells were sedimented at 1500 rpm for 10 min, resuspended in 5 ml fresh culture medium and then incubated at 37°C and 0.5 % CO_2 in a 25cm^2 cell culture flask.

Equipment and solutions:

Equipment	***Additional equipment needed***	***Solutions***
2 metal cannulas	2 single use syringes 50 mL	1XPBS, 50 mL, autoclaved
3 compresses	1 single use syringe 15 mL	Cord buffer
2 small pieces of aluminium foil	1 50 mL centrifuge tube	0.2% collagenase, 10 ml
4 plastic straps	1 cell flask 25 cm^2	Medium
4 plastic tubes (2-3 cm)	Sterile surgical glows	
3 glass vials, 2x200 mL and 1x100 mL	Water bath, 37^oC	
A sterile tray to work on	1 sterile surgical blade	

All equipment was autoclaved

4.1.2 Culturing HUVEC

HUVECs were grown at 37°C and 0.5% CO_2 in plastic bottles or wells of different sizes, in complete endothelial basal medium of 7 % FCS (foetal calf serum), and fed twice a week.

Solutions:

Complete MCDB medium

Components	Volume	Final concentration
MCDB-131 medium	Powder for 500 ml	
$NaHCO_3$	0.59 g	
mQ-H_2O	500 mL	
FGF 10µg/mL	50 µL	1 ng/mL
Hydrocortisone 10 mg/ mL	50 µL	1 µg/mL
EGF 10 µg/mL	500 µL	10 ng/mL
Gentamicine 50 mg/mL	500 µL	50 µg/mL
Fungisone 250 µg/mL	500 µL	250 ng/mL
FCS (heat inactivated)	37.5 mL	7%

MCDB-131 medium powder and $NaHCO_3$ were dissolved in the water, and the pH was adjusted to 7.3 adding 1M HCl or NaOH while stirring. This solution was sterilized by filtration and aseptically dispensed into a sterile container before additional sterile ingredients was aseptically added.

HUVECs were split at a 1:3 ratio when 100% confluent, usually once or twice a week. This was done by adding a solution of trypsin and EDTA, detaching the cells from the plastic and each other. Trypsin is a protease braking down proteins on the cell surface needed for adhesion, thereby releasing the cells from the plastic. The chelating agent EDTA binds to calcium and prevents joining of cadherins between cells. Cadherins are calcium dependent transmembrane proteins important for cell-cell adhesion, thus EDTA prevents clumping of cells.

Procedure:

1. Trypsin/EDTA solution and complete medium was heated to 37ºC in water bath.

2. The culturing medium was collected and the cells were washed in trypsin solution in order to remove FCS remnants.

3. Cells were incubated in trypsin / EDTA until detached from the plastic and each other. When observed in microscope; the cells will get a round shape.

4. The trypsin was inactivated by adding equal volumes of medium containing 7% FCS.

5. The cells were pelleted at 1200 rpm for 3 minutes and re-suspended in a desired volume of complete medium, before added to cell culture flasks or wells.

6. The cells were incubated at 37°C and 0.5% CO_2.

4.1.3 Freezing and thawing of cells

After isolation the cells can be frozen and stored in liquid nitrogen. This was performed in the presence of DMSO (dimethyl sulfoxide) to prevent crystal formation. The cells were trypsinized, pelleted and resuspended in *freezing-medium I*. An equal volume of *freezing-medium II* was added drop by drop while stirring carefully. The cell suspension was transferred to cool cryovials and put in liquid nitrogen for long-term storage.

When needed, the frozen cells could be removed from the nitrogen tank and thawed rapidly in a water bath of 37^{o}C. The thawed cells were carefully mixed with 5 ml MCDB-medium and pelleted at 1200 rpm for 3 min to remove the DMSO. The pellet was resuspended in the desired volume of culture medium and incubated as previously described.

Solutions:

Freezing medium I

Components	Volume	Final concentration
MCDB-medium	2 ml	50%
FCS (heat inactivated)	2 ml	50%

Freezing medium II

Components	Volume	Final concentration
MCDB-medium	4 ml	80%
DMSO	1 ml	20%

4.2 General Experimental Outline

Generally, the cells were grown in 12 wells culture plates for counting, 6 well plates or small cell culture flasks for sulfate-labelling and finally cell culture flasks of different sizes for Western analysis. The cells were cultured until confluent in MCDB-medium with 5.0 mM glucose and 7% FCS

The cells were exposed to either high glucose (25.0 mM) (54), GlcN (0, 0.1, 1.0, 2.0, 5.0 or10.0 mM), IL-1α (2 ng / ml) or TNF-α (7 ng / ml)(60). Low glucose (5.0 mM) was used as control in all experiments.

Cell exposures were performed for the indicated time, usually 24 hours. Medium was changed to sulfate free RPMI 1640 medium containing 5.0 mM glucose and 2 % FCS for all radiolabelling experiments. When exposing to high glucose, glucose was added to a total of 25 mM. In experiments not including radiolabelling (i.e Western

blotting), MCDB medium of 2 % FCS and 5.0 mM glucose was used. Also here, when exposing to high glucose, glucose was added to a total of 25 mM.

Regarding the experimental outline when collecting data such as cell number, protein contents or cpm (counts per minute); each exposure was performed in parallels and from each of these, two samples were taken. Thus, these data are based on duplicates of parallels. Each experiment was usually performed on cells from umbilical cords from at least three different individuals.

4.3 Cell count

In order to determine differences in cell growth and viability of the different culturing conditions, the cells were stained and counted visually using a hemacytometer (Bürker chamber).

Trypan blue is a stain commonly used in estimating the proportion of viable cells in a population. The negatively charged chromophore will react only with damaged cell membranes, dying only dead cells. In this way the staining facilitates the visualization of the amount of dead and live cells.

Procedure:

1. The cells were trypsinized by standard techniques (section 4.1.2) and MCDB-medium containing 7% serum was added to inactivate the trypsin. The cells were dispersed thoroughly by vigorously pipetting the suspension. Equal amounts of cell suspension and trypan blue solution (f ex 50 µl of each) was mixed and allowed to rest between 5 and 15 minutes.

2. The cover slip was fastened and a small amount of cell solution was transferred to the edges; with the help of capillary forces both chambers were filled.

3. The hemacytometer was placed on a microscope, and in each of the two chambers the number of dead and alive cells in 16 small squares was counted twice.

16 squares contain 0.1 µl solution. The original number of cells can thus be calculated taking all dilutions into account: Cells/ml = (average count in 16 squares) x (dilution factor) x 10^4 [chamber conversion factor]. Total cell number = (cells/ml) x original or pre-dilution volume.

Example: (20 cells) x (2) x (10^4) = 0.4 x 10^6 cells/ml. This is the contents of cells solubilised in trypsin, typically 3 ml in a small cell culturing flask. Then, the total cell number is: 0.4 x 10^6 cells/ml x 3 ml = 1.2 million cells.

4.4 Labelling with ^{35}S-sulfate

The GAG-chains of PGs are highly sulfated and ^{35}S-sulfate added to the medium will be taken up by the cells and incorporated into newly synthesized PGs. Supplying the cells with radioactively labelled sulfate will thus enable us to detect and study the *de novo* synthesis of PGs, without any interference of PGs already present in the cells, medium, serum etc. Other molecules containing sulfate will also be labelled, but after purification by G-50 fine gel chromatography, PGs have been shown to comprise the major part of the labelled macromolecules (63). Thus, the amount of ^{35}S-sulfate incorporated into macromolecules is used as a measurement of the amount of PG synthesized.

The cells were grown in MCDB-medium with 7% FCS and 5.0 mM glucose in cell-culture flasks or wells, until confluent. Because both medium and FCS contained sulfate, which will compete with the ^{35}S-sulfate for uptake by cells, the medium was changed to sulfate free RPMI 1640 medium during radiolabelling, and the amount of serum reduced to 2%. As sulfate and other ingredients could obscure the results, the cells should ideally be cultured under serum-free conditions. However, the cells grow poorly under such conditions, and the serum concentration is reduced rather than

eliminated. The cells were incubated for 24 hours in 0.1 mCi ^{35}S-sulfate/ml medium. In some experiments this was increased to 0.2 mCi, in order to increase the labelling efficiency.

After metabolic labelling with ^{35}S-sulfate for 24 hours, the medium and cell fraction were harvested as described below. The samples contained both free, unbound ^{35}S-sulfate and other ^{35}S-labelled macromolecules besides the radio-labelled PGs. Unbound ^{35}S-sulfate and other small molecules were removed by gelfiltration, in which molecules are separated according to size. Separation of PGs from other macromolecules can also be performed by ion-exchange chromatography, where molecules are separated according to charge**.**

4.5 Harvesting

After different types of stimulation and radiolabelling, the cells and conditioned medium was harvested using Guanidine/Triton X-100 buffer. RIPA buffer was used for lysis of cells for Western blotting analysis. Fosfatase inhibitor was added to the latter to slow down the proteolysis, defosforylation and denaturation of the cell lysate.

Procedure:

1. Medium fractions were collected and centrifuged 3 min at 1200 rpm to remove cell debris
2. Cells were carefully washed in 37°C PBS to remove rests of medium
3. The cells were lysed for 10-15 min before carefully mixed and harvested
4. Samples were purified and further analysed, or frozen.

Solutions:

Guanidine / Triton X-100 harvesting buffer for ^{35}S-labelled cells

600 ml 4M Guanidine HCl in 0.1M acetate buffer with 2% Triton X-100, pH 6.0

Components	Volume	Final concentration
Guanidine HCl	229.27 g	4M
Triton X-100	12 ml	2 %
0.1M Acetatebuffer pH 6,5	Up to 600 ml	0.1M

Guanidine HCl was added to the Ac buffer and the volume adjusted to 600 mL. Then the solution was rinsed while stirring with charcoal over night, and then filtered twice before Triton X-100 was added to a final concentration of 2 %. PH was adjusted to 6.0.

RIPA lysis buffer – for cell harvesting before Western blotting analyses.

Components	Final concentration
Tris-HCl pH 7.4	50 mM
NaCl	150 mM
Triton X-100	1 %
SDS	1 %
Na-Deoxycholate	1 %
EDTA	10 mM
$Na_4PO_2O_7$ Sodium pyrophosphate	10 mM
Fosfatase-inhibitor tablet (freshly added)	1 tabl.

4.6 Scintillation counting

The amount of radio-labelled molecules in a metabolically labelled sample can be estimated using a liquid scintillation counter, which measures radiation from β-emitting nuclides such as ^{35}S.

Radio-labelled samples were mixed with a liquid scintillation 'cocktail' of solvent, emulsifier and Flurophore. The kinetic energy of the β-particles is absorbed by solvent molecules, and the energy of these excited molecules is emitted as UV-light. The UV-light is absorbed by Fluor, which in turn emits blue light upon returning to ground state. The samples were placed in small transparent vials loaded into a liquid scintillation counter, where light flashes emitted per minute are counted. In this way, each beta emission results in a pulse of light, and the amount of light emitted will reflect the amount of radioactivity of the sample. Each sample was counted for three minutes, and measured as cpm.

4.7 Protein quantitation

Protein measurement of cell lysate is a way of monitoring the cell growth and proliferation. When taken together with cell counts, protein quantification can give information about cell growth. Increasing protein concentrations could indicate either hyperplasia (increasing number of cells) or hypertrophy (increasing size of the cells).

Determination of the protein concentration of a solution can be done using the Uptima BC Assay protein quantitation kit. This method is based on the reduction of Cu^{2+} to Cu^{+} by protein peptidic bonds. This reduction can be quantified by adding bicinchoinic acid which in the presence of Cu^{+} forms a coloured complex with absorption maxima at 562 nm. The absorbance is directly proportional to the protein concentration, which can be calculated using a standard curve. The method is modified after Paul Smith et al (64).

Procedure:

The cells were cultured in wells or flasks as described and stimulated as required before harvested and analyzed. Only cell lysates were analysed for protein content.

1. Cells were harvested as described for the experiment in question. ^{35}S-labelled cell fractions were subjected to Sephadex G-50 fine chromatography.

2. Standards were made out of a BSA stock solution of 2 mg protein / ml diluted in the same buffer as in the cell-samples. The stock is diluted 1:10 sequentially for 11 times achieving a standard curve of 12 different concentrations of protein (including one blank).

3. A+B solution was made from 2 % assay reagent A and 98 % assay reagent B, in volumes appropriate to the number of samples being analyzed.

4. 25 µl of sample or standard were added in doublets to a 96-well microtitrer plate, and 200 µl of A+B solution was added to each well. The samples are re-suspended thoroughly before application.

5. The plate was gently stirred for 2 min, and then incubated at 37ºC for about 30 min (depending on the colour development). Bubbles were poked a hole in.

6. The absorbance was measured at 562 nm using the Titertec multiscan PLUS spectrophotometer.

7. A standard curve was created plotting the absorbance (Y-axis) versus their corresponding known protein concentrations (X-axis), and the concentrations of the unknown samples was calculated from this. Taking dilutions into account, the original protein concentration was calculated.

4.8 Sample purification

In order to study the PGs, they need to be purified to different degree, depending on the methods of further analyses.

4.8.1 Gelfiltration– Sephadex G-50 fine

After radiolabelling, the samples will contain both free ^{35}S-sulfate and ^{35}S-sulfate incorporated in macromolecules; which thus can be separated according to size using gelfiltration.

Gelfiltration separates proteins according to molecular size. This separation is achieved using a porous matrix to which the molecules, for steric reasons, have different degrees of access; smaller molecules have greater access than larger molecules. The matrix is packed in a column, the sample mixture added, and the separation is achieved by passing an aqueous buffer through the column and sampling eluted fractions. The size of the molecules separated will depend on the matrix chosen; Sephadex G-50 fine will separate proteins of 0.5-10 kDa. Small molecules like unbound sulfate will penetrate the matrix and will be eluted in decreasing order of size. Larger protein molecules, like PGs, will be confined in the volume outside the matrix beads and will be swept through the column by the mobile phase and be eluted first.

Procedure:

1. Sephadex G-50 fine powder was swollen into a gel over night in the buffer of choice, we used 0.05M NaCl 0.05M, Tris-HCl pH 8,0

2. Columns were made of 10mL pipettes cut at the 7 mL mark and filled with glass wool in the bottom. Each column was filled with 4 ml of Sephadex G-50 fine gel.

3. 1 ml of sample was applied.

4. The first 1 ml of elute was discarded.

5. PGs and other macromolecules were eluted in the void volume with 1.5 ml buffer, and collected. Free ^{35}S remained associated with the column, which was discarded.

6. Aliquots of this elute (2x50µL) was counted for radioactivity using the scintillation counter.

Solutions:

500 ml G50-fine buffer: 0.05M NaCl in 0.05M Tris-HCl pH 8.0

Components	Volume	Final concentration
1.0M Tris	25 ml	0.05M
NaCl	1.461 g	0.05M
mQ-H_2O	Up to 500 ml	

pH was adjusted to 8.0 adding 5.0M HCl

Sephadex G50-fine solution

Components	Volume
Sephadex G-50 fine powder	10 teaspoons
0.05M NaCl in 0.05M Tris-HCl, pH 8.0	500 ml

The solution was swollen overnight

4.8.2 DEAE anion-exchange chromatography

Ion-exchange chromatography separates molecules according to charge. DEAE (Diethylaminoethyl) is a weak anion-exchanger, binding the highly negative charged PGs by ionic bonds. Slightly negative, neutral or positively charged molecules will not bind and can be washed out. Then, the PGs can be eluted by high salt concentration (2M NaCl). Thus, by this method PGs are separated from other macromolecules according to charge (65).

Procedure:

1. The ethanol in which the DEAE was solved was removed by washing twice in equal amount of low salt Tris buffer (0.15M NaCl 0.05M Tris-HCl pH 8.0). The mixture was shaken thoroughly, spinned down in centrifuge and the supernatant was removed before solved in equal amount of buffer.

2. 600 µl washed DEAE was added to every sample (about 1.5 mL) and mixed 5 min on shaker before spinned down by centrifugation. Negatively charged proteins as PGs will bind to the DEAE, and the supernatant containing other macromolecules can be removed.
3. The sediment was washed twice in Tris buffer of slightly higher salt (0.3M NaCl/0.05M Tris), eluting weakly negatively charged proteins like BSA.
4. Finally the PGs were eluted in high salt, in which the ionic bonds between the DEAE and PGs are broken, by washing three times in 500µl 2M NaCl/ 0.05M Tris (alternatively 2M NH_4HCO_3) and collecting the supernatant containing the PGs.

Low salt Tris buffer: 0.15 M NaCl in 0.05M Tris-HCl pH 8.0

Components	Volume	Final concentration
1.0M Tris buffer	25 ml	0.05M
4.0M NaCl	18.75 ml	0.15M
mQ-H_2O	Up to 500 ml	

pH was adjusted with 1M HCl to 8.0

Medium salt Tris buffer: 0.3 M NaCl in 0.05 M Tris pH 8.0

Components	Volume	Final concentration
1.0M Tris buffer	25 ml	0.05M
4.0M NaCl	37.5 ml	0.3M
mQ-H_2O	Up to 500 ml	

pH was adjusted with 1M HCl to 8.0

High salt Tris buffer: 2 M NaCl in 0.05 M Tris-HCl pH 8

Components	Volume	Final concentration
1.0M Tris buffer	25 ml	0.05M
NaCl	58.44 g	2.0M
mQ-H_2O	Up to 500 ml	

pH was adjusted with 1M HCl to 8.0

4.9 Concentrating the samples

In order to apply enough material per well when performing electrophoresis, the samples were concentrated prior to mounting. This was done by different methods, depending on the sample volume and prior treatment. Vacuum centrifuge and freeze-dryer could be used when the samples were not eluted with salt (DEAE). Freeze-drying is better suited for large volumes, but could be harsh treatment. Concentration on microcon is suited for small samples eluted in salt, as the samples in this way also are desalted.

In SDS-PAGE of the radio-labelled material samples of equal protein content and ~ 10 000 cpm were mounted in each well. For Western blotting, cell lysate or media equivalent to at least one small culturing flask was used per well.

4.10 GAG-depolymerisation

4.10.1 Chondroitinase ABC

Polysaccharide-lyases are a class of enzymes especially suited for GAG- and PG analyses, as they cleave specific glycosidic bonds and facilitate a depolymerisation of polysaccharides (GAG-chains). Choindroitin lyases are prokaryotic GAG-degrading lyases that will depolymerise GAG by an elimination mechanism. (Eucaryotic enzymes act by hydrolysis). There are two classes of choindroitin lyases,

chondroitinase AC and ABC. The latter will act on CS-A, CS-C and DS (CS-B), as illustrated by figure 4.2.

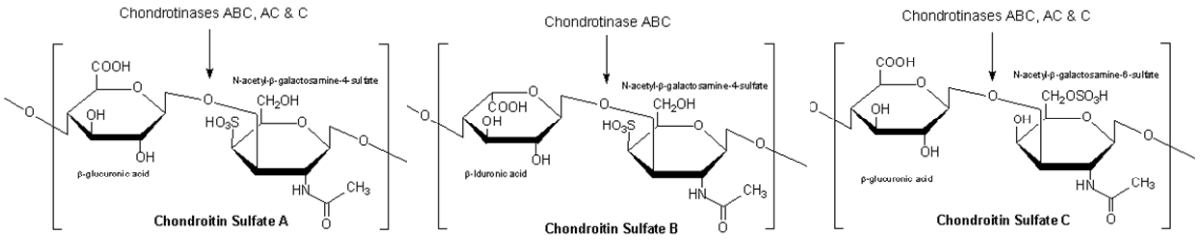

Figure 4.2. Illustration of the cleavage action of chondroitinase ABC*, which will act on both chondroitin sulfate A and C, as well as DS (CS-B).*

Chondroitinase ABC (cABC) was used for identification of CS/DS-PGs. Optimal conditions for this enzyme is Tris-HCl/NaAc buffer, 0.05 M and incubation at 37ºC. It will depolymerise CS and DS GAG-chains at pH 8 into disaccharides, without affecting HS.

Procedure:

1. 0.01U of cABC enzyme was added to each sample.
2. 10x cABC-buffer was added until 1x.
3. Samples were incubated over night at 37°C

Solutions:

10 x c-ABC buffer- 0.5M Tris-HCl pH 8.0, 0.5 M sodium acetate, 10 mL

Components	**Volume**	**Final concentration**
1M Tris pH 8.0	5 ml	0.5M
$NaAc{\cdot}3H_2O$	0.68 g	0.5M
mQ-H_2O	Until 10 ml	

4.10.2 HNO_2 – Cleavage of N-sulfated GAGs

All GAG-chains consists of an amino sugar in every second position, which normally are N-acetylated (GalNAc in CS and DS, GlcNAc in HS, heparin, hyaluronic acid). In heparin and heparan sulfate a high percentage of the N-acetyl substituents are replaced by N-sulfate groups. N-sulfated glucosamines ($GlcNSO_3$) are sites that are unique in their susceptibility to facilitate cleavage by nitrous acid at room temperature and low pH (~1.5). Thus, when heparins or heparan sulfates are treated with nitrous acid, they are specifically cleaved into fragments with ranges of molecular weight depending on the distribution of the $GlcNSO_3$ residues in the chain. N-acetylated amino sugars are not affected by this treatment, and only HSPG GAG-chains will be cleaved (66).

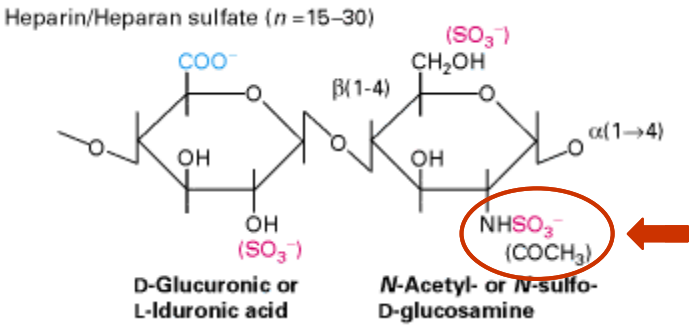

Figure 4.3. Illustration of heparin / heparan sulfate and the location of the target site of nitrous cleavage. *The location of the possible N-sulfate is unique for heparin/HS and is the target of nitrous cleavage at low pH, as indicated by the red arrow. Adapted from http://courses.cm.utexas.edu.*

Procedure:

1. Equal volumes of sample and HNO_2 was mixed and incubated for 10 minutes at room temperature.

2. The reaction was stopped by increasing the pH to 8.5 by adding Na_2CO_3.

Solutions:

0.5 M H_2SO_4 50 mL

Components	Volume	Final concentration
H_2SO_4	1.33 g	0.5M
mQ-H_2O	Up to 50 mL	

0.5 M $Ba(NO_2)_2$, 10 mL, made fresh for each experiment

Components	Volume	Final concentration
$Ba(NO_2)_2 \cdot H_2O$	1.24 g	0.5M
mQ-H_2O	Up to 10 mL	

HNO_2 pH 1.5

Components	Volume
0.5 M H_2SO_4	Equal volumes
0.5M $Ba(NO_2)_2$	Equal volumes

Equal volumes of ice cold reagents was mixed, centrifuged and the supernatant which comprises the HNO_2collected. This reagent must be stored on ice, and must be used immediately. $H_2SO_4 + Ba(NO_2)_2 \rightarrow 2HNO_2 + BaSO_4(s)$

2 M Na_2CO_3

Components	Volume	Final concentration
Na_2CO_3	2.12 g	2.0M
mQ-H_2O	Up to 10 mL	

4.11 SDS – PAGE sodium dodecyl sulfate polyacrylamide gel electrophoresis

Generally, gelelectrophoresis is a technique in which charged molecules, such as protein or DNA, are separated according to physical properties as they are forced through a gel by an electrical current. Proteins are commonly separated using Poly Acrylamide Gel Electrophoresis (PAGE) to characterize individual proteins in a complex sample or to examine multiple proteins within a single sample. PAGE can be used as a preparative tool to obtain a pure protein sample, or as an analytical tool to provide information on the mass, charge, purity or presence of a protein. Several forms of PAGE exist and can provide different types of information about the protein(s). SDS-PAGE, the most widely used electrophoresis technique, separates proteins primarily by mass. The size and mass of the protein will be inversely related to the degree of migration in the gel. For PGs the GAG-chains also affects the migration. Proteins can also be separated in non-denaturating conditions; not containing SDS.
Polyacrylamide gels are formed from the polymerization of acrylamide and bis (N,N-methylenebisacrylamide) in the presence of ammonium persulfate and TEMED (N,N,N,N'-tetramethylenediamine). The size of the pores created in the gel is inversely related to the amount of acrylamide used. Gels with a low percentage of acrylamide are typically used to resolve large proteins and high percentage gels are used to resolve small proteins. A gradient gel allows separation of a mixture of proteins with a greater molecular weight range than a gel with a fixed acrylamide concentration.

The samples were treated with sample buffer containing the detergent SDS prior to application on the gel. This ionic detergent denatures the proteins and binds tightly to the uncoiled molecule. Because of the sulfate groups, the SDS molecules mask the intrinsic charge of the protein and create a relatively uniform negative charge distribution. When an electric current is applied, all proteins will migrate through the gel toward the anode, which is placed at the bottom of the gel. Because of the

uniform charge:mass ratio created by SDS-binding, the SDS-PAGE gel then separates the proteins primarily according to size. Proteins with less mass travel more quickly through the gel than those with greater. Protein molecular weights can be estimated by running standard proteins of known molecular weights in separate lanes of the same gel.

In addition to SDS, the sample buffer also contains 2-β-mercaptoethanol (alternatively DDT) for further denaturation (reduction of disulphide bridges), glycerol (to increase loading efficiency) and bromophenol blue-marker dye. Boiling or heating is also a common way of denaturating the proteins, but PGs tends to aggregate so heating is not used here.

Procedure:

1. In order to be detectable, the samples must contain a quantity of PGs equivalent to a minimum of 10 000 cpm in each radio-labelled sample, and it is often necessary to concentrate the samples prior to loading.

2. Loading buffer containing glycerol, bromophenol blue marker dye, denaturating SDS and 2-mercaptoethanol was added to the samples, and incubated in room temperature for 15 min.

3. The gel was mounted in the electrophoresis apparatus and running buffer was added to the top and bottom reservoirs.

4. Samples and standards were carefully loaded in a predetermined order to the wells, after “rinsing” the well with a pipette.

5. The apparatus was attached to an electric power supply and a voltage of 110V was applied to the gel until the bromophenol blue reached the bottom of the gel, after approximately 2 hours.

6. As soon as the power was turned off, the gel was treated with fixing solution to prevent diffusion of proteins.

7. Gels containing radio-labelled samples were fixed, treated with amplifier, dried and subjected to autoradiography. Alternatively, the gel was subjected to electroblotting and analysed further by Western blotting

Solutions:

4x Loading buffer, 10 ml

Components	**Volume**	**Final concentration**
0.1M Tris buffer pH 6,5	2.5 ml	0.025 mM
Glycerol	4.0 ml	40 %
SDS	0.8 g	0.08 % (w/v)
Bromphenol blue	1.0 ml	10%
2-mercaptoethanol	1.0 ml	10%
mQ-H_2O	Up to 10.0 ml	

10x Running buffer, 1000 ml

Components	**Volume**
Tris base	29.0 g
Glycin	144.0 g
SDS	10.0 g
mQ-H_2O	Up to 1000 ml

1x Running buffer

Components	**Volume**	**Final concentration**
10x running buffer	100 ml	1x
mQ-H_2O	900ml	

Fixing solution

Components	Volume	Final concentration
Isopropanol	200 ml	25%
Acetic acid, glacial	80 ml	10%
mQ-H_2O	520 ml	65%

Drying of SDS-PAGE gel

Before autoradiography the radio-labelled SDS-PAGE gel must be dried. After removing the gel from the electrophoresis apparatus, the gel was incubated for 30 min in fixing solution, then 15 min in amplifier. The gel was then put on a filter paper with protective plastic foil on top, and placed on the gel dryer. The lid was tightly closed with suction and heated to 70°C for about two hours. The dry gel attached to the filter is then removed from the dryer, plastic removed, and ready for autoradiography.

Autoradiography

Gels containing radioactive material were subjected to autoradiography. The dried gel was placed on a film in -70°C for about 7 days, depending on the amount of radioactivity in the samples, and then developed. After development, the radioactivity was observed as dark regions on the film.

Generally, in SDS-PAGE, PGs are visualized as smears of high molecular size, in contrast to the distinct bands of proteins. This is due to the heterogeneity in PG size, caused by the variation in size, number and composition of the GAG chains attached. The intensity of the bands is generally lower in the cell lysate than in the medium, indicating that the majority of the PGs are secreted.

4.12 Western blotting

SDS-PAGE is useful in separating PGs, detecting the presence of PGs of different sizes and distinguishing between CS and HS-PGs. However, in order to detect individual proteins or PGs from a mixture, we can use the technique *Western blotting*, where the PGs are electroblotted from the SDS-PAGE gel to a membrane. Then immuno-staining is performed in order to visualize specific proteins bound to the membrane.

Preparation of the samples separated by SDS-PAGE differ as they can be reduced and/or denaturated. As the epitope[1] may reside within the 3D conformation of the protein, the samples usually are denaturated and the proteins separated on a reducing SDS-PAGE gel. Alternatively, proteins can be separated both under non-denaturating (no SDS) and/or non-reducing (no β-mercaptoethanol) conditions, depending on the epitope.

After separation on SDS-PAGE, proteins were transferred from the gel to a PVDF (polyvinylidene fluoridine) blotting membrane using BIORAD Criterion blotter system. Wet transfer was performed, as recommended for large proteins.

The membrane can be probed for specific proteins using antibodies. Blocking the membrane in non-fat milk, BSA or another unrelated protein prior to antibody-incubation prevents non-specific binding of the antibodies to the membrane. Then the membrane is exposed to an unlabeled antibody (Ab) specific for the target protein. The membrane is washed several times in TBST to remove excess antibody. This washing solution contains a detergent (tween 20) and high salt that eliminates non-specific binding to the membrane through hydrophobic or ionic interactions.

The Ab bound to the membrane is detected when binding to a secondary Ab coupled to horseradish peroxidase (HRP), followed by enhanced chemiluminiscence (ECL).

[1] antigenic determinant , portion of protein recognised by the antibody

After incubation and carefully washing away unbound secondary antibody, the Western blot is ready for detection of the labelled probes. The HRP-linked secondary antibody is used in conjunction with a chemiluminescent detection method. A substrate of HRP is added and the formation of a luminescence is catalyzed. The amount of luminescence produced is proportional to the amount of protein on the membrane, and can be detected by exposing to a photographic film. Thus, only the proteins immuno-stained will be visualized. From the bands on the film you can determine the size of the protein relative to the standard, or amount of immunostained protein relative to other bands.

Procedure:

1. **SDS-PAGE**.

   The samples were denaturated and the PGs were separated according to size on a reducing 4-20 % precast SDS-PAGE gel, as described in section 4.11**.** The amount of protein loaded in each well corresponded to the amount of one confluent 25 cm^2 cell-culturing flask.

2. **Electro-blotting**

   The transfer of proteins from the gel on to a solid support using electricity is referred to as electroblotting. The gel was removed from the electrophoresis apparatus and equilibrated for 15 min in blotting-buffer to remove SDS-remnants. The proteins were electroblotted from the gel to a membrane using wet transfer. PVDF-membrane and filter papers were cut to cover the gel. The membrane was rehydrated by soaking in methanol for 15 seconds, then rinsed for 2 min in milliQwater and equilibrated for 10 minutes in blotting buffer. Whatman filter-papers and fibre pads was soaked in cold transfer buffer. Then gel, membrane, filter papers and fibre pads was placed in the cassette according to the instructions of the distributor, and put in the blotting tank. Care is taken to remove any air bubbles. A cooling agent and a stir bar were added, and the tank was placed on top of a magnetic stirrer, filled with blotting

buffer and set at 1,0A for two hours. This high current creates a lot of heat, and the cooling agent is renewed when needed, after approx 1 hour.

3. Blocking

In order to prevent non-specific binding of the antibodies, the membrane was blocked prior to immuno-staining. The membrane was agitated in non-fat milk or BSA (depending on the primary antibody) for 1 hour at room temperature.

4. Immunostaining

The membrane was incubated in antibody/TBST-solution at 4ºC over night at an agitator. The antibody-solution can be reused if always kept at low temperature. Unbound antibodies are removed by washing 6x 5 minutes in TBST.

A HRP-linked secondary antibody recognizing the primary antibody is diluted in TBST. The membrane is incubated in this solution for 1 hour at room temperature, before removing unbound probes in 6x 5 minutes TBST.

5. Development

The HRP-enzyme will convert the luminol of the ECL to a light-releasing substance, and this light is detected as dark areas on a film. ECL, ECL plus or ECL advanced solution was prepared and the membrane was incubated for the recommended period of time. The membrane was then transferred to a cassette and developed using Hyperfilm^{TM} MP and Curix 60 AGFA developer.

6. Stripping and re-probing

The probes bound to the membrane can be stripped off before re-probing the membrane with another antibody. This is done by washing 5 min in milli-Q H_2O, blocking buffer, milli-Q H_2O, and then 10 min in 2M NaOH, 5 min in milli-Q H_2O, and 15 min TBST. Finally blocking for 1 hour and rinsing for15

minutes in TBST, before incubating with another antibody using the same procedure.

Solutions:

10x Transfer buffer pH 7.4, 1000 ml

Components	Volume
Tris-HCl	39.4 g
Glycin	143 g
mQ-H_2O	Up to 1000 ml

pH was adjusted to 7,4 with 1.0 M HCl or NaOH

1x Transfer buffer

Components	Volume	Final Concentration
Methanol	200 ml	20 %
10x transfer buffer	100 ml	1x
mQ-H_2O	700 ml	

10x TBS pH 7.5, 1000 ml

Components	Volume
Tris base	24.22 g
NaCl	80.15 g
1M HCl	38 ml
mQ-H_2O	Up to 1000 ml

After adding about 800 ml mQ-H_2O, the pH was adjusted to 7,5 using 10M HCl (~50 mL), before adding mQ-H_2O up to 1000 ml. 10x TBS was stored at 4ºC.

TBST

Components	Volume	Final Concentration
10x TBS	200 ml	1x
Tween 20	2 ml	1%
mQ-H_2O	Up to 2000 ml	

Blocking buffer

Components	Volume	Final Concentration
TBST	200 ml	0.1% Tween 20
Dried milk	10 g	5 %

The blocking buffer was used immediately or stored in refrigerator for a few days

4.13 Statistical analysis

In this section we provide a brief introduction to concepts of statistical analysis relevant in this work. We then proceed by describing the typical experiments performed and the assumptions we have made to give an analysis of the results presented in this thesis.

Introduction

A normal distribution N(μ, σ) is described by the two parameters, the mean μ and the standard deviation σ. Typically these two parameters are unknown, and needs to be estimated. Let $\{X_i\}$ be a random sample of the normal distribution, consisting of n measurements. Then the estimate of the mean $\overline{X}$ is given by:

$$\overline{X} = \frac{1}{n}\sum_{i=1}^{n} X_i, \qquad (1)$$

And the estimate of the standard deviation SD by

$$SD = \sqrt{\frac{1}{n-1}\sum_{i=1}^{n}(X_i - \overline{X})^2} \quad (2)$$

The estimate of the mean follows a normal distribution as well, with a standard deviation that is termed the standard error. The estimate of the standard error SE, given by

$$SE = SD/\sqrt{n} \quad (3)$$

is inversely proportional to the square-root of the number of measurements n. About 95 % of all estimates of the mean $\overline{X}$ are within two standard errors SE of the mean μ. The estimated standard error therefore gives an indication of how accurate the estimated mean is, and should be taken into account when comparing the mean values of different populations.

When taking the ratio Z = X/Y between two means X and Y , with corresponding standard errors SE(X) and SE(Y), the standard error of the ratio is given by

$$SE(Z) = \frac{X}{Y}\sqrt{\frac{SE(X)}{X} + \frac{SE(Y)}{Y}} \quad (4)$$

Experiments and assumptions

In order to get statistically significant results one would typically need a larger number of measurements than what we have performed in this work. Nevertheless, we provide a statistical analysis to assess the results in a qualitative fashion. In this work the HUVEC of several individuals were exerted to different exposures. The measurement of one individual at a given exposure was typically composed of two parallel samples of cells grown in two parallels. We take the mean of these four samples to be one measurement of the individual. There is an error associated with each such measurement, and for a thorough statistical analysis one should include this error in the analysis. However, for simplicity we disregard this error. All experiments contain a control, in which only low glucose has been given. To better compare the results between different individuals, we first scale the results of a given individual

(at each exposure) with the control of the same individual. In the figures included in this work, we present the means of these scaled measurements and their corresponding standard errors, using Eq. (1) and Eq. (3) respectively. All results are presented as percentages of the control. Note that in some cases we also present the ratios between the results of different experiments. The corresponding standard error is calculated via Eq. (4).

5. Results

DM is associated both with hyperglycemia and atherosclerotic chronic inflammation of the vessels. The endothelium is the prime organ to be exposed to hyperglycemia and is one of the main targets of diabetic complications. PGs are important components of the healthy endothelium, and are also involved in a number of processes important to the development of DM and atherosclerosis. In this way, changes in PG expression can be linked to the development of diabetic complications. In order to study these changes, we mimicked the diabetic conditions by exposing ECs to a hyperglycaemic environment, or to pro-inflammatory cytokines, and studied the effects on PG expression.

General comments

All experiments were performed on primary HUVECs isolated from different donors, carrying distinct qualities. Like other studies performed on HUVEC, we experienced varying results from the different donors (61;67). To be able to compare the results of the different individuals, all results were presented as percent of the control.

The cells were grown in complete MCDB 131 culturing medium containing 5,0 mM glucose and 7 % FCS, referred to as “MCDB- medium”, unless otherwise noted (see section 4.1.2.) and used for experiments when in passage 2-4. In all experiments exposures were performed with cells cultured in only 2% FCS, in order to reduce the level of cold sulfate, and to create identical culturing conditions for cells later compared. All data were based on cells from several, usually three, individuals. Each experiment was performed in parallels, and duplicates of measurements were taken from each parallel.

5.1 Effect of hyperglycemia on PG synthesis

In order to investigate the role of PGs in DM, HUVECs were exposed to hyperglycemic conditions. The effect of hyperglycemia on PG synthesis was investigated in two ways; both through direct exposure to high concentration of sugar (25 mM glucose), as well as by stimulating the hexosamine pathway by adding the glucose metabolite GlcN. High levels of sugar increase the concentration of glucose-metabolites in the cells and increase the flux trough many metabolic pathways. High levels of glucose will increase the level of the metabolite GlcN (25), and GlcN will increase the flux trough the hexosamine pathway (25).

5.1.1 Effect of GlcN on HUVEC

The glucose metabolite GlcN will bypass the rate limiting GFAT enzyme of the hexosamine pathway. Increased flux trough this pathway is thought to affect PG synthesis by increasing the level of UDP-GlcN. The effect of GlcN on HUVEC was investigated trough the effects on proliferation and expression of ^{35}S-macromolecules and ^{35}S-PGs.

Effect of GlcN on HUVEC proliferation

As we had no previous experience in exposing HUVEC to GlcN; the appropriate dose and time of stimulation had to be established. The effect of GlcN on HUVEC proliferation was investigated by exposing HUVEC to different concentrations of GlcN. This effect was further investigated as a function of exposure time.

GlcN dose-response

The effect of GlcN on cell proliferation was to be studied. The relation between the number of cells and the protein concentrations was investigated to assess whether the protein content was a suitable measure for cell proliferation.

HUVECs from three cell cultures were seeded onto 12-wells cell culture plates and grown in MCDB medium until confluent. A 24 hour exposure to parallels of 0, 0.1, 1.0, 2.0, 5.0 and 10.0 mM GlcN was performed in sulfate free RPMI 1640 medium with 2% FCS. Cells were dissolved by trypsin treatment, prior to trypan blue staining, and counted as doublets on a hemacytometer in a microscope.

Cells from the same three different individuals were also exposed in parallels to different concentrations of GlcN, and the corresponding protein concentrations were measured to assess the effect on cell proliferation. Cells were seeded onto 6-well culture plates and grown in MCDB medium until confluent. A 24 hour exposure to 0, 0.1, 1.0, 2.0, 5.0 and 10.0 mM GlcN was performed in sulfate free RPMI 1640 medium with 2% FCS. Cells were harvested in Guanidine/Triton X-100 and samples purified by gelfiltration, prior to the protein measurements presented in figure 5.1, as percent of control.

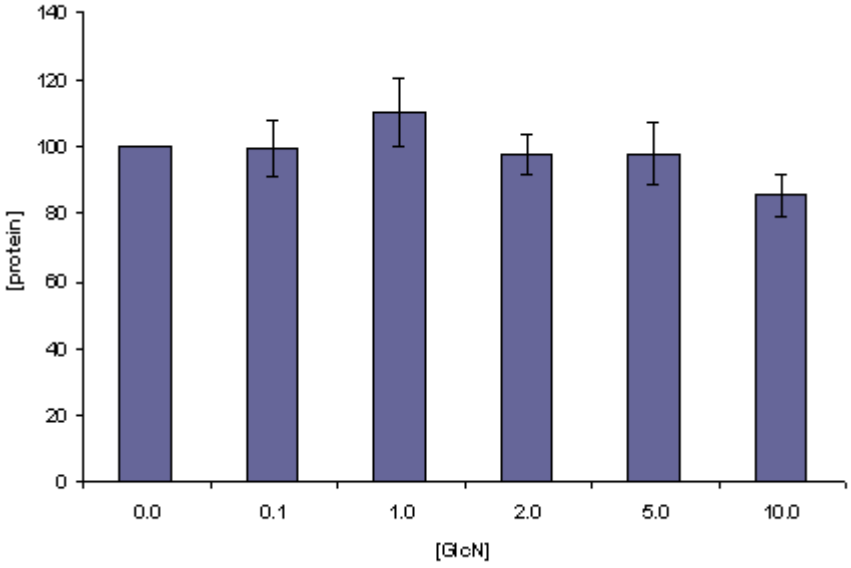

Figure 5.1. Protein concentration in HUVEC exposed to different concentrations of GlcN. *Proliferation of HUVEC cultured for 24 hours in GlcN and sulfate free RPMI 1640 medium with 2 % FCS. Cells was harvested in Guanidine / Triton X-100 and purified by gel filtration before protein determination. The results are based on doublets of parallels from three different donors, and presented as % of control with error bars.*

No differences in protein content were observed after HUVEC exposure to different amounts of GlcN, except a possible reduction at 10.0 mM. GlcN concentrations up to 10.0 mM do not seem to affect HUVEC proliferation using this parameter. There was a stable relationship between number of cells and protein concentration until exposure to 1.0 mM GlcN (results not shown). At concentrations above 1.0 mM cellular effects were observed, such as vulnerability to trypsin treatment. As a consequence, GlcN concentrations above 1.0 mM were not used in later experiments, and protein could hence be utilized as a measurement for cell viability for GlcN concentrations of 1.0 mM and below.

GlcN time-response

To determine the necessary exposure time in order to detect effects of GlcN on proliferation, parallels of HUVECs from three individuals were exposed to 1.0 mM GlcN for 0, 24, 48 and 72 hours. Proliferation was assessed by protein measurements.

Cells were grown to confluence in 6-well plates, before changing the culturing conditions to sulphate-free RPMI 1640 medium with 2% FCS. The cells were exposed to 1.0 mM GlcN for 0, 24, 48 and 72 hours respectively, prior to harvesting and gel filtration purification of the samples.

A slight increase in protein content was observed with increasing incubation time, as can be seen in figure 5.2. This increase in protein concentrations suggests a continued cell proliferation along with increasing time, as expected for healthy cells. The cell viability in 1,0 mM GlcN was clearly not affected during the course of the experiment.

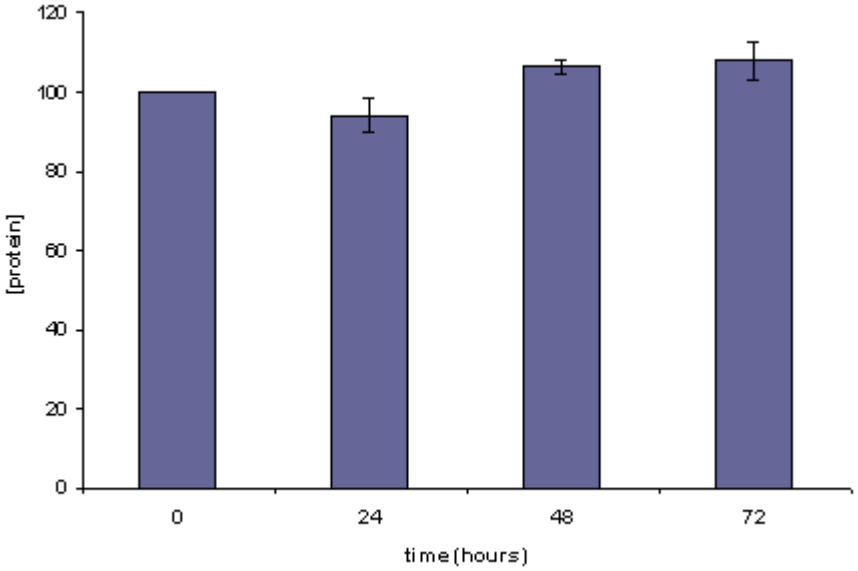

***Figure 5.2*. Protein concentration in HUVEC in 1,0 mM GlcN over time.** *Cell viability in HUVEC exposed to 1.0 mM GlcN for 0, 24, 48 and 72 hours in sulfate free medium containing 2 % FCS. Cells were harvested in Guanidine/Triton X-100 and samples purified by gelfiltration before protein concentrations were determined. The data are based on doublets of parallels from three experiments, and presented as % of control with error bars.*

Effect of GlcN on ^{35}S-macromolecules in HUVEC

The effect of different concentrations of GlcN on the *de novo* synthesis of ^{35}S-macromolecules in HUVEC was investigated exposing HUVEC to different concentrations of GlcN. This effect was further investigated in relation to exposure time.

GlcN dose-response

Parallels of HUVECs from the same three individuals as used for cell count and protein measurements were exposed to different GlcN concentrations during metabolic labelling with ^{35}S-sulfate. The corresponding *de novo* synthesis of ^{35}S-macromolecules was measured.

HUVECs were seeded onto 6-wells culture plates and grown in MCDB medium until confluent. A 24 hour exposure to different concentrations of GlcN was performed in sulfate free RPMI 1640 medium with 2% FCS. After metabolic labelling in 0.1 mCi

^{35}S-sulfate / ml medium for 24 hours, medium and cell fraction was harvested and purified by gelfiltration.

The amount of ^{35}S-macromolecules recovered was related to the protein concentration. This was used as an assessment of the *de novo* ^{35}S-macromolecule synthesis per cell. The secretion of ^{35}S-macromolecules per cell did not seem to be affected until at 1.0 mM GlcN, where we observed a decrease of 42 ± 18 % as compared to the control (figure 5.3, panel A). This decline continued with increasing GlcN concentration, reaching 20 ± 9 % of the control at 10.0 mM. As mentioned earlier, the cells showed altered behaviour when exposed to concentrations above 1.0 mM. Thus, a concentration of 1.0 mM GlcN seems to be sufficient in order to see changes in the secreted ^{35}S-macromolecules. As can be seen in figure 5.3 panel B, there was a reduction also of intracellular macromolecules, but not to the same extent as in the conditioned medium. The reduction at 1.0 mM was 26 ± 23 %, reaching a reduction of 54 ± 20 % compared to the control at 10.0 mM.

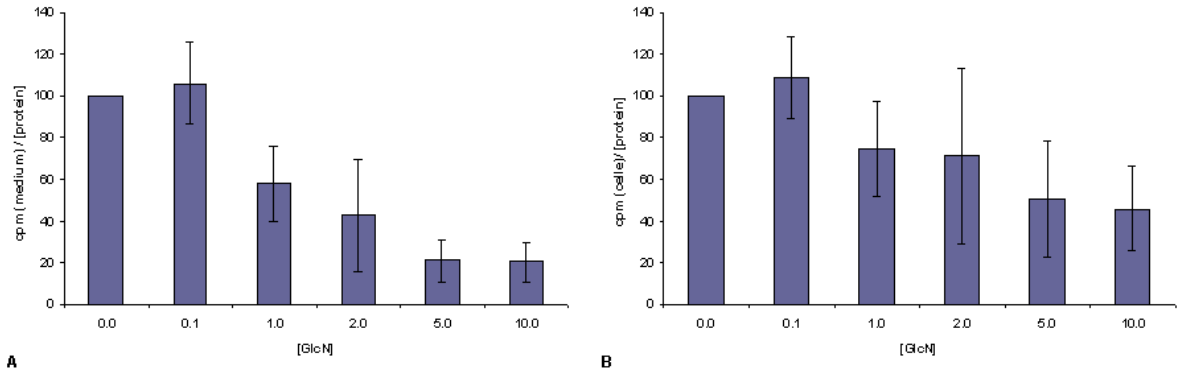

Figure 5.3. ^{35}S-macromolecules in HUVEC exposed to GlcN*. HUVECs were cultured for 24 hours in 0.0, 0.1, 1.0, 2.0, 5.0 and 10.0 mM GlcN and sulfate free RPMI-medium with 2% FCS. Metabolic labelling was performed in 0.1mCi / ml ^{35}S-sulfate. Cells and medium was harvested and samples purified by gelfiltration. The amount of ^{35}S-labeled macromolecules in conditioned medium (A) and cell lysate (B) was measured as cpm and adjusted to the cellular protein concentration. The results are based on doublets of parallels from three different individuals, and presented as % of control with error bars.*

GlcN time-response

A change in ^{35}S-macromolecule expression was seen after 24 hours incubation. To further investigate the effect of time exposure to GlcN, parallels of HUVECs from three individuals were exposed to 1.0 mM GlcN for more extended time periods.

HUVECs were seeded onto 6-wells culture plates and grown in MCDB medium until confluent. Exposure to 1.0 mM GlcN was performed in sulfate free RPMI 1640 medium with 2% FCS for 0, 24, 48 and 72 hours. After metabolic labelling in 0.1 mCi ^{35}S-sulfate / ml medium for 24 hours, medium and cell fractions were harvested and purified as previously described.

From figure 5.4, panel A, it is evident that there was a reduction of 29 ± 16 % in secreted ^{35}S-macromolecules from 0 to 24 hours, compared to the control. This trend seemed to continue with time, reaching a reduction of 57 ± 4 % of the control at 72 hours. In cell lysates, figure 5.3 panel B, this reduction was less obvious. The reduction reached 51 ± 5 % of the control after 72 hours. A 24 hours exposure appeared to be sufficient in order to detect effects of GlcN on the expression of ^{35}S-macromolecules in HUVEC.

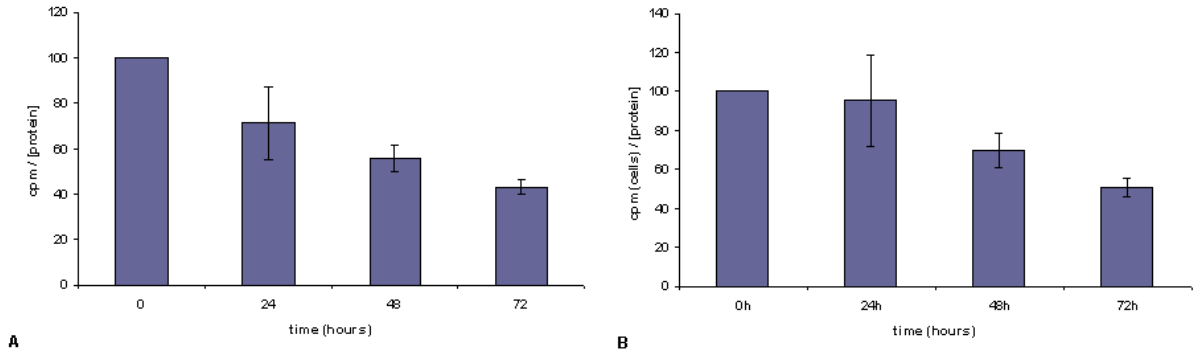

Figure 5.4. ^{35}S-macromolecules after HUVEC exposure to 1.0 mM GlcN for 0, 24, 48 and 72 hours*. Confluent cells were cultured in sulfate free RPMI-medium with 2% FCS and 1.0 mM GlcN for the indicated times. 0.1mCi ^{35}S-sulfate was added per ml medium for the last 24 hours before harvesting in Guanidine / Triton X-100. Samples from both conditioned medium (A) and cell-lysate (B) were purified by gelfiltration. The amount of ^{35}S-labelled PGs was measured as cpm and adjusted to the cellular protein concentration. The results are based on doublets of parallels from three different individuals, and presented as % of control with error bars.*

Effect of GlcN on ^{35}S-proteoglycans

Investigation of the effect of GlcN on PG expression was performed on samples purified from HUVEC exposed to different GlcN concentrations and for different durations. As mentioned in section 4.11, PGs are seen on SDS-PAGE as broad smears, typically at approximately >220, 220 and 95 kDa. Thus, high molecular bands of this kind on a SDS-PAGE of ^{35}S-macromolecules are thought to represent PGs.

GlcN dose-response

The effect of different doses of GlcN on the *de novo* PG synthesis was investigated by visualization of ^{35}S-PGs on SDS-PAGE.

Parallels from the three different HUVEC cultures previously used for protein and ^{35}S-macromolecule measurements, were seeded onto 6-wells culture plates and grown in MCDB medium until confluent. The cells were exposed to 0, 0.1, 1.0, 2.0, 5.0 and 10.0 mM GlcN and metabolically labelled with ^{35}S-sulfate. Purified samples of equal protein contents and a minimum of 10 000 cpm were subjected to SDS-PAGE, as shown in figure 5.5. Radioactive molecules of different sizes were visible as dark areas at different locations in each lane, relative to the migration in the gel. The size was determined by comparison to molecular weight markers.

PGs were separated on the gel into three distinct bands of >220, ~220 and ~ 95 kDa, as shown in figure 5.5, and the intensity of the bands correspond to the amount of radioactive material present. The SDS-PAGE indicated a decrease in the secretory PGs relative to the increasing GlcN concentration, starting at 1,0 mM GlcN (figure 5.5, panel A). The intensity of the bands was measured by the program *Scion Image* (Table 5.1). Additionally, no new bands appeared, nor did any bands disappear. This suggested that there was no change in the individual PG expressions, although this could not be concluded, as each band theoretically could be comprised of several PGs. From figure 5.5, panel B it is evident that the cell fractions contained much less radiolabelled PGs than the medium fractions. As illustrated by Table 5.1, the total intensity at 1.0 mM was reduced with 28 ± 7 % relative to control. In cell-lysate, the

total PG amount was lower, and the decrease in intensity with increasing GlcN concentration was less obvious.

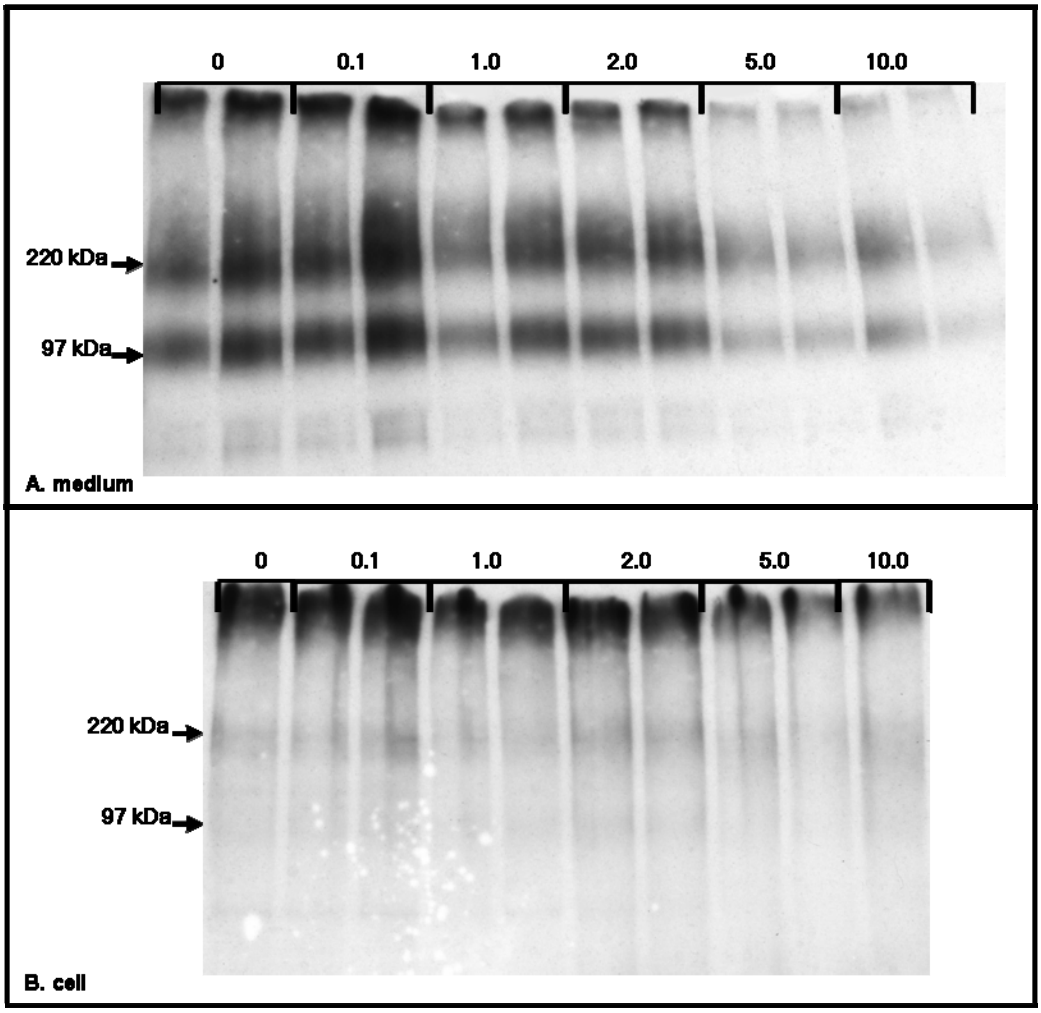

Figure 5.5. SDS-PAGE of ^{35}S-PGs in HUVEC exposed to 0, 0.1, 1.0, 2.0, 5.0 and 10.0 mM GlcN for 24 hours. *After grown to confluency,* ***t****he exposure was performed in sulfate free RPMI 1640 medium with 2% FCS and metabolic labelling with 0.1 mCi ^{35}S-sulfate/ ml medium. Conditioned medium (panel A) and cell lysate (panel B) was harvested, purified by gelfiltration, and sample volumes of equal protein contents and a minimum of 10 000 cpm were separated according to size on SDS-PAGE (4-20%). Radio-labelled PGs were detected by film exposure. This represents the results obtained from one of three individual experiments, in which each concentration is performed in parallel and accordingly loaded to two separate lanes (except for 0 and 10.0 mM in cell lysate, due to technical problems). The migration positions of molecular weight markers (in kDa) are shown on the left side of the panel.*

Table 5.1. *Intensity of the ^{35}S-PG-bands of the SDS-PAGE from all three experiments, detected with the program Scion Image. The mean intensity of each band (>250, 220 and 95 kDa) and the mean total intensity of each lane are shown for medium (A.) and cellysate (B.) for each GlcN concentration. The data are presented as % of control with standard errors.*

	Band size (kDa)	[GlcN] (mM)					
		0	0.1	1.0	2.0	5.0	10.0
A. Medium	>250	100	98	65	49	25	21
	220	100	112	75	69	29	23
	95	100	105	75	63	27	22
	Total	**100**	**104 ± 1**	**72 ± 7**	**63 ± 2**	**27 ± 1**	**22 ± 2**
B. Cell	>250	100	91	80	89	59	59
	220	100	91	83	108	63	88
	Total	**100**	**91 ± 3**	**81 ± 10**	**99 ± 3**	**61 ± 1**	**73 ± 2**

GlcN time-response

The effects of GlcN on ^{35}S-PGs were further investigated on parallels of HUVECs from three individuals exposed to 1.0 mM GlcN for 0, 24, 48 and 72 hours, as previously described. This *de novo* synthesis of PGs is illustrated in figure 5.6 by SDS-PAGEs of ^{35}S-sulfate labelled macromolecules from cell lysate and conditioned medium.

In line with previous observations, figure 5.6 illustrate the separation of PGs into three distinct bands of approximately 100, 220 and >220 kDa. The intensity of the bands varied with the amount of radiolabelled PGs present, and the total intensity of the medium samples dominated the cell lysate by far. In cell lysates, there was a total domination of PGs comprising the uppermost band. In both medium and cell fractions, there was a decreasing intensity of the bands with increasing incubation time. This suggested an increasing effect of GlcN with exposure time, supported by the data previously presented in figure 5.4. Measured as SDS-PAGE band intensity, the total amount of secreted ^{35}S-PGs was reduced by 33 ± 16 % after 24 hours, as can be seen from table 5.2. The corresponding reduction in cell-lysate was 34 ± 11 %. These data were supported by the previous findings that 24 hours incubation with 1.0 mM GlcN reduces the secretory ^{35}S-PGs. A more modest reduction was seen in cell-lysate with increasing time periods. The secretory PGs were of a much greater

abundance than the intracellular, and were increasingly affected by GlcN with increasing exposure time.

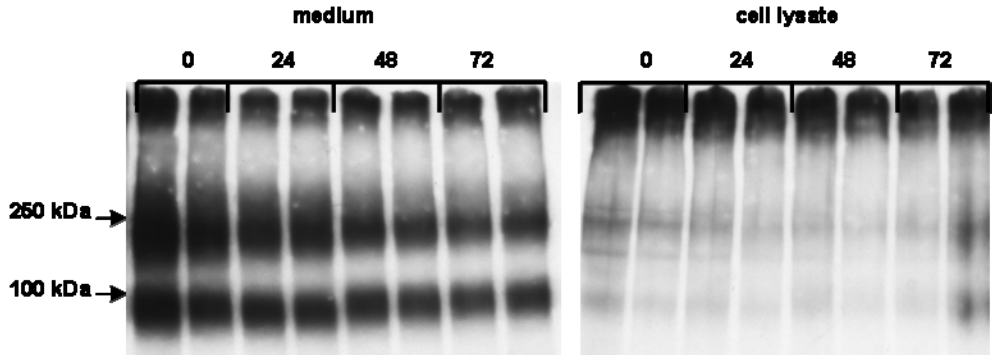

Figure 5.6. Effect of 0, 24, 48 and 72 hours GlcN exposure on ^{35}S-PGs in HUVEC*. SDS-PAGE of ^{35}S-sulfate labelled macromolecules in cell lysate and conditioned medium of HUVECs exposed to 1.0 mM GlcN for the indicated times. After grown to confluency, the exposure was performed in sulfate free RPMI 1640 medium with 2% FCS and metabolic labelling by 0.1 mCi ^{35}S-sulfate/ ml medium. Cells and medium was harvested, purified by gelfiltration, and sample volumes of equal protein contents and a minimum of 10 000 cpm were separated according to size on SDS-PAGE. Radiolabelled PGs were detected by film exposure. This is one representative of three individual experiments. The migration positions of molecular weight markers (in kDa) are shown on the left side of the panel.*

Table 5.2. *Intensity of the PG-bands at SDS-PAGE shown in figure 5.6, detected with the program Scion Image. The intensity of each band (>220, 220 and 95 kDa) and the total intensity of the lanes are shown for medium and cell-lysate for 0, 24, 48 and 72 hours, respectively. The data are presented as % of control with standard deviations.*

	Medium				Cell			
Band size (kDa)	0 h	24 h	48 h	72 h	0 h	24 h	48 h	72 h
450	100	48	48	57	100	79	74	71
220	100	77	61	57	100	59	45	75
95	100	76	66	49	100	62	53	104
Total	**100**	**67 ± 16**	**58 ± 9**	**54 ± 4**	**100**	**66 ± 11**	**57 ± 15**	**83 ± 18**

Collected effects of GlcN on HUVEC

GlcN in concentrations up to 10.0 mM did not affect the protein concentration of HUVEC. Concentrations above 1.0 mM were however observed to alter cell qualities, and 1.0 mM GlcN was therefore chosen for further experiments. Increasing exposure time did not seem to alter the effect of 1.0 mM GlcN on protein concentrations. Exposure to 1.0 mM GlcN reduced the expression of both ^{35}S-macromolecules and ^{35}S-PGs. A sufficient magnitude of effect was seen after 24

hours. In conditioned medium, the reduction of ^{35}S-macromolecules was 42 ± 18 %, and the reduction of ^{35}S-PGs was 28 ± 7 %. In summary; HUVEC exposure to 1.0 mM GlcN did not affect cell proliferation or viability, but did affect the expression of ^{35}S-macromolecules and ^{35}S-PGs. 24 hours was sufficient time to observe this effect.

5.1.2 Effects of high glucose and GlcN on HUVEC

The effects of glucose and GlcN on ECs were compared by exposing HUVEC to 25.0 mM glucose or 1.0 mM GlcN for 24 hours. Growth was monitored by cell protein measurements, as well as monitoring the biosynthesis of ^{35}S-macromolecules, ^{35}S-PGs and individual PGs.

Effect of Glucose and GlcN on HUVEC proliferation

We wanted to compare the effects of glucose and GlcN on HUVEC proliferation. This was done by exposing HUVECs to GlcN or high levels of glucose, and monitoring the protein concentration as compared to concentrations from HUVECs grown in low levels of glucose.

Seven confluent HUVEC cultures were exposed to low glucose (5.0 mM), high glucose (25.0 mM) or GlcN (1.0 mM) in RPMI 1640 sulfate free medium with 2% FCS for 24 hours before harvesting and purification.

No obvious differences in protein concentration were observed when comparing the effect of low glucose to high glucose or to GlcN, as shown in figure 5.7. In other words; neither high glucose nor GlcN affected cell viability or proliferation, and there were no differences between glucose and GlcN in their effect on proliferation.

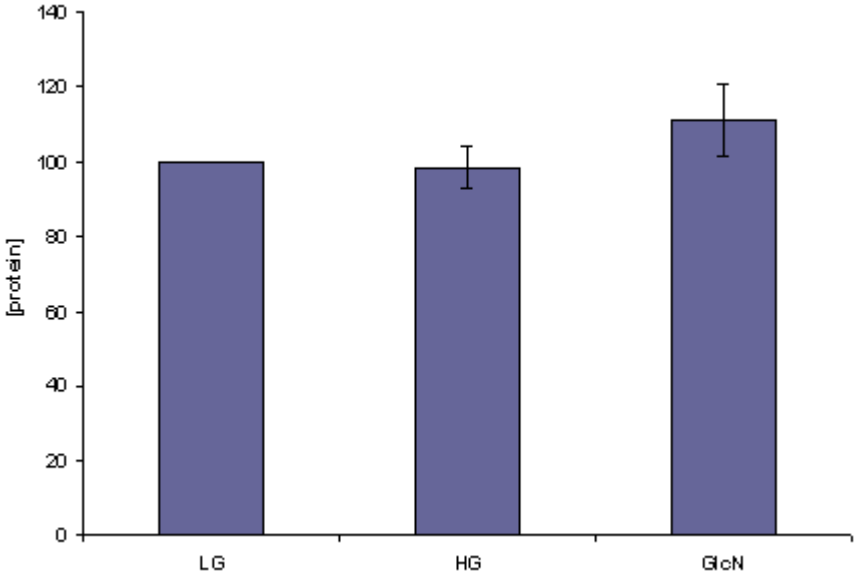

Figure 5.7. Protein concentration in HUVEC after 24 hours in low glucose (5.0 mM), high glucose (25.0 mM) or GlcN (1.0 mM). *Confluent HUVEC cells were cultured in sulfate free medium with 2% FCS and low glucose (LG), high glucose (HG) or GlcN for 24 hours, prior to harvesting, gel-chromatography purification and protein measurements. The data are based on doublets of parallels from seven individuals and presented as % of control, with error bars.*

Effect of Glucose and GlcN on ^{35}S-macromolecules

The effect of high glucose and GlcN on ^{35}S-macromolecules was investigated, both in relation to low glucose, and to each other.

HUVEC were grown to confluency and exposed to low glucose, high glucose or GlcN, in RPMI 1640 sulfate free medium with 2% FCS, and radiolabelled with ^{35}S-sulfate 24 hours prior to harvesting, G50 Fine purification, and finally protein and scintillation measurements.

From figure 5.8, panel A, it is evident that GlcN reduced the secretion of ^{35}S-macromolecules with 41 ± 13 %. Intracellular macromolecules were reduced by 31 ± 7 % (figure 5.8, panel B). High levels of glucose on the other hand, decreased the secretion (13 % ± 7 %) and increased intracellular levels (+ 27 % ± 16 %).

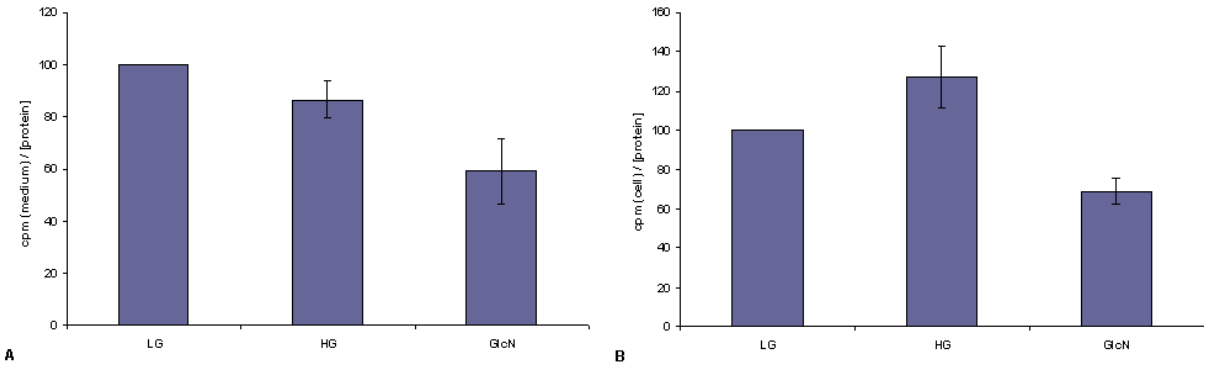

***Figure 5.8**: ^{35}S-macromolecules from HUVEC grown in low glucose (5.0 mM), high glucose (25.0 mM) or GlcN (1.0 mM) for 24 hours. Confluent HUVEC cells were cultured in sulfate free medium with 2% FCS and low glucose (LG), high glucose (HG) or GlcN, as well as 0.1 - 0.2 mCi ^{35}S-sulfate / ml medium. Cells were lysed and conditioned medium harvested, before gel-chromatography purification and cpm and protein measurements. The de novo PG synthesis is illustrated as amount of ^{35}S-macromolecules measured as cpm and adjusted to the protein concentration. Data from conditioned medium are found in panel A and from cell lysate in panel B. The data are based on doublets of parallels from five individuals and presented as % of control, with error bars.*

Effect of Glucose and GlcN on ^{35}S-proteoglycans

We wanted to investigate the effects of glucose and GlcN on the PG synthesis in HUVEC. The *de novo* synthesis of PGs can be assessed trough separation and visualization of radiolabelled macromolecules after SDS-PAGE.

Cell cultures grown to confluence on 6-well plates were exposed to low glucose (5.0 mM), high glucose (25.0 mM) or GlcN (1.0 mM) and radiolabelled with ^{35}S-sulfate for 24 hours prior to harvesting and G50 fine purification, and finally separation and visualization of PGs on SDS-PAGE (4-20 %) as previously described.

Separation of the ^{35}S-PGs gave rise to three distinct bands on the SDS-PAGE, and the intensity of the bands indicates their relative amounts. From figure 5.9 panel A it is observed that the ^{35}S-PG bands in the medium from cells treated with high glucose were overall equally intense, and the bands from GlcN treatment less intense, as compared to low glucose. From Table 5.3 it is evident that there were a minimal increase of 2 ± 1 % from low to high glucose, and a more markedly reduction of 55 ± 7 % from low glucose to GlcN in secreted PGs. This illustrate a markedly reduction

in the release of ^{35}S-PGs upon GlcN exposure. In cell lysate (figure 5.9, panel B), the total intensity of the bands was lower. The total cellular reduction in GlcN relative to low glucose was 19 ± 10 %, and in high glucose relative to low glucose the reduction was 12 ± 1 % (Table 5.3).

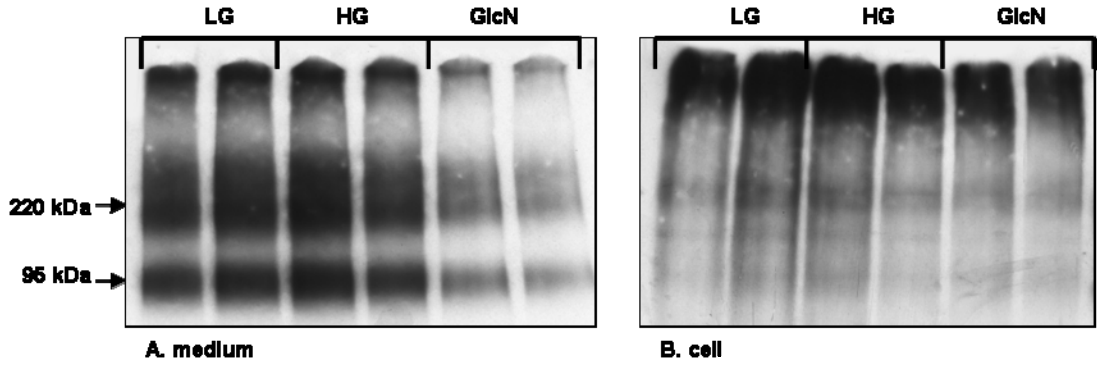

Figure 5.9. ^{35}S-PGs in HUVEC exposed to LG, HG or GlcN for 24 hours*. SDS-PAGE (4-20 %) visualisation of ^{35}S-sulfate labelled macromolecules from conditioned medium (A) and cell lysate (B) of HUVEC exposed to low glucose (LG, 50mM), high glucose (HG, 25.0 mM) and GlcN (1.0 mM) for 24 hours. Confluent cells were labelled in 0.1 mCi / ml and samples were purified by gelfiltration after harvesting. Samples of equal volumes and protein content was loaded on the gel and separated before visualization by film exposure. This represents the results obtained from three experiments, in which each concentration is performed in parallel and accordingly loaded to two separate lanes. The migration positions of molecular weight markers (in kDa) are shown on the left side of the panel.*

Table 5.3. *Intensity of the PG-bands in the SDS-PAGE shown in figure 9, detected with the program Scion Image. The intensity of each band (>220, 220 and 95 kDa) and the total intensity of each lane is shown for cell-lysate (A.) and medium (B.) for each concentration of GlcN. The data are presented as % of control (LG) with standard deviations.*

	Medium			Cell		
Band size (kDa)	LG	HG	GlcN	LG	HG	GlcN
>220	100	101	40	100	89	74
220	100	103	53	100	87	88
95	100	103	43			
Total	**100**	**102 ± 1**	**45 ± 7**	**100**	**88 ±1**	**81 ± 10**

Effect of Glucose and GlcN on PG composition in HUVEC

SDS-PAGE separation of ^{35}S-macromolecules gave rise to broad "PG-bands" at >220, 220 and 95 kDa. We wanted to investigate whether these were composed of HS or CS PGs.

Three HUVEC cultures were grown to confluence and exposed to low glucose, high glucose or GlcN and radio-labelled with 0.2 mCi ^{35}S-sulfate/ml medium 24 hours prior to harvesting and purification both by gelfiltration and ion-exchange chromatography. Each sample of conditioned medium was divided in four, of which were either left untreated or treated with cABC, HNO_2 or both, and subjected to SDS-PAGE.

Treatment of PGs with cABC will depolymerise CS- and DS-PGs into disaccharides, leaving only the core protein. HS is resistant to this enzyme, and HSPGs will remain unaffected. HNO_2 treatment on the other hand will depolymerise HS and heparin without affecting CS/DS. Radio-labelled HSPGs will thus not be visible at the SDS-PAGE of the HNO_2 treated samples.

As illustrated in figure 5.10, both in the low glucose, high glucose and GlcN samples, we observed that the uppermost bands at >220 kDa in the untreated samples, nearly disappeared after HNO_2 treatment. This showed that the PGs of this band were predominately of the HSPG type. A band of this size corresponds to the size of perlecan, which can be both of the HS and of the CS type. These data thus suggested that perlecan in HUVEC might be a HSPG.

In the cABC-digested samples the bands at ~ 220 and 95 kDa were markedly reduced, suggesting that the PGs in these bands were predominately of the CS/DS type. This was in agreement with the assumption that these bands consist, amongst others, of the HS/CS PGs serglycin and syndecan-1 at ~ 220 kDa, as well as the CS/DS PGs decorin and biglycan at ~ 95 kDa.

In the double digested samples all three bands were reduced, supporting these observations.

The PG composition of the low glucose, high glucose and GlcN treated cells were apparently identical, as the same effects were seen after cABC and HNO_2 in all treatments (figure 5.10, panel A, B, C). Therefore hyperglycemia did not seem to influence on the CS / HS ratio of PGs. The previous results illustrated in figure 5.9 and table 5.3, show that the change in intensity of the >220 kDa band of medium was negligible after high glucose treatment (increase of 1 %). After GlcN exposure, however, a reduction of 60 % was observed. Corresponding numbers for cellysate were 11 % decrease in high glucose and 26 % decrease in GlcN. The intensity of the 95 kDa band in cell lysate was to wage for identification, but in medium we observed a trend towards an increase (3 %) in high glucose and a decrease of 57 % in GlcN.

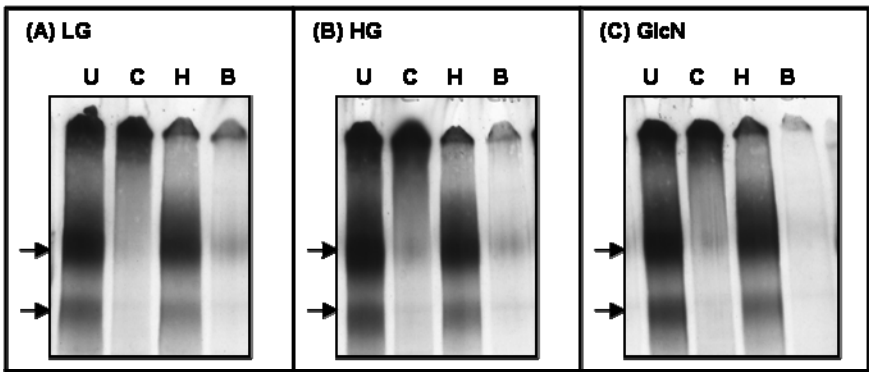

Figure 5.10. Secreted ^{35}S-PGs in HUVEC exposed to low glucose, high glucose or GlcN for 24 hours*. SDS-PAGE (4-20 %) visualisation of ^{35}S-sulfate labelled macromolecules from conditioned medium of HUVEC exposed to low glucose (LG, 50mM), high glucose (HG, 25.0 mM) and GlcN (1.0 mM) for 24 hours, in panel (A), (B) and (C) respectively. Confluent cells were labelled in 0.2 mCi / ml and samples were purified by gelfiltration and ion-exchange chromatography after harvesting, after which each sample was divided in four and treated with HNO_2, cABC, both or none. Samples of equal volumes and protein content was loaded on the gel and separated before visualization by film exposure. Indication if the treatments are given by U: Untreated, C: cABC, H: HNO_2, B: Both cABC and HNO_2. The upper arrow indicate a molecular size of ~ 220 kDa, the lower ~ 95 kDa. This represents the result of three experiments.*

Effect of Glucose and GlcN on perlecan and decorin

HNO_2 exposure and cABC digestion suggest that the >220 kDa PG in HUVEC is perlecan, and that the 95 kDa band contained decorin. This was investigated further, by Western blotting identification of the individual PGs.

HUVEC were grown to confluence, before exposed for 24 hours in MCDB medium with 2% FCS and either low glucose (5.0 mM), high glucose (25.0 mM) or GlcN (1.0 mM). Conditioned medium was recovered before cell lysis and harvesting in RIPA-buffer. The PGs were separated from other macromolecules by DEAE ion-exchange chromatography, and the samples were desalted and concentrated. Each sample was divided in three, in which two were subjected to cABC or HNO_2 digestion. Samples of equal protein contents were separated on SDS-PAGE (4-20 %) and the proteins were electroblotted on to a PVDF membrane. The blots were analyzed with antibodies against perlecan and decorin. The experiment was repeated three times with HUVEC from three different individuals. One representative blot is shown for perlecan in figure 5.11 and for decorin in figure 5.12.

The fully glycosylated perlecan was identified at >220 kDa by Western blotting in the untreated and cABC digested samples. In HNO_2 treated samples, the core was shown to have a molecular weight above 250 kDa. These results support the finding that perlecan in HUVEC is a HSPG, and that perlecan is the PG of the >220 kDa band on SDS-PAGE of ^{35}S-macromolecules. Due to uneven transfer of the large PGs from the gel to the PVDF membrane, the Western blots were not suited for quantitative analyses. However, the previous experiments showed that on SDS-PAGE the >220 kDa band was reduced with 60 % in GlcN, and unchanged in high glucose, related to low glucose (see Table 5.3).

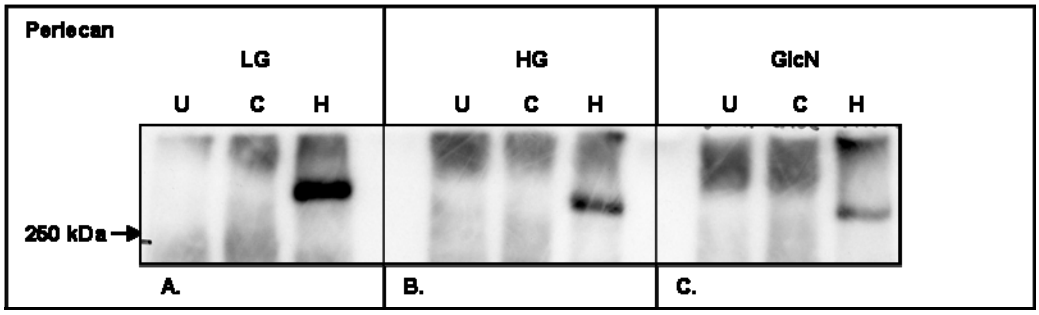

Figure 5.11. Perlecan expression in conditioned medium of HUVEC exposed 24 hours to low glucose, high glucose and GlcN. *HUVEC was exposed to low glucose (5.0 mM, LG), high glucose (25.0 mM, HG) or GlcN (1.0 mM). Conditioned medium was collected and purified by ion-exchange chromatography. The samples were either untreated (U) or treated with cABC (C) or HNO_2 (H), before amounts of equal protein contents was loaded on the gel (4-20 % SDS-PAGE gel) and PGs separated according to size. Perlecan was identified by Western blotting. The results present one representative of three experiments. The migration positions of molecular weight markers (in kDa) are shown on the left side of the panel.*

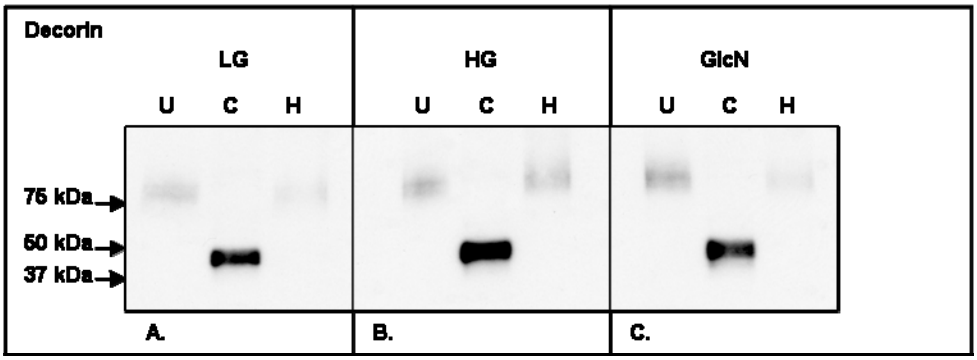

Figure 5.12. Decorin expression in conditioned medium of HUVEC exposed 24 hours to low glucose, high glucose and GlcN. *HUVEC were exposed to low glucose (5.0 mM, LG), high glucose (25.0 mM, HG) or GlcN (1.0 mM). Conditioned medium was collected and purified by ion-exchange chromatography. The samples were either untreated (U) or treated with cABC (C) or HNO_2 (H), before amounts of equal protein contents was loaded on the SDS-PAGE (4-20%) and PGs separated according to size. Decorin was identified by Western blotting. The results presented are representatives from three experiments. The migration positions of molecular weight markers (in kDa) are shown on the left side of the panel.*

In figure 5.12, decorin core protein was identified as strong bands at approximately 40 kDa in the cABC treated samples. The intact decorin was seen as somewhat fainter bands around 95 kDa in the untreated samples and HNO_2 treated samples. These data illustrated the fact that decorin was present and detectable in HUVEC as a CS/DS PG. This was supported by the results from the previous SDS-PAGE of ^{35}S-PGs (figure 5.9), showing that the band at ~ 95 kDa was of the CS/DS type. This band was decreased 57 % by GlcN and increased 3 % by high glucose, as illustrated by Table 5.3.

The PGs perlecan and decorin were detected by Western blotting of conditioned medium from HUVEC, and qualitative analyses confirmed perlecan as a HSPG and decorin as a CS/DS PG. They were both found in HUVEC during normoglycemic and hyperglycemic conditions, and both PGs were found to be secretory products under *in vitro* conditions.

Collected effects of Glucose and GlcN on HUVEC

Glucose and GlcN did not seem to affect HUVEC viability and proliferation. A reduction in both ^{35}S- macromolecules and PGs was observed in conditioned medium of GlcN exposed cells, by 41 ± 13 % and 55 ± 7 % respectively. The observed effects of high concentrations of glucose however, were more conflicting. The overall composition of PGs did not appear to be affected, neither with respect to PG size or the CS/DS composition. Perlecan and decorin were expressed in HUVEC exposed to both a normal and hyperglycaemic environment. Perlecan was shown to comprise the >220 kDa ^{35}S-PG SDS-PAGE band, and decorin was found in the ~ 95 kDa band. Perlecan in HUVEC has HS-chains and decorin has CS/DS chains, and the CS/HS composition did not seem to be affected by GlcN or high levels of glucose. Results from the previous experiment show that the relative intensities of the >220 (perlecan) and 95 kDa band (decorin) on SDS-PAGE were reduced by 60 % and 57 %, respectively, upon GlcN exposure. High glucose did not show conclusive effects on either PG

5.2 Effect of inflammatory conditions on proteoglycan synthesis

Hyperglycemia induces the atherosclerotic chronic inflammation of the vessels seen in DM. To further study PGs as a link between DM and vascular damage, ECs were exposed both to inflammatory conditions.

5.2.1 Effect of inflammatory conditions on HUVEC

Diabetic hyperglycemic conditions may lead to low-grade inflammatory conditions in the circulatory system. To study the possible implications of inflammation on PGs, ECs were exposed to the pro-inflammatory mediators IL-1α and TNF-α, and the effect on both cell proliferation and on radiolabelled macromolecules / PGs was studied.

Effect of inflammatory conditions on HUVEC proliferation

We wanted to investigate the effect on HUVEC proliferation upon exposure to IL-1α and TNF-α. Confluent HUVEC were cultured in RPMI sulfate free medium with 2% FCS and 5.0 mM glucose, and exposed for 24 hours to IL-1α (2.0 ng/ml) or TNF-α (7.0 ng/ml) (60), compared to cells grown only in the low glucose medium. The cells were harvested in Guanidine / Triton X-100, before gel filtration purification and protein determination.

These data indicate a slight increase in protein concentration after IL-1α exposure, as seen in figure 5.13. However, there was no change in protein concentration after exposure to TNF-α.

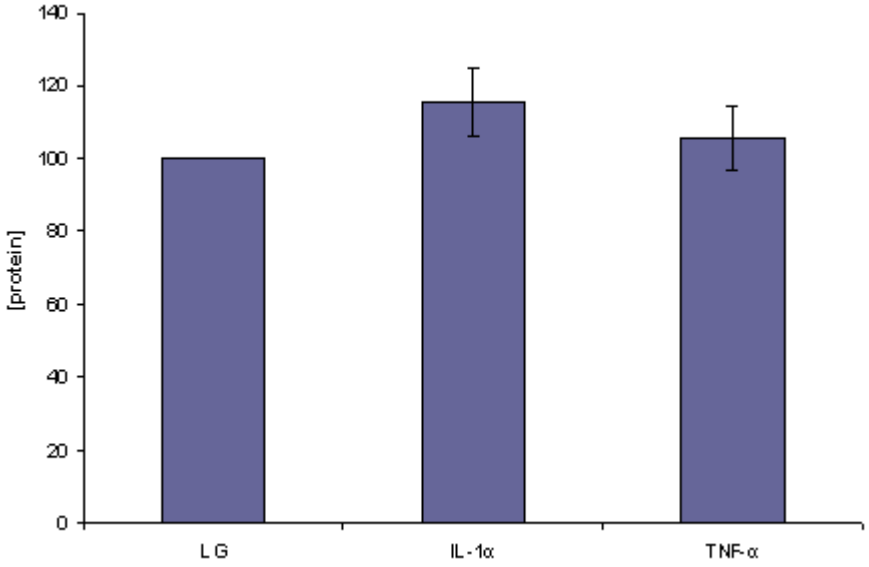

Figure 5.13. Protein concentration in HUVEC after 24 hours in low glucose (5.0 mM), IL-1α (2.0 ng/ml) or TNF-α (7.0 ng/mL). *Confluent HUVEC cells were cultured in sulfate free medium with 2% FCS and low glucose, IL-1α or TNF-α for 24 hours, prior to harvesting, gel-chromatography purification and protein measurements. The data are based on doublets of parallels from three individuals and presented as % of control, with error bars.*

Effect of inflammatory conditions on ^{35}S macromolecules

The effect of the inflammatory mediators on macromolecules was further investigated after ^{35}S-labelling.

HUVEC was cultured to confluence in MCDB-medium, after which they were grown in sulfate free RPMI 1640 medium with 2% FCS and low glucose (5 mM), IL-1α (2.0 ng/ml) or TNF-α (7.0 ng/ml) for 24 hours. The *de novo* synthesis of ^{35}S-macromolecules during these 24 hours was assesses by measuring the amount of ^{35}S macromolecules after gelfiltration.

From figure 5.14, panel A, it is evident that there was a profound increase in secreted ^{35}S- macromolecules after IL-1α exposure of 20 % ± 10 %. A trend towards a reduction was seen after TNF-α exposure; which decreased 14 ± 13 %. Intracellular macromolecules were reduced by 11 ± 8 % in IL-1α and 36 ± 21 % in TNF-α exposed samples, as illustrated in figure 5.14, panel B.

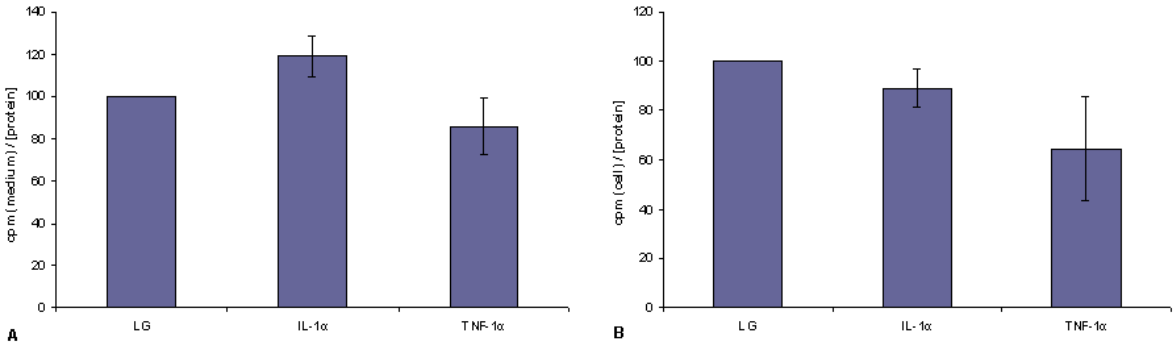

Figure 5.14. ^{35}S-macromolecules from HUVEC grown in low glucose (5.0 mM), IL-1α (2.0 ng/ml) or TNF - α (7.0 ng/mL) for 24 hours. *Confluent HUVECs were cultured in sulfate free medium with 2% FCS and low glucose (LG), IL-1α or TNF-α for 24 hours, as well as 0.2 mCi ^{35}S-sulfate / ml medium. Cells were lysed and conditioned medium harvested, before gel-chromatography purification and cpm and protein measurements. The de novo PG synthesis in conditioned medium (A) and cell-lysate (B) is illustrated as amount of ^{35}S-macromolecules measured as cpm and adjusted to the protein concentration. The data are based on doublets of parallels from two individuals and presented as % of control, with error bars.*

Effect of inflammatory conditions on ^{35}S-proteoglycans

The effect of inflammation on the *de novo* synthesis of total amount of PGs was studied by radiolabelling and visualisation on SDS-PAGE.

HUVEC from two individuals were cultured and exposed 24 hours to low glucose (5.0 mM), IL-1α (2.0 ng / mL) or TNF-α (7.0 ng / ml) and radiolabelling, and analysed by SDS-PAGE in the previously described manner. Due to limited amount of material, only conditioned medium was analysed, not cell-lysates. From figure 5.15 and table 5.4 it is evident that there was a small increase in ^{35}S-PGs in the medium after IL-1α exposure, whereas no effect was observed after TNF-α treatment.

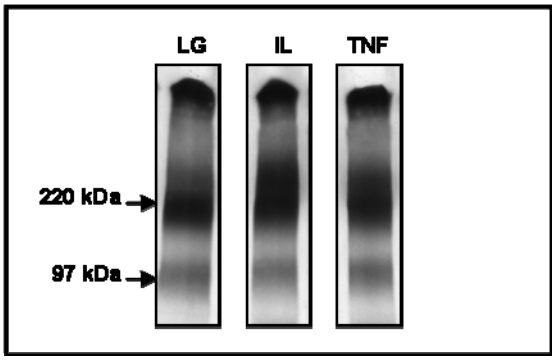

Figure 5.15 . SDS-PAGE of secreted ^{35}S- labelled PGs in HUVEC. *^{35}S- labelled macromolecules was recovered from the medium of HUVEC treated for 24 hours with low glucose (LG), IL-1α or TNF-α and purified by gelfiltration. Samples of equal volume and protein contents were subjected to SDS-PAGE (4-20 %). The migration of high molecular weight markers is shown on the left side (in kDa). This is one representative of two experiments.*

Table 5.4. *Intensity of the PG-bands from the SDS-PAGE shown in figure 5.16, detected with the program Scion Image. The intensity of each band (>220, 220 and 95 kDa) and the total intensity of the lanes are shown for low glucose (LG), IL-1α and TNF-α. The data are presented as % of control.*

Band size (kDa)	LG	IL-1α	TNF-α
450	100	103	94
220	100	104	105
95	100	113	111
Total	100	107	101

Effect of inflammatory conditions on PG composition in HUVEC

The SDS-PAGE separation of ^{35}S-macromolecules shown in Figure 5.16 gave rise to broad "PG-bands" at >220, 220 and 95 kDa. We wanted to investigate whether inflammatory conditions affected the synthesis of HSPGs or of CSPGs.

HUVEC from two individuals were cultured and exposed for 24 hours to low glucose (5.0 mM), IL-1α (2.0 ng / ml) or TNF-α (7.0 ng / ml) as previously described. Samples obtained were treated with c-ABC, HNO_2 or both, and subjected to SDS-PAGE.

Both in the low glucose, IL-1α and TNF-α treated samples, we observed that the uppermost bands at >220 kDa nearly disappeared when HNO_2 treated, indicating that the PGs in this band are predominately of the HSPG type (figure 5.16). This size corresponds to the size of the PG perlecan, which can be both of the HS and of the CS type. These data support the finding from the high glucose and GlcN treated cells; that perlecan in HUVEC is a HSPG.

After cABC-digestion, the bands at ~ 220 and 95 kDa were markedly reduced, suggesting that the PGs comprising these bands are predominately of the CS/Ds type. This is in agreement with our previous assumption that these bands consist, amongst others, of the HS/CS PGs serglycin and syndecan-1 at ~ 220 kDa, as well as the CS/DS PGs decorin and Biglycan at ~ 95 kDa.

No conclusions could be made about the changes in the >220 kDa "perlecan" band after IL-1α or TNF-α treatment, shown in previous experiments (Table 5.4) to be increased 3 % by IL-1α and reduced 6 % by TNF-α. A more distinct reduction was seen in the "decorin band" which was increased 13 % by IL-1α and 11 % by TNF-α.

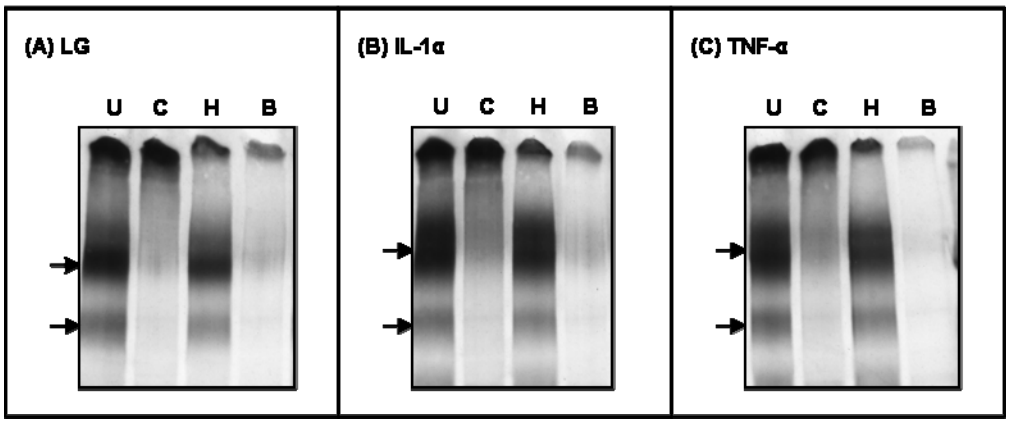

Figure 5.16. Secreted ^{35}S-PGs in HUVEC exposed to low glucose, IL-1α or TNF- α for 24 hours*. SDS-PAGE (4-20 %) visualisation of ^{35}S-sulfate labelled macromolecules from conditioned medium of HUVEC exposed to low glucose (LG, 5.0 mM), panel A, IL-1α (2.0 ng/ml), panel B and TNF-α (7.0 ng/ml), panel C. Confluent cells were labelled in 0.2 mCi / ml and samples were purified by gelfiltration and ion-exchange chromatography after harvesting, after which each sample was divided in four and treated with HNO_2, cABC-enzyme, both or none. Samples of equal volumes and protein content was loaded on the gel and separated before visualization by film exposure. Indication if the treatments are given by U: Untreated, C: cABC, H: HNO_2, B: Both cABC and HNO_2. The upper arrow indicate a molecular size of ~ 220 kDa, the lower ~ 95 kDa. This represents results from two experiments.*

Effect of inflammatory conditions on perlecan and decorin

HNO_2 exposure and cABC digestion to HUVEC in normal and inflammatory conditions suggest that the >220 kDa PG in HUVEC is perlecan, and that the 95 kDa band contains decorin. This was investigated further by Western blotting.

Confluent HUVEC were exposed to IL-1α or TNF-α for 24 hours. Cells were lysed in RIPA-buffer, and conditioned medium and cell lysates collected and purified as previously described. Samples of equal protein contents were separated on SDS-PAGE (4-20 %) and analyzed for perlecan (figure 5.17) and decorin (figure 5.18) using Western blotting.

Perlecan was identified by Western blotting both in medium (figure 5.17, panel A), and only faintly in cell-lysate (figure 5.17, panel B). The intact perlecan PG was observed mainly in untreated and cABC digested samples, at >220 kDa. The core protein was seen only in the HNO_2 treated samples as a band at approximately 200 kDa. These findings implicate that perlecan is predominately a HSPG, both during

normal and inflammatory conditions. These findings support the results obtained from the SDS-PAGE of figure 5.16 that the >220 kDa band is perlecan. As demonstrated in table 5.4, no changes were detected in the intensity of this band on SDS-PAGE after IL-1α or TNF treatment.

In contrary to perlecan, decorin was only identified in the medium fractions (figure 5.18). The core protein was observed as strong bands at approximately 40 kDa in the cABC treated samples, and the intact PG was seen as bands around 95 kDa in the untreated and HNO_2 treated samples. These data illustrates the fact that decorin is present in HUVEC and detectable on SDS-PAGE and after Western at 95 kDa, and supports the fact that decorin is a CS/DS PG. This seemed to be the case both in normal and inflammatory conditions. This supports the data from the SDS-PAGE (figure 5.16) that the 95 kDa band was comprised of CSPGs. This band was increased 13 % upon IL-1α exposure and 11 % after TNF-α stimulation as detected from SDS-PAGE (figure 5.15, table 5.4).

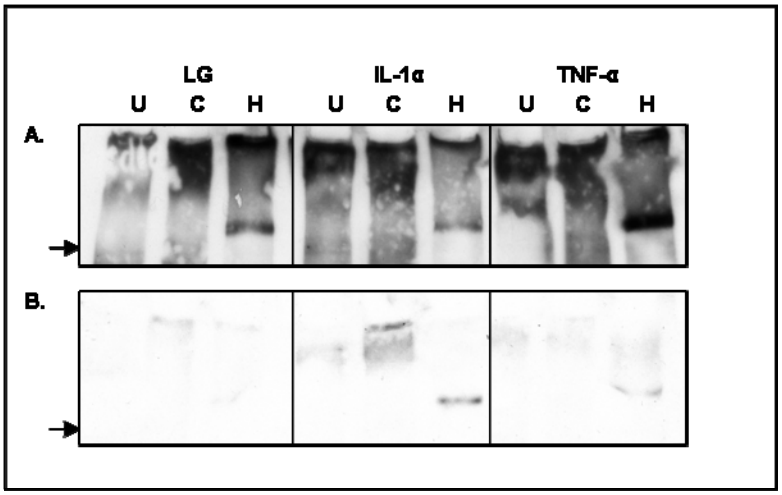

Figure 5.17. Perlecan expression in HUVEC exposed 24 hours to low glucose, IL-1α and TNF-α. *HUVEC was exposed to low glucose (5.0 mM, LG), IL-1α (2.0 ng/ml) and TNF-α (7.0 ng/ml). Both conditioned medium (panel A) and cell-lysate (panel B) was collected and purified by ion-exchange chromatography. The samples were either untreated or treated with cABC or HNO_2, before samples of equal protein contents was loaded on the SDS-PAGE (4-20 %) and PGs separated according to size. Perlecan level was determined by Western blotting. These data are representative of three experiments. The arrows indicate a molecular size of 220 kDa.*

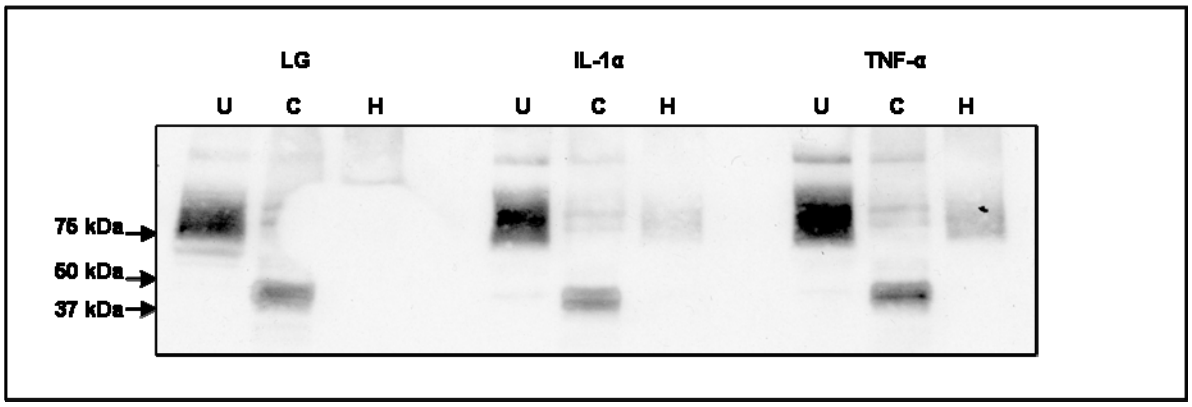

Figure 5.18. Decorin expression in HUVEC exposed 24 hours to low glucose, IL-1α and TNF-α. *HUVEC was exposed to low glucose (5.0 mM, LG), IL-1α (2.0 ng/ml) and TNF-α (7.0 ng/ml). Conditioned medium was collected and purified by ion-exchange chromatography. The samples were either untreated or treated with cABC or HNO_2, before samples of equal protein contents was loaded on the SDS-PAGE gel (4-20 %), and PGs separated according to size. decorin level was determined by Western blotting. The blot is representative of three different experiments. The migration positions of molecular weight markers (in kDa) are shown on the left side of the panel.*

Collected effects of IL-1α and TNF-α on HUVEC

IL-1α, but not TNF-α, have possibly stimulating effects on HUVEC proliferation, measured as increase in protein contents. There were indications of a stimulating effect of IL-1α on ^{35}S-macromolecule and ^{35}S-PGs secretion in HUVEC, whereas the effect of TNF-α was more questionable. Cellular levels seemed to be less affected. Perlecan and decorin were identified as the >220 and 95 kDa PGs in HUVEC. Perlecan was identified as a HSPG in HUVEC, and decorin as a CS/DS PG. This was true in HUVEC both during inflammatory and normal conditions.

5.3 Assembled effects of hyperglycemic and inflammatory conditions on HUVEC

Exposure to 1.0 mM GlcN did not affect cell proliferation or viability of HUVEC. It did however affect the level of secreted ^{35}S-macromolecules in the range of 29 ± 16 % to 42 ± 18 % and ^{35}S-PGs in the range of 28 ± 7 % to 55 ± 7 %. The corresponding reductions observed in cell lysate were in the range of a 5 ± 23 % to 31 ± 19 % reduction in ^{35}S-macromolecules, and in the area of a 19 ± 10 % to 34 ± 11 %

reduction in ^{35}S-PGs. 24 hours exposure under *in vitro* conditions was sufficient to see this effect.

Neither Glucose nor GlcN seemed to affect HUVEC viability and proliferation. However, as noted, a reduction in both ^{35}S- macromolecules and PGs was observed in the conditioned medium of GlcN exposed cells. The effects of high glucose, however, were more uncertain. IL-1α, but not TNF-α, had a possibly stimulating effect on HUVEC proliferation, measured as protein contents. There were also indications of a stimulating effect of IL-1α on secreted ^{35}S-macromolecules (20 ± 10 % increase) and ^{35}S-PGs (7 % increase) in HUVEC, whereas the effect of TNF-α was more questionable. Cellular levels seemed to be less affected.

Perlecan in HUVEC was found to be a HSPG, and decorin a CS/DS PG. The >220 kDa band on the SDS-PAGE of ^{35}S-macromolecules was identified as the PG perlecan, and decorin was identified in the 95 kDa band. Thus, after metabolic labelling with ^{35}S-sulfate and purification of the samples, the radiolabelled macromolecules obtained consisted mainly of PGs. The amount of ^{35}S-PGs detected on film can be used as an assessment of the *de novo* PG synthesis.

Exposure of GlcN resulted in a 60 % reduction in perlecan and a 57 % reduction in decorin, whereas no such changes were observed in high glucose. IL-1α The level of perlecan was shown to be reduced by 60 % upon GlcN exposure. The effects of inflammation were more variable. Decorin was reduced by 57 % in GlcN, and increased by 13 and 11 % by IL-1α and TNF-α. The effects of high glucose on perlecan and decorin were inconclusive.

6. Discussion

Changes in PG expression are suspected to be involved in the development of diabetic complications (58;59;68). DM is associated both with hyperglycemia and atherosclerotic chronic inflammation of the vessels. Hyperglycemic conditions can be mimicked *in vitro* both by exposing cultured cells to high glucose, as well as high concentrations of glucose metabolites such as GlcN, and diabetic inflammatory conditions can be mimicked by using pro-inflammatory cytokines such as TNF-α and IL-1α (18).

With this is mind; In order to explore the role of PGs in DM, we studied the effects of hyperglycemic and inflammatory conditions on PG synthesis in HUVEC. We studied the effects of high glucose, GlcN, IL-1α and TNF-α on cell proliferation, total PG production and changes in the expression of the important PGs perlecan and decorin, in particular.

The most commonly used sources of human endothelial cells to study specific characteristics and a range of patho-physiological processes, are Human Umbilical Vein Endothelial Cells, HUVEC, isolated from the vein of the umbilical cord (69). HUVEC were isolated from different donors of different backgrounds, and therefore carry distinct qualities. The biological variation of the population will therefore be more visible than if working with an established cell line. This is reflected in the variation of the data obtained. A possible objection to the use of HUVEC however, could be the fact that they are derived from immune-privileged foetal tissue, and may not be representative for adult endothelium.

Hyperglycemia is an independent risk factor for cardiovascular disease in diabetic patients, although the link is unclear. *In vivo* studies associate high glucose with a decrease in HSPGs (30;68;70;71). A decrease in HSPG in vitro, will increase monocyte adhesion to endothelium and accelerate atherogenesis (54;68), and a loss of endothelial HS has been postulated to lead to severe pathological events, in particular

event related to atherosclerosis. Loss of endothelial glycocalyx *in vivo* is also observed during hyperglycemia (20). Perlecan is the major extracellular HSPG, shown to be negatively correlated to inflammation, atherosclerosis and DM (24). CS/DS PGs are possibly increased, showing an increase in expression in human placentas of patients with gestational DM (72). Other studies do not demonstrate such an effect (68). Decorin is a prominent CS/DS PG, which is observed to increase during atherosclerosis (30). GlcN is a glucose metabolite increased in hyperglycemia. Current studies show that glucose and GlcN have distinct effects on vascular HSPG (24). Unlike glucose, GlcN was suggested to increase matrix HSPG (perlecan) in endothelial cells (24). However, the opposite effect is observed in chondrocytes (73). Finally, others report that vascular PG synthesis is not affected at all by metabolic factors associated with DM such as high glucose (74). Hyperglycemia is known to promote inflammation (55). The effect of the pro-inflammatory cytokines IL-1α and TNF-α are reported to increase PG production (60).

6.1 Effects of hyperglycemia on PG synthesis

6.1.1 Effect of GlcN on HUVEC

Among several mechanisms proposed to explain the link between hyperglycemia and vascular dysfunction is changes in the hexosamine pathway, where glucose is converted to GlcN. GlcN is the precursor for PG biosynthesis, as well as serving as substrate for O-GlcNAcylation of proteins. The effects of GlcN on HUVEC were investigated, both by looking at the effects on proliferation, and by investigating the effects on expression of ^{35}S- macromolecules and ^{35}S-PGs.

Different concentrations of GlcN were administered to the cells, and the effects on both ^{35}S- macromolecules and ^{35}S-PGs were investigated. A substantial reduction in PG expression was seen after incubating HUVEC in 1.0 mM GlcN for 24 hours, without seeing any effect on cell viability.

A decrease in HSPGs in endothelial cells is associated with increased atherosclerosis. The results obtained here thus suggest that diabetic complications associated with hyperglycemia could, in part, be due to an increase in the glucose metabolite GlcN. The observed reduction in PGs upon GlcN exposure is in conflict with some other findings, such as the report of Duan, W. et al. (24). As GlcN is a precursor for GAG biosynthesis, an increase in GAGs following increased GlcN levels, is comprehensible. However, GlcN is also utilized for the glycosylation of proteins including certain transcription factors (23). Glycosylation state of the transcription factors affects their activity (26). Thus, it is conceivable that GlcN treatment increase the glycosylation of transcription factors involved in PG expression, which is a challenging topic for further research.

Additionally, different endothelial cells could respond very differently to identical environments. Duan et al. performed experiments on Bovine aortic endothelial cells, exposing them to 2.5 mM GlcN for 16 hours. This represents different conditions than in the present study. Contradictory effects of GlcN in different cells could be the result of variations in GLUT expression. GlcN are transported into cells by GLUT 1, 2 and 4. GLUT 1 and 4 has the same affinity for glucose and GlcN, but GLUT 2 has a 10-20 fold higher affinity for GlcN (75). Thus, the expression of glucose transporters by various cells could affect the uptake, cytosolic concentration and hence the effect of GlcN. GLUT l is expressed at high levels in all foetal tissues, and is also abundant in adult tissue endothelial cells (15;16).

The concentration of GlcN used in the experiments also influence on the results; GlcN concentration found in the blood is normally in the range of 60-80 μM (75), much lower than the 1.0 mM used in the present study, and far lower than the 2.5 mM used by Duan et al. Also, administering GlcN extracellularly might not mimic hyperglycaemic conditions in a satisfactory way. In hyperglycemia, high levels of glucose in the blood will lead to increased uptake by concentration-dependent glucose transporters and hence increased intracellular levels of glucose. This increasing intracellular level of glucose will lead to an increased conversion into

GlcN, and hence increased flux trough the hexosamine pathway. Thus, increased levels of GlcN are seen intracellularly, but not extracellularly in hyperglycemia (76;77), and it is not known whether extracellularly administration will give the same effects.

6.1.2 Effects of high glucose and GlcN on HUVEC

The effect of glucose and GlcN on PGs in endothelial cells was compared. Glucose is thought to exert some of its effects by way of the metabolite GlcN and the hexosamine pathway. Therefore, GlcN was administered as a way of enhancing the possible effects of glucose. Comparison of the effect of GlcN and glucose will give information about how glucose affects PG synthesis in endothelial cells; whether the effects of glucose are trough transformation to the metabolite GlcN and the hexosamine pathway, or whether other effects could be of more importance.

In contradiction to GlcN, exposing HUVEC to high glucose is a more established procedure. The aim is to mimic human hyperglycaemic conditions. DM is diagnosed by a non fasting plasma glucose of ≥ 11.1 mM (78), and will vary throughout the day. 25 mM glucose is a common concentration used when mimicking hyperglycemia in cell cultures (54;79). This concentration is higher than 11 mM, but is a concentration observed in human with hyperglycemia. Additionally, glucose is only added when changing medium, whereas human has a constant supply of glucose. Finally, *in vitro* experiments often require an exaggerated exposure in order to show the effects experienced *in vivo* in short term experiments.

Neither glucose nor GlcN was shown to affect cell proliferation. The *de novo* biosynthesis and secretion was assessed by investigation of ^{35}S-macromolecules and ^{35}S-PGs (figure 5.8 & 5.9). The effect of high glucose on PG expression was not as pronounced as the effect of GlcN. GlcN was shown to decrease PGs, but we could not observe such changes after high glucose treatment. These results could possibly support the notion that glucose and GlcN has distinct effects on PGs (24). A great deal of publications suggest a decrease in HSPG upon high glucose exposure of cells

in vitro (30;68;70;71). CSPGs however, are observed to remain unaffected (71) or to increase (30). Thus, the total expression of PGs could remain unaltered, even if the expression of individual PGs were altered. In contrast, a reduction in total secreted PGs upon high glucose was reported by Gharagozlian et al. (54). These experiments were performed on HUVEC, but under slightly different conditions than in the present study. 80 % confluent cells, as opposed to 100 % confluent, were exposed to high glucose for a length of 4 days, in contrast to 24 hours. Also, the labelling with ^{35}S-sulfate was performed under serum-free conditions. All this taken together could possibly explain the lack of ability to reproduce the results of Gharagozlian et al. Clearly, effects on HSPGs versus CSPGs must be investigated further.

In order to address the question of how hyperglycemia will affect the expression of HS versus CS PGs, ^{35}S-macromolecules were separated according to size on SDS-PAGE. The GAG-chain composition of the PGs was investigated by comparing untreated samples to samples treated with cABC, HNO_2, or both, as illustrated in figure 5.10. The >220 kDa band was found to be composed predominately of HSPGs, and the 220 and 95 kDa bands was dominated by CS/DS PGs. This pattern after SDS-PAGE separation was identical in HUVEC exposed to low glucose, high glucose and GlcN, thus the CS/HS composition of each band was not altered under these circumstances. Additionally, these results also suggest that the observed effects of GlcN and high glucose on total PGs are also representative for the effect on HSPGs and CSPGs. It would however be interesting to investigate the effects on individual PGs, as both the HSPG-band and the CSPGs bands could represent more than one PG each, with different functions and responses to hyperglycemia.

Thus, analysis of the individual PGs perlecan and decorin were performed. Perlecan is the most prominent HSPG in endothelial cells (30;44;50;80), a major basementmembrane PG with a multitude of important functions such as modulation of growth factors and angiogenic activity, effect on cell-cell and cell-matrix adhesion and motility. Structural changes in perlecan in endothelium is observed during hyperglycemia (71). Decorin is a smaller SLRP matrix PG found in endothelium

(45;81), which may have a pathogenic role in DM. Decorin is observed to be produced by capillary ECs during angiogenesis associated with a profound inflammation (82).

Western blotting analyses identified perlecan as the > 220 kDa PG and decorin as the 95 kDa PG in HUVEC (figure 5.11 and 5.12). HNO_2 and cABC digestion of the samples identified perlecan as being a HSPG with a core protein of approximately 350 kDa. Decorin was shown to be a CS/DS PG with a core protein of approximately 40 kDa. This is in correspondence to earlier findings, identifying decorin as a 90 kDa CSPG with a core protein of 40 kDa (83). Perlecan may contain both HS and CS chains (42;43;84), but is previously fond to be an HSPG in endothelium (71). These results then suggest perlecan as the major HSPG in HUVEC.

Hyperglycemic conditions such as high glucose or GlcN did not seem to affect the presence of perlecan or decorin (figure 5.11 and 5.12). Thus, there were no indications of a change in the composition of different PGs during hyperglycemia. Also, the HS / CS composition of each of the PGs present did not seem to be altered (figure 5.10). Perlecan was found to be a HSPG in all cases.

Both Western blots illustrate the fact that the core protein is frequently visible as a more intense band than the fully glycosylated PG. This is probably due to the improved availability of the antibody for binding to the core protein after removal of GAG-chains. Similarly, HNO_2 treatment occasionally gave rise to a nearly invisible core protein. This result could be due to the harsh HNO_2treatment at pH 1.5. PGs with few GAG-chains protecting the core protein, such as decorin, could suffer from degradation of the core protein in HNO_2. To avoid this problem, in future experiments heparitinase will be used and not HNO_2.

The quantity of the individual PGs could not be assed by Western blotting due to uneven transfer from the SDS-PAGE to the PVDF-membrane. This is most likely due to the big size of the PGs. To obtain more quantitative data, blotting methods for PGs should be optimized. The success of blotting could be affected by a multitude of

factors, such as blotting buffer composition, time and current of electroblotting, and type of membrane. Alternatively, precise quantifications could rather be performed by for instance ELISA assays. Sufficient and even transfer of the PGs can be controlled by visualization of proteins in way of Coomassie blue staining of the gel after blotting, or by reversible staining of the membrane with Ponceau red. However, having identified perlecan as the >220 kDa PG and decorin as the 95 kDa PG, these could be quantified from the SDS-PAGE separation of the PGs. The most apparent changes were seen for perlecan and decorin after GlcN treatment, were the reduction were 60 and 57 % respectively. GlcN is thus suggested to affect the total expression of PGs.

GlcN was observed to inhibit PG expression, while no such effect could be observed by glucose. However, if glucose exerts some of its effects via GlcN and the hexosamine pathway, a direct stimulus by GlcN would be expected to give a more obvious effect than when stimulating with glucose alone. These experiments thus do not exclude the fact that glucose might act on PG synthesis trough stimulation of the hexosamine pathway. The effects of GlcN could be masked by opposite effects of glucose, exerted trough other metabolic pathways. Clearly, more experiments must be conducted to clarify this issue.

Effect of inflammatory conditions on PG synthesis

Arterial PGs are considered to be important in atherogenesis due to their ability to trap lipid inside the vessel wall and to influence cellular migration and proliferation. Atherosclerotic lesions have displayed an altered PG content and distribution (59). In order to understand the possible implications of inflammation on PGs, ECs were exposed to the pro-inflammatory mediators IL-1α and TNF-α, and the effect on both cell proliferation and on *de novo* biosynthesis and secretion of PGs was studied.

The serum levels of TNF-α in diabetic subjects have been measured in the range 2.45 – 3.8 pg / ml (55;55;85). In the same studies, the normal controls were in the range of

1.58 – 3.3 pg / ml. IL-1α serum concentrations in subjects with recently diagnosed DM type have shown to be in the range 59 – 1421 pg / ml, whereas normal controls were in the range 23 – 233 pg / ml (86). The concentrations used in these studies are based on the reports from Kulset et al (60), showing that 2 ng/ml IL-1α and 7 ng/ml TNF-α were the most potent concentrations in inducing HUVEC serglycin mRNA expression *in vitro* for 24 hours.

The data presented in figure 5.13 indicate an increase in protein concentration after IL-1α exposure. However, there are no indications towards a change in protein content after exposure to TNF-α. The latter is in correspondence to the observations by Kulseth et al. where incubation in TNF-α and IL-1α did not significantly affect the viability of HUVEC (60).

Our experiments, describing the effect of IL-1α and TNF-α on ^{35}S-macromolecules, indicated an increase in secretion upon IL-1α exposure, but suggest a slight reduction upon TNF-α (figure 5.14A). Corresponding data from cell-lysate indicated a reduction upon both cytokines (Figure 5.14B). However, the standard errors are of such a great magnitude, making it difficult to conclude with certainty. Analyses of the changes in secreted ^{35}S-PGs upon the same conditions did suggest an increase after IL-1α exposure, and a negligible increase after TNF-α exposure. However, this also are merely indications, as the experiments were not performed with sufficient number of parallels. These experiments must be repeated with more HUVEC cultures in order to show the trends more clearly.

As previously mentioned and discussed later, the ^{35}S-macromolecules can be taken to represent the PGs in our samples. Thus an increase in the *de novo* PG biosynthesis and secretion is observed upon IL-1α, but no effect is seen after TNF-α exposure. This observed increase in PGs after IL-1α exposure in HUVEC is also seen in the study performed by Kulseth et al.(60). Our observations of the effects of TNF-α however, are in conflict with the results obtained from this study, where they showed a 2.5 times increase of serglycin mRNA levels upon 24 hours TNF-α exposure. The increase with IL-1α was lower, but significant. The serglycin m-RNA level was taken

to represent the total PG production. However, the experiments of Kulseth et al. were performed under slightly different conditions than ours, which could have influenced on the results. As an example, the m-RNA data were obtained from HUV-EC-C (Human umbilical vein endothelial cell line) in contrast to the primary HUVEC used in our experiments. These could possibly have some different characteristics. Also, the experiments were performed under slightly different culturing conditions, regarding the composition of the culturing medium and the culture flask coating. On the other hand, other researchers has reported a decrease in endothelial HSPG when exposed to TNF-α (87), and suggest a decrease in HS might be a general inflammatory reaction (24).

Atherosclerosis is considered in part to be a consequence of the chronic low-grade inflammation seen in DM (18). Inflammation is an important feature of plaque initiation and progression, and recruitment of leukocytes from the circulation to the site of tissue injury is essential for effective immune response. HSPGs are required for several stages of this entry process, binding and presenting chemokines, inducing adhesion of leucocytes (31). Additionally, PGs are thought to act as co-receptors for several signalling molecules such as growth factors and cytokines, binding to HSPGs on the EC surface (57). Thus, an increase in PGs upon IL-1α exposure could be a direct response to an inflammatory environment. In contrast to these considerations, evidence suggests that a disruption of the glycocalyx upon atherogenic stimuli increase vascular vulnerability for atherogenesis (19;33). An inflammation-induced shedding of the endothelial glycocalyx has been suggested to be an essential component in the inflammatory response of the vasculature. Thus, whether a reduction in HSPGs is linked to inflammation or not, is not yet determined. Alternatively, other metabolic alterations of HSPGs could be important during inflammation, such as changed GAG composition, length or sulfation.

HSPGs are suggested as important players in the inflammatory process. The effect of inflammation on PGs was further investigated trough the effects on HS/CS composition. The HS/CS composition of the bands resulting from separation of ^{35}S-

macromolecules on SDS-PAGE was determined by cABC and HNO_2 treatment. The >220 kDa band was composed of HSPGs, and the 220 and 95 kDa bands were CS/DS PGs. This composition was not altered when exposing HUVEC to inflammatory conditions. The pattern was identical after all three treatments (Figure 5.16), which indicate that inflammation does not alter the composition of the PG GAGs. This cannot be concluded, however, because each band on the SDS-PAGE could possibly be composed of different PGs. There could be individual changes in PG composition, but if opposite not visible in the total band. Investigation of the individual PGs are needed to address this. In addition, analyses of possible changes in HS and CS structure should be undertaken.

Analyses of the individual PGs perlecan and decorin were performed. Western blotting identified both perlecan as the > 220 kDa PG and decorin as the 95 kDa PG in HUVEC (Figure 5.17 & 5.18). Inflammatory conditions did not seem to affect the presence of perlecan or decorin, as the ratio of the PGs was not altered during IL-1α or TNF-α exposure. Neither was the CS/HS composition of each of the PG affected, as perlecan was identified as a HSPG and decorin as a CSPG in all cases. Collectively, these results indicate that the observed effects of inflammation on the total PG expression might also be representative for the effects on individual PGs. Inflammation was not shown to change the total composition of PGs, nor the HS/CS composition of each PG.

Perlecan and decorin could not be quantified by Western blotting due to uneven transfer of the large PGs, as previously discussed. However, as discussed later, ^{35}S-macromolecules separated on SDS-PAGE visualize the PGs found in the samples. Perlecan was identified as the >220 kDa PG on SDS-PAGE, and decorin was identified as the 95 kDa CSPG. This implies that perlecan and decorin could be quantified by analysing the intensity of these two bands on the SDS-PAGE (figure 5.16). The data presented suggest a possible decrease in decorin release both in IL–1α and TNF-α treated HUVEC, but no consistent change was observed in perlecan

expression. However, the changes observed by this method, are not reproducible enough to allow definitive conclusions.

The change in ^{35}S-macromolecules and ^{35}S-PGs observed after IL-1α exposure correspond to the change seen in the expression of decorin, but not in perlecan. This indicates a change in the expression of PGs other than perlecan. However, the >220 kDa band representing perlecan at the SDS-PAGE is saturated and changes could thus be undetectable. More detailed studies including time-studies are clearly needed to address this question.

The changes described in PG expression are based upon radiolabelling of the highly sulfated PGs with ^{35}S-sulfate added to the medium and incorporated into newly synthesized PGs. This method is excellent, enabling us to detect and study the *de novo* synthesis of PGs, without any interference of PGs already present in the cells, medium, serum etc. Thus, the amount of ^{35}S-sulfate incorporated into macromolecules is used as a measurement of the amount of sulfated macromolecules synthesized. Sulfate containing macromolecules in addition to PGs will also be labelled, but after purification by G-50 fine gel chromatography, PGs was shown to comprise the major part of the labelled macromolecules. ^{35}S-macromolecules were purified by gelfiltration before separated according to size on SDS-PAGE. This gave rise to broad smears at >220, ~220 and ~95 kDa, recognized as bands typically observed when separating PGs on SDS-PAGE (52;54;63;71;83;88). These bands were found to be composed of HS or CS PGs, respectively. Western blotting demonstrated that the >220 kDa band was comprised of the HSPG perlecan, and the 95 kDa band was found to contain CS/DS PG decorin. Thus; the ^{35}S-macromolecules was demonstrated to be predominately PGs, and this method could be used further as a tool to describe the *de novo* biosynthesis and secretion of PGs, both by radioactivity measurements or by visualization on SDS-PAGE. This finding is also supported by others (54;89).

Alterations in ^{35}S-PGs could indicate a change in number of PGs. However, the alterations in ^{35}S-sulfate incorporation into PGs may indicate structural modifications of the PGs rather than altered numbers of PGs. Both the number of GAGs, size of each GAG and sulfation of the GAGs could be affected and give rise to the observed changes in ^{35}S-PGs. Finally, changes in PG expression could be due to alteration in the degradation of both GAGs and PGs, in contrast to PG synthesis.

Additional analyses are clearly demanded in order to make any conclusions regarding the causes of the observed changes in ^{35}S-PGs. Changes in sulfation can be investigated by radiolabelling of both sulfate and sugar residues, using ^{35}S-sulfate and ^{3}H-GlcN and disaccharide analyses of HS and CS. GAG-chain length could be investigated trough ^{35}S-sulfate labelling of GAGs after separation from the protein core. GAGs could then be separated into CS and HS by CS/HS degradation, before separated according to size. Labelling of core proteins with for instance ^{35}S-cys/met and the GAG chains with ^{3}H-GlcN, make it possible to detect changes in GAG / core ratio. Also, a change in PG could be due to changes in degradation rather than synthesis, which also would be an interesting field of continuing research. Regarding quantitative analyses of individual PGs, Western blotting protocols should be optimized. Alternatively, ELISA assays could be used.

Finally, the composition of the 220 kDa PG band observed on SDS-PAGE was not evaluated in these experiments. This band was shown to consist of HSPGs, but the individual PGs were not identified. The HS/CS PG syndecan-1 has been identified in HUVEC by in our lab only by immunoprecipitation, but we have not been able to reproduce these results by western blotting or ELISA assays, and further studies are clearly needed. Another possible candidate, however, is the HS/CS PG serglycin. Current experiments are performed in our lab, both Western blotting and ELISA assays, in order to elucidate if serglycin might be the 220 kDa PG found in HUVEC.

7. Conclusions

There is need to increase our knowledge of the molecular mechanisms linking hyperglycemia to the pathogenesis of diabetic complications. A change in the endothelial expression of PGs in diabetic conditions might constitute a piece of the puzzle, and this was further investigated in this work.

Perlecan was demonstrated to be a HSPG in HUVEC. Additionally, ^{35}S-macromolecules purified by gelfiltration, was shown to be predominately PGs, and this method could be used further as a descriptive tool of the *de novo* biosynthesis of PGs.

Exposure of GlcN as an inducer of hyperglycemic effects, without affecting cell viability but still affecting PG expression, should be performed with GlcN concentrations close to 1.0 mM in HUVEC. The major findings of this study revealed a decreased biosynthesis and secretion of ^{35}S-PGs and of the individual PGs perlecan and decorin in HUVEC exposed to 1.0 mM GlcN for 24 hours. This suggests an effect of glucose in hyperglycemia on the total PG expression trough the hexosamine pathway. The effects of exposing HUVEC to high levels of glucose were inconclusive. The HS/CS composition of PGs was not altered, neither with high glucose nor GlcN.

Exposure of HUVEC to the proinflammatory cytokine IL-1α increased the total *de novo* synthesis of PGs, while the effects of TNF-α were more inconclusive. The HS/CS composition of the PGs did not seem to be altered during these conditions. However, only decorin was increased by cytokine stimulation, while the level of perlecan appeared to be unaffected. This might indicate a different effect on the expression of various PGs in inflammation.

Atherosclerosis is associated with a decrease in HSPGs in endothelial cells. Contrastingly, an increase in PGs was seen upon IL-1α exposure. Thus, whether a reduction in HSPGs is linked to inflammation or not, is yet to be determined.

Alternatively, in addition to synthesis and degradation, other alterations of HSPGs could be of importance during inflammation, such as changed GAG composition, length or sulfation.

Additional analyses are clearly demanded in order to make any conclusions regarding the causes of the observed changes in PG expression. The experiments with IL-1α and TNF-α must be repeated with more cell cultures, in order to verify the indicated trends. Additionally, the cause of the observed changes in ^{35}S-PGs must be found, by investigation of core proteins and GAG composition, length and sulfation. The different PGs expressed by endothelial cells should also be determined in further detail, including studies on syndecan-1 and serglycin.

8. Appendix I - Materials

8.1 Cells

Human Umbilical Vein Endothelial Cells (HUVEC)	Rikshospitalet, Norway

8.2 Chemicals

2-mercaptoethanol C_2H_6OS	Sigma Aldrich, Germany
^{35}S-sulfate as Na_2SO_4	Perkin Elmer, USA
Acetic acid /HAc, glacial (CH_3COOH)	Merck, Germany
Ammonium bicarbonate (NH_4HCO_3)	VWR, Germany
Amplifier	Amersham Biosciences, UK
Antibodies primary:	
decorin goat	R&D systems, USA
perlecan rabbit Polyclonal	Gift from Iozzo, R.(Department of Pathology, Anatomy and Cell Biology and the Kimmel Cancer Centre, Thomas Jefferson University, Philadelphia, Pennsylvania 19107, USA)
Antibodies, secondary:	
Anti goat HRP-linked,	R&D systems, USA
Anti rabbit HRP-linked	Amersham, UK
Barium nitrite ($BaN_2O_4xH_2O$)	Sigma Aldrich, USA
BC Assay: Protein Quantification kit	Uptima Interchim, France
Bromophenol blue	Sigma Aldrich, Norway
BSA (Bovine Serum Albumin)	Sigma Aldrich, Germany
Charcoal, activated	Merck, Germany

Collagenase 0.2%	Sigma Aldrich, Germany
Chondroitin ABC lyase	Sigma Aldrich, Germany
Coomassie Blue R250	BIO-RAD, USA
D-(+)-Glucosamine hydrochloride (GlcN HCl)	Sigma Aldrich, Norway
D-(+)-Glucose	Sigma Aldrich, USA
DEAE (diethyl aminoethyl)	Sephacel, Amersham Biosciences, Sweden
DMSO (dimethyl sulphoxide)	Sigma Aldrich, Germany
ECL Western blotting detection reagent, (Advance, Plus)	Amersham, UK
EDTA (ethylene diamine tetraacetic acid)	Merck, Germany
EGF (Epidermal Growth Factor)	R&D Systems, UK
FCS (Foetal Calf Serum)	Sigma Aldrich, Germany
FGF (Fibroblast Growth Factor)	R&D Systems, UK
Fungisone	GIBCO Invitrogen Corporation, UK
Gentamicine	GIBCO Invitrogen Corporation, UK
Glycerol	Sigma Aldrich, Germany
Glycine	Sigma Aldrich, Germany
Guanidine hydrochloride	Fluka Bio Chemica, Germany
Hydrocortisone	Sigma Aldrich, Germany
Hydrogen Chloride (HCl)	Merck, Germany
IL-1α (interleukin-1 α)	R&D systems, UK
Insulin Actrapid® Pennfill®	Novo Nordisk AS, Denmark
Isopropanol	Arcus, Norway
MCDB 131 medium basis powder	Sigma Aldrich, USA
Methanol	Merck, Germany
Precision Plus protein standard, All blue	BIORAD, USA

Precision Plus protein standard, Dual Colour	BIORAD, USA
Protease inhibitor Complete Mini EDTA-free cocktail tablet	Roche, Germany
Purified MQ water (mQH_2O)	Elix Millipore, USA
Rainbow ^{14}C methylated protein molecular weight standard	Amersham Biosciences, UK
RPMI 1640 sulfate free medium	GIBCO Invitrogen, Norway
SDS (sodium dodecyl sulfate)	Sigma Aldrich, Norway
Sephadex G50-fine	GE Healthcare, Sweden
Skim Milk Powder	Fluka, Switzerland
Sodium Acetate (NaAcx3H_2O)	Merck, Germany
Sodium Carbonate (Na_2CO_3)	Sigma Aldrich, USA
Sodium Chloride (NaCl)	Merck, Germany
Sodium deoxycholate	Sigma-Aldrich, USA
Sodium Hydrogencarbonate, ($NaHCO_3$)	Kebo, Denmark
Sodium Hydroxide (NaOH)	Merck, Germany
Sodium Pyrophosfate ($Na_4PO_2O_7$)	Sigma Aldrich, USA
Sulfuric Acid (H_2SO_4)	Merck, Germany
TNF-α (tumour necrosis factor- α)	R&D systems, UK
Trisma base	Calbiochem, USA
Trisma HCl	Sigma Aldrich, UK
Triton X-100	Sigma Aldrich, UK
Trypan blue solution	Sigma Aldrich, UK
Trypsin / EDTA	Sigma Aldrich, Norway
Tween®-20	Sigma Aldrich, Germany
Ultima Gold XR Scintillation fluid	Laborel AS, Norway

8.3 Equipment

96 well ELISA microplate	Greiner bio-one, Germany
Autoradiography cassette, Hypercassette™	Amersham Biosciences, UK
Cell culture flasks (25, 75, 150 cm^2)	BD Labware, USA
Cell culture plastic plates (6 and 12 wells)	BD Labware, USA
Compresses, Meosoft	Tendra, Sweden
Criterion Precast Gel, 4-20% Tris-HCl, 12+2 & 18 wells	BioRad, USA
Criterion ™ gel system, for SDS-PAGE and Western blotting	BioRad, USA
Eppendorf tubes (1,5 ml & 2,0 ml)	Sarstedt, Germany
Falcon pipette tubes 5, 10, 25 ml	BD Labware, Germany
Falcon tubes, 15 and 50 ml	BD Labware, USA
Filter flask (for medium), sterile	TPP, Switzerland
Finnpipette	Thermo labsystems, Finland
Glass wool	Paragon, UK
Hemacytometer, Bürker	Marlenfield, Germany
Hyperfilm ECL, Amersham	GE Healthcare, UK
Microcon Centrifugal Filter Devices	Millipore corporation, USA
pH paper	Merck, Germany
Pipetboy	IBS Integra Biosciences
Pipette tips	FinnTip, Thermo Electron Corporation & TipOne, Starlab, GMBH, Germany
PVDF membrane, Immobilion™ Transfer Membranes	Millipore, USA
Scalpel, single use	Paragon, UK
Sterile needle, Sterican	Braun, Germany
Sterile surgical glows with biogel coating	Regent, USA

Syringe filter 0.2 µm, sterile	VWR
Syringe, single use 15/50 ml, Omnifix®	B.Braun, Germany
Whatman® filter paper	Schleicher & Schwell

8.4 Apparature

Centrifuge	
Centrifuge 5417C	Eppendorf
Centri Kubota 5930	Kubota
DNA speedvac, DNA 100	Savant
IEC Centra –M centrifuge	Heigar
Labofuge 400	Heraeus
Film developer	AGFA Curix 60
Freeze-dryer	Hetosicc
Gel dryer, SGD 2000 Slab Gel Dryer	Thermo Savant
Gel Imager	Gel Logic Imaging system, Olympus
Incubator, 37°C, 5% CO_2	
Mini Galaxy A	E. Pedersen & Sønn laboratorieutstyr
Forma	Scientific Incorporation
Liquid Scintillation counter. Win spectral 1414	Wallac
Magnetic stirrer, heated	Heigar
Microscope, Olympus CKX415F	Olympus Corp.
pH meter, pHM210	Radiometer Analytical
Scale, Mettler	Toledo
Shaker	

Celloshaker variospeed	Vialta
Bibby	Stuart Scientific
Titertek Multiscan PLUS, absorbance measurer	Eflab
Water bath	Lauda

9. Appendix II - Solutions

Cord buffer

Components	Volume	Final concentration
Streptomycin	0.5 g in 1.0 mL sterile mQ-H_2O	50.0 mg/l
1xPBS (sterile)	1000 ml	

1.0 L 10xPBS, pH 7.4 – stock solution

Components	Volume	Final concentration
$NaH_2PO_4 \cdot 2H_2O$ (Mm 120 g/mol)	8.6 g	0.072M
KH_2PO_4	2.5 g	0.018M
NaCl	85 g	1.45M
mQ-H_2O	Up to 1000 ml	

pH was adjusted to 7.4 with 3M HCl or 4M NaOH. Autoclaved if needed.

1.0 L 1xPBS, pH 7,4

Components	Volume	Final concentration
10xPBS	100 ml	1x
mQ-H_2O	900 ml	

Autoclaved if needed

1.0 L 0.1M Acetate buffer pH 6,5

Components	Volume	Final concentration
NaAc ($NaC_3H_3O_2 \cdot 3H_2O$)	13.608 g	0.1M
mQ-H_2O	Up to 1000 ml	

0.2M HAc was added until pH 6.5

1.0 L 1.0M Tris buffer, pH 8, stock solution

Components	Volume	Final concentration
Tris base $C_4H_{11}NO_3$	121.1 g	1.0 M
mQ-H_2O	800 ml	
HCl concentrated	42 ml	
mQ-H_2O	Up to 1000 ml	

pH was adjusted to 8.0 with HCl

1.0 L 1.0M Tris buffer, pH 7.4, stock solution (for RIPA-buffer)

Components	Volume	Final concentration
Tris base $C_4H_{11}NO_3$	121.1 g	1.0 M
mQ-H_2O	800 ml	
HCl concentrated	70 ml	
mQ-H_2O	Up to 1000 ml	

pH was adjusted to 7.4 with HCl

1.0 L 0.05M Tris buffer, pH 8.0 (for G50 Fine buffer and ion exchange buffers)

Components	Volume	Final concentration
1.0 M Tris buffer pH 7,4	50 ml	0.05 M
mQ-H_2O	950 ml	

pH was adjusted to 8.0

1.0 M Tris buffer pH 6.8 (for sample buffer)

Components	Volume	Final concentration
Tris base $C_4H_{11}NO_3$	121.1 g	1.0 M
mQ-H_2O	800 ml	
HCl concentrated	Until pH 6.8	
mQ-H_2O	Up to 1000 ml	

0.2 M HAc/Acetic acid

Components	Volume	Final concentration
Glacial acetic acid (17,3M)	1.0 mL	0.2M
mQ-H_2O	Up to 86.5 ml	

100 ml 10.0 M HCl

Components	Volume	Final concentration
HCl concentrated (12,1M)	30 ml	10M
mQ-H_2O	Up to 100 ml	

100 ml 1.0 M HCl

Components	Volume	Final concentration
10M HCl	10 ml	1.0M
mQ-H_2O	Up to 100 ml	

10.0 M NaOH

Components	Volume	Final concentration
NaOH	40g	10M
mQ-H_2O	Up to 100 ml	

1.0 M NaOH

Components	Volume	Final concentration
10 M NaOH	10 ml	1.0 M
mQ-H_2O	Up to 100 ml	

100 mL 4.0 M NaCl (for ion-exchange chromatography)

Components	Volume	Final concentration
NaCl	23.38 g	4.0 M
mQ-H_2O	Up to 100 mL	

List of references

Reference List

(1) Type 2 diabetes in children and adolescents. American Diabetes Association. Diabetes Care 2000 Mar;23(3):381-9.

(2) Stene L, Midthjell K, Jenum A, Skeie S, Birkeland K, Lund E, et al. Hvor mange har diabetes mellitus i Norge? Tidsskr Nor Lægeforen 2004;124:1511-4.

(3) Wild S, Roglic G, Green A, Sicree R, King H. Global prevalence of diabetes: estimates for the year 2000 and projections for 2030. Diabetes Care 2004 May;27(5):1047-53.

(4) Frayn KN. Metabolic regulation - A human perspective. second edition ed. Blackwell Science; 2003.

(5) Metzger BE CDE. Proceedings of the Fourth International Work-shop-Conference on Gestational Diabetes Mellitus. Diabetes Care 1998 Aug;21 (Suppl.2):B1-B167.

(6) Schalkwijk CG, Stehouwer CD. Vascular complications in diabetes mellitus: the role of endothelial dysfunction. Clin Sci (Lond) 2005 Aug;109(2):143-59.

(7) Iivanainen E, Kahari VM, Heino J, Elenius K. Endothelial cell-matrix interactions. Microsc Res Tech 2003 Jan 1;60(1):13-22.

(8) Alberts B, Bray D, Lewis J, Raff M, Roberts K, Watson JD. Molecular Biology of The Cell. 3 ed. 1994.

(9) Reitsma S, Slaaf DW, Vink H, van Zandvoort MA, oude Egbrink MG. The endothelial glycocalyx: composition, functions, and visualization. Pflugers Arch 2007 Jun;454(3):345-59.

(10) Brownlee M. The pathobiology of diabetic complications: a unifying mechanism. Diabetes 2005 Jun;54(6):1615-25.

(11) Sheetz MJ, King GL. Molecular understanding of hyperglycemia's adverse effects for diabetic complications. JAMA 2002 Nov 27;288(20):2579-88.

(12) The effect of intensive treatment of diabetes on the develompent and long-term complications in insulin-dependent diabetes mellitus. The Diabetes Control and Complications Research Group. N Engl J Med 1993 Sep;329(14):977-86.

(13) Effect of intensive blood-glucose control with metformin on complications on overweight patientswith type 2 diabetes (UKPDS 34) UK Prospective Diabetes Study (UKPDS) Group. Lancet 1993 Sep;352(9131):854-65.

(14) Jeffcoate SL. Diabetes control and complications: the role of glycated haemoglobin, 25 years on. Diabet Med 2004 Jul;21(7):657-65.

(15) Olson AL, Pessin JE. Structure, function, and regulation of the mammalian facilitative glucose transporter gene family. Annu Rev Nutr 1996;16:235-56.

(16) Rask-Madsen C, King GL. Mechanisms of Disease: endothelial dysfunction in insulin resistance and diabetes. Nat Clin Pract Endocrinol Metab 2007 Jan;3(1):46-56.

(17) Endemann DH, Schiffrin EL. Endothelial dysfunction. J Am Soc Nephrol 2004 Aug;15(8):1983-92.

(18) Maiti R, Agrawal NK. Atherosclerosis in diabetes mellitus: role of inflammation. Indian J Med Sci 2007 May;61(5):292-306.

(19) Nieuwdorp M, Meuwese MC, Vink H, Hoekstra JB, Kastelein JJ, Stroes ES. The endothelial glycocalyx: a potential barrier between health and vascular disease. Curr Opin Lipidol 2005 Oct;16(5):507-11.

(20) Nieuwdorp M, van Haeften TW, Gouverneur MC, Mooij HL, van Lieshout MH, Levi M, et al. Loss of endothelial glycocalyx during acute hyperglycemia coincides with endothelial dysfunction and coagulation activation in vivo. Diabetes 2006 Feb;55(2):480-6.

(21) King GL, Brownlee M. The cellular and molecular mechanisms of diabetic complications. Endocrinol Metab Clin North Am 1996 Jun;25(2):255-70.

(22) Brownlee M. Biochemistry and molecular cell biology of diabetic complications. Nature 2001 Dec 13;414(6865):813-20.

(23) Kjellen L, Lindahl U. Proteoglycans: structures and interactions. Annu Rev Biochem 1991;60:443-75.

(24) Duan W, Paka L, Pillarisetti S. Distinct effects of glucose and glucosamine on vascular endothelial and smooth muscle cells: evidence for a protective role for glucosamine in atherosclerosis. Cardiovasc Diabetol 2005;4:16.

(25) Du XL, Edelstein D, Rossetti L, Fantus IG, Goldberg H, Ziyadeh F, et al. Hyperglycemia-induced mitochondrial superoxide overproduction activates the hexosamine pathway and induces plasminogen activator inhibitor-1 expression by increasing Sp1 glycosylation. Proc Natl Acad Sci U S A 2000 Oct 24;97(22):12222-6.

(26) Han I, Kudlow JE. Reduced O glycosylation of Sp1 is associated with increased proteasome susceptibility. Mol Cell Biol 1997 May;17(5):2550-8.

(27) Brownlee M. Negative consequences of glycation. Metabolism 2000 Feb;49(2 Suppl 1):9-13.

(28) Basta G, Schmidt AM, De CR. Advanced glycation end products and vascular inflammation: implications for accelerated atherosclerosis in diabetes. Cardiovasc Res 2004 Sep 1;63(4):582-92.

(29) Rifai N, Ridker PM. Inflammatory markers and coronary heart disease. Curr Opin Lipidol 2002 Aug;13(4):383-9.

(30) Pillarisetti S. Lipoprotein modulation of subendothelial heparan sulfate proteoglycans (perlecan) and atherogenicity. Trends Cardiovasc Med 2000 Feb;10(2):60-5.

(31) Kolset SO, Salmivirta M. Cell surface heparan sulfate proteoglycans and lipoprotein metabolism. Cell Mol Life Sci 1999 Nov 30;56(9-10):857-70.

(32) Kolset SO, Tveit H. Serglycin - Structure and biology. Cell Mol Life Sci 2007 Dec 8.

(33) Svennevig K, Kolset SO, Bangstad HJ. Increased syndecan-1 in serum is related to early nephropathy in type 1 diabetes mellitus patients. Diabetologia 2006 Sep;49(9):2214-6.

(34) Sternlicht MD, Werb Z. How matrix metalloproteinases regulate cell behavior. Annu Rev Cell Dev Biol 2001;17:463-516.

(35) Perrimon N, Bernfield M. Cellular functions of proteoglycans--an overview. Semin Cell Dev Biol 2001 Apr;12(2):65-7.

(36) Knudson CB, Knudson W. Cartilage proteoglycans. Semin Cell Dev Biol 2001 Apr;12(2):69-78.

(37) Tryggvason K, Patrakka J. Thin basement membrane nephropathy. J Am Soc Nephrol 2006 Mar;17(3):813-22.

(38) Lusis AJ. Atherosclerosis. Nature 2000 Sep 14;407(6801):233-41.

(39) Quarto N, Amalric F. Heparan sulfate proteoglycans as transducers of FGF-2 signalling. J Cell Sci 1994 Nov;107 (Pt 11):3201-12.

(40) Border WA, Ruoslahti E. Transforming growth factor-beta 1 induces extracellular matrix formation in glomerulonephritis. Cell Differ Dev 1990 Dec 2;32(3):425-31.

(41) Hayashida K, Chen Y, Bartlett AH, Park PW. Syndecan-1 is an in vivo suppressor of Gram-positive toxic shock. J Biol Chem 2008 May 22.

(42) Iozzo RV. Matrix proteoglycans: from molecular design to cellular function. Annu Rev Biochem 1998;67:609-52.

(43) Iozzo RV. Basement membrane proteoglycans: from cellar to ceiling. Nat Rev Mol Cell Biol 2005 Aug;6(8):646-56.

(44) Segev A, Nili N, Strauss BH. The role of perlecan in arterial injury and angiogenesis. Cardiovasc Res 2004 Sep 1;63(4):603-10.

(45) Iozzo RV. The biology of the small leucine-rich proteoglycans. Functional network of interactive proteins. J Biol Chem 1999 Jul 2;274(27):18843-6.

(46) Rapraeger AC, Krufka A, Olwin BB. Requirement of heparan sulfate for bFGF-mediated fibroblast growth and myoblast differentiation. Science 1991 Jun 21;252(5013):1705-8.

(47) Bellin R, Capila I, Lincecum J, Park PW, Reizes O, Bernfield MR. Unlocking the secrets of syndecans: transgenic organisms as a potential key. Glycoconj J 2002 May;19(4-5):295-304.

(48) Reitsma S, Slaaf DW, Vink H, Van Zandvoort MA, oude Egbrink MG. The endothelial glycocalyx: composition, functions, and visualization. Pflugers Arch 2007 Jun;454(3):345-59.

(49) Kolset SO, Prydz K, Pejler G. Intracellular proteoglycans. Biochem J 2004 Apr 15;379(Pt 2):217-27.

(50) Bishop JR, Schuksz M, Esko JD. Heparan sulphate proteoglycans fine-tune mammalian physiology. Nature 2007 Apr 26;446(7139):1030-7.

(51) Abrink M, Grujic M, Pejler G. Serglycin is essential for maturation of mast cell secretory granule. J Biol Chem 2004 Sep 24;279(39):40897-905.

(52) Kolset SO, Zernichow L. Serglycin and secretion in human monocytes. Glycoconj J 2008 May;25(4):305-11.

(53) Prydz K, Dalen KT. Synthesis and sorting of proteoglycans. J Cell Sci 2000 Jan;113 Pt 2:193-205.

(54) Gharagozlian S, Borrebaek J, Henriksen T, Omsland TK, Shegarfi H, Kolset SO. Effect of hyperglycemic condition on proteoglycan secretion in cultured human endothelial cells. Eur J Nutr 2006 Oct;45(7):369-75.

(55) Esposito K, Nappo F, Marfella R, Giugliano G, Giugliano F, Ciotola M, et al. Inflammatory cytokine concentrations are acutely increased by hyperglycemia in humans: role of oxidative stress. Circulation 2002 Oct 15;106(16):2067-72.

(56) Little PJ, Ballinger ML, Osman N. Vascular wall proteoglycan synthesis and structure as a target for the prevention of atherosclerosis. Vasc Health Risk Manag 2007;3(1):117-24.

(57) Parish CR. Heparan sulfate and inflammation. Nat Immunol 2005 Sep;6(9):861-2.

(58) Edge AS, Spiro RG. A specific structural alteration in the heparan sulphate of human glomerular basement membrane in diabetes. Diabetologia 2000 Aug;43(8):1056-9.

(59) Wasty F, Alavi MZ, Moore S. Distribution of glycosaminoglycans in the intima of human aortas: changes in atherosclerosis and diabetes mellitus. Diabetologia 1993 Apr;36(4):316-22.

(60) Kulseth MA, Kolset SO, Ranheim T. Stimulation of serglycin and CD44 mRNA expression in endothelial cells exposed to TNF-alpha and IL-1alpha. Biochim Biophys Acta 1999 Aug 5;1428(2-3):225-32.

(61) Johansen LM. Efects of Methylglyoxal, TNF-alfa and IL-1alfa on Proteoglycan Synthesis in Human Endothelial Cells *in vitro* 2007.

(62) Jaffe EA, Nachman RL, Becker CG, Minick CR. Culture of human endothelial cells derived from umbilical veins. Identification by morphologic and immunologic criteria. J Clin Invest 1973 Nov;52(11):2745-56.

(63) Svennevig K, Prydz K, Kolset SO. Proteoglycans in polarized epithelial Madin-Darby canine kidney cells. Biochem J 1995 Nov 1;311 (Pt 3):881-8.

(64) Smith PK, Krohn RI, Hermanson GT, Mallia AK, Gartner FH, Provenzano MD, et al. Measurement of protein using bicinchoninic acid. Anal Biochem 1985 Oct;150(1):76-85.

(65) Salmivirta M, Safaiyan F, Prydz K, Andresen MS, Aryan M, Kolset SO. Differentiation-associated modulation of heparan sulfate structure and function in CaCo-2 colon carcinoma cells. Glycobiology 1998 Oct;8(10):1029-36.

(66) Conrad HE. Degradation of heparan sulfate by nitrous acid. Methods Mol Biol 2001;171:347-51.

(67) Bergli I. Proteoglycaner i endotelceller isolert fra venen i navlesnor (HUVEC) 1997.

(68) Vogl-Willis CA, Edwards IJ. High glucose-induced alterations in subendothelial matrix perlecan leads to increased monocyte binding. Arterioscler Thromb Vasc Biol 2004 May;24(5):858-63.

(69) Marin V, Kaplanski G, Gres S, Farnarier C, Bongrand P. Endothelial cell culture: protocol to obtain and cultivate human umbilical endothelial cells. J Immunol Methods 2001 Aug 1;254(1-2):183-90.

(70) Edwards IJ, Wagner JD, Vogl-Willis CA, Litwak KN, Cefalu WT. Arterial heparan sulfate is negatively associated with hyperglycemia and atherosclerosis in diabetic monkeys. Cardiovasc Diabetol 2004 Apr 29;3:6.

(71) Vogl-Willis CA, Edwards IJ. High-glucose-induced structural changes in the heparan sulfate proteoglycan, perlecan, of cultured human aortic endothelial cells. Biochim Biophys Acta 2004 Apr 7;1672(1):36-45.

(72) Chen CP, Chang SC, Vivian Yang WC. High glucose alters proteoglycan expression and the glycosaminoglycan composition in placentas of women with gestational diabetes mellitus and in cultured trophoblasts. Placenta 2007 Feb;28(2-3):97-106.

(73) Terry DE, Rees-Milton K, Smith P, Carran J, Pezeshki P, Woods C, et al. N-acylation of glucosamine modulates chondrocyte growth, proteoglycan synthesis, and gene expression. J Rheumatol 2005 Sep;32(9):1775-86.

(74) Wilson P, Drennon K, Tannock LR. Regulation of vascular proteoglycan synthesis by metabolic factors associated with diabetes. J Investig Med 2007 Jan;55(1):18-25.

(75) Uldry M, Ibberson M, Hosokawa M, Thorens B. GLUT2 is a high affinity glucosamine transporter. FEBS Lett 2002 Jul 31;524(1-3):199-203.

(76) Nowak A, Szczesniak L, Rychlewski T, Dylewicz P, Przywarska I. Glucosamine levels in people with ischaemic heart disease with and without type II diabetes. Pol Arch Med Wewn 1998 Nov;100(5):419-25.

(77) Nowak A, Stankiewicz W, Szczesniak L, Korman E. [Glucosamine in the blood serum of young people with diabetes mellitus type 1]. Endokrynol Diabetol Chor Przemiany Materii Wieku Rozw 1999;5(2):97-101.

(78) Shils EM, Olson JA, Shike M, Ross AC. Modern Nutrition in Health and Disease. 9 ed. 1999.

(79) Gharagozlian S, Henriksen T, Kolset SO. High glucose and Nepsilon-(carboxymethyl) lysine bovine serum albumin modulate release of matrix metalloproteinases in cultured human endothelial cells. Eur J Nutr 2006 Aug;45(5):283-90.

(80) Charonis A, Sideraki V, Kaltezioti V, Alberti A, Vlahakos D, Wu K, et al. Basement membrane peptides: functional considerations and biomedical applications in autoimmunity. Curr Med Chem 2005;12(13):1495-502.

(81) Jarvelainen HT, Kinsella MG, Wight TN, Sandell LJ. Differential expression of small chondroitin/dermatan sulfate proteoglycans, PG-I/biglycan and PG-II/decorin, by vascular smooth muscle and endothelial cells in culture. J Biol Chem 1991 Dec 5;266(34):23274-81.

(82) Nelimarkka L, Salminen H, Kuopio T, Nikkari S, Ekfors T, Laine J, et al. Decorin is produced by capillary endothelial cells in inflammation-associated angiogenesis. Am J Pathol 2001 Feb;158(2):345-53.

(83) Fischer DC, Henning A, Winkler M, Rath W, Haubeck HD, Greiling H. Evidence for the presence of a large keratan sulphate proteoglycan in the human uterine cervix. Biochem J 1996 Dec 1;1(320):393-9.

(84) Danielson KG, Martinez-Hernandez A, Hassell JR, Iozzo RV. Establishment of a cell line from the EHS tumor: biosynthesis of basement membrane constituents and characterization of a hybrid proteoglycan containing heparan and chondroitin sulfate chains. Matrix 1992 Feb;12(1):22-35.

(85) Lindmark S, Buren J, Eriksson JW. Insulin resistance, endocrine function and adipokines in type 2 diabetes patients at different glycaemic levels: potential impact for glucotoxicity in vivo. Clin Endocrinol (Oxf) 2006 Sep;65(3):301-9.

(86) Hussain MJ, Peakman M, Gallati H, Lo SS, Hawa M, Viberti GC, et al. Elevated serum levels of macrophage-derived cytokines precede and accompany the onset of IDDM. Diabetologia 1996 Jan;39(1):60-9.

(87) Ramasamy S, Lipke DW, McClain CJ, Hennig B. Tumor necrosis factor reduces proteoglycan synthesis in cultured endothelial cells. J Cell Physiol 1995 Jan;162(1):119-26.

(88) Schick BP, Gradowski JF, San Antonio JD. Synthesis, secretion, and subcellular localization of serglycin proteoglycan in human endothelial cells. Blood 2001 Jan 15;97(2):449-58.

(89) Fjeldstad K. Proteoglycans in polarized epithelial Madin Darby Canine Kidney cells 1995.